CHALMERS
UNIVERSITY OF TECHNOLOGY

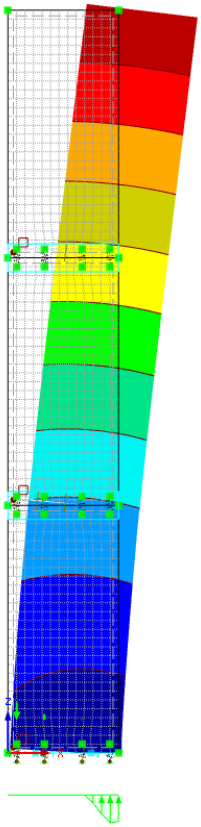

Finite-element modelling of 3D timber structures

Efficient pre- and postprocessing modelling strategies for 3D timber shear walls

Master's thesis in Master Program Structural Engineering and Building Technology

FILIP GÖTBORG

Department of Architecture and Civil Engineering
CHALMERS UNIVERSITY OF TECHNOLOGY
Master's thesis ACEX30
Gothenburg, Sweden 2022

Master's thesis ACEX30

Finite-element modelling of 3D timber structures

Efficient pre- and postprocessing modelling strategies for 3D timber shear walls

FILIP GÖTBORG

CHALMERS
UNIVERSITY OF TECHNOLOGY

Department of Architecture and Civil Engineering
Division of Structural Engineering
Lightweight Structures
Chalmers University of Technology
Gothenburg, Sweden 2022

Finite-element modelling of 3D timber structures
Efficient pre- and postprocessing modelling strategies for 3D timber shear walls

FILIP GÖTBORG

Supervisor: Dr. Laurent Giampellegrini, Associate Director knippershelbig GmbH.
Examiner: Assist. Professor Robert Jockwer, Department of Architecture and Civil Engineering.

Department of Architecture and Civil Engineering
Division of Structural Engineering
Lightweight Structures
Chalmers University of Technology
SE-412 96 Gothenburg
Telephone +46 31 772 1000

Cover: Global displacement of a three storey cross-laminated timber shear wall subjected to a unit load in horizontal and vertical direction at each floor level. Modelled in FE-software Dlubal RFEM using the proposed modelling strategy developed within this thesis.

Department of Architecture and Civil Engineering
Gothenburg, Sweden 2022

Finite-element modelling of 3D timber structures
Efficient pre- and postprocessing modelling strategies for 3D timber shear walls
FILIP GÖTBORG
Department of Architecture and Civil Engineering
Divison of Structural Engineering
Lightweight Structures
Chalmers University of Technology

Abstract

This thesis investigates, develops and proposes finite-element modelling strategies for timber shear walls constructed as timber frame walls and cross-laminated timber walls. The thesis recommends various techniques to reach reliable results and at the same time reduce the modelling efforts. Studies are made on the effects of scaling the structure to multiple floors as well as the influence of the length of the individual wall elements. Discussions are made on the behaviour of the different modes of deformation and it is found that there is a significant potential to reduce the calculated deformation of timber shear walls by taking into account the friction to the foundation or floor as well as considering the weak axis strength of shear and tension connectors. Further a discussion is held concerning modelling strategies suitable for linear dynamic analysis and recommendations are made to take precautions of how the non-linearities in the model are linearized in the analysis.

Keywords: Timber structure, Shear wall, Finite-element method, Modelling strategy, Stiffness assessment.

Acknowledgements

I have written this thesis with support from my friends and colleagues at knippershelbig GmbH in Stuttgart. A special thanks goes out to my supervisor Laurent Giampellegrini who initiated the idea of the thesis topic and together with Guillaume Caussarieu has given great support and guidance throughout the writing process. Thanks also to my examiner Robert Jockwer for good discussions and advice. Last but not least a big thanks to my opponents Mattias Udén & Kalle Thorsager for constructive criticism and invaluable support.

Filip Götborg, Stuttgart, June 2022

Contents

List of Figures

1

Introduction

In view of the increasing use of timber in construction and the trend to build taller buildings with this natural material, the need for reliable and robust 3D numerical models becomes an unavoidable necessity to the structural engineer. At present, little guidance is available on the subject and traditional, code-based methods, that for instance rely upon direct proportionality of the length and stiffness of timber walls are not suitable for modern high-rise timber construction, in particular for hybrid timber-concrete structures.

The stiffness of timber walls, whether cross-laminated timber (CLT) or timber frame, depends significantly on its connections to the floors and the linear shear-connection in-between individual panels. However, a detailed modelling of all the connectors in a 3D-model (see Figure 1.1) quickly becomes cumbersome and unmanageable in large scale 3D-models.

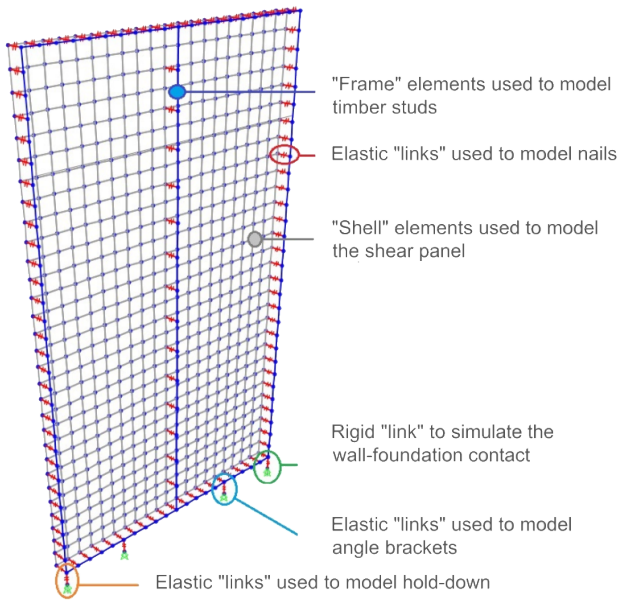

Figure 1.1: Example of an intricate modelling technique for a timber frame wall in a finite-element software.

Therefore, the following thesis proposes a pragmatic approach to modelling timber shear walls, both for cross-laminated timber as well as timber frame walls, for use

in large scale 3D finite-element models. The modelling approach should thereto consider all aspects to allow for efficient post-processing. For example, how to isolate the elements at shear joints to easily read out the shear flow directly from the 3D-model.

1.1 Aims

The aim of the thesis is to propose general FE-modelling strategies for timber shear walls constructed as timber frame and cross-laminated timber walls. The main focus is to achieve a correct wall stiffness, along with a scaleability to global models with systems of shear walls. The proposed strategy should at the same time capture the behaviour of all the applicable modes of deformation for the type of construction. A central topic will be to balance the level of model simplifications in proportion to the exactness of the results and the post-processing possibilities. Where the global behaviour of the shear wall and the possibility to view results at wall boundaries, across surfaces or at certain connection points might be in conflict due to the FE-modelling strategy.

The aim is also that the provided modelling strategy can be modified for use in modal analysis of the timber structure. The main issue here being the linearity of the model since, for example, non-linear springs would get linearized in a linear dynamic analysis. Which in turn leads to an incorrect stiffness of the structure. Essentially the modelling strategy could have two alterations for a non-linear and a linear model with a clear conversion procedure.

1.2 Limitations

The focus of the thesis is to provide a pragmatic general FE-modelling strategy for timber frame shear walls and cross laminated timber shear walls such as applicable for use in high rise timber construction. The subject of tall timber buildings and its applicable FE-modelling techniques is however far broader with influences from several building parts and their behaviour under different loading. Limitations are therefore adapted on both structural and material level.

The stiffness definitions of layered and orthotropic materials will be investigated and various reduction factors discussed. Different cross-section build-ups of cross-laminated timber will also be briefly mentioned but the stiffness assessment methods will be concentrated to symmetric build-ups with 90° alternating board layers. Likewise, the influence of the shear wall length will be discussed but the studied test structures will have a fixed wall height.

Although the scaleability of shear walls are studied the investigation is limited to stacked walls and walls in series in 2D and 3D. The rigidity of floor/roof systems and their influence on the force distribution on the shear walls are not included in the report. The studied structures presented in section 1.3.1 are chosen to cover

the general behaviour of timber shear walls as stand alone walls, walls in series and stacked walls. Walls with openings such as windows and doors will not be investigated. This is partly to concentrate the scope but also due to the common method to consider that wall partitions with openings does not contribute to the stiffness of the structure. There are also several different types of shear wall connection systems on the market and within the report only a selection of connectors commonly used in modern practice are discussed.

1.3 Method

As a first step in the workflow a literature study will be conducted with three main topics to be investigated.

- The construction principles and types of connections used for shear walls constructed both as timber frame and cross-laminated timber walls.
- The stiffness definition of cross-laminated timber in a finite-element software.
- Finite-element modelling approaches for shear walls in general and for timber shear walls and their connections in particular.

Along with the literature study of the state-of-the-art a software study will also be performed on the methods currently used by different commercially available finite-element softwares. With the knowledge base from the literature and software study optimized modelling strategies will then be developed. The proposed strategies will be evaluated for criteria concerning the included modes of deformation, the level of pre-processing needed, the scaleability to global building models, the post-processing possibilities and if they are general enough to not rely on the performance of specific FE-softwares. As a guidance in the evaluation the following three questions are established to ensure that the produced models actually provides the results needed.

- Which results are needed from the model?
- To calculate and present these results which demands are set on the FE-model regarding geometry, element types, stiffness, meshing and boundary conditions?
- How are these modelling demands met in an arbitrary FE-environment?

Within the thesis all proposed modelling strategies will be developed decoupled from a specific FE-environment. The strategies should be such that independently of which FE-software that is used the strategy is feasible and produces equal results. Within the investigative work however the FE-softwares SOFiSTiK, with Rhinoceros and Grasshopper as pre-processor, and Dlubal RFEM with the RF-LAMINATE add-on is used to test and evaluate methods, Sofistik (2020), Dlubal Software GmbH (2016). It is kept in mind that possible limitations of the software might have an effect on the direction of work. If situations like this occur, considerations will be made on using additional testing and proofing software.

1.3.1 Reference structure

The reference structure is a 3-storey residential timber building. The construction is in cross-laminated timber with floors spanning the width of each apartment unit. The floors attach rigidly to the walls and acts as a diaphragm transferring the loads from wind or seismic events to the shear walls and ultimately the ground. The shear walls provide the primary lateral bracing system for the building. The vertical load transfer occurs through the cross-laminated timber walls and perimeter glue-laminated beams. While the load path through the inner walls is direct, the staggered arrangement of the walls on the perimeter gives rise to cantilever constructions. Stability of these cantilevers is achieved through the story high cross-laminated timber walls that are supported off-center but connected rigidly to the floor slabs above and below. They are stabilized by a horizontal force pair in the floor slabs which act like horizontal beams tied back to the inner shear walls. The foundation of the building is concieved as a shallow foundation in conventional manner.

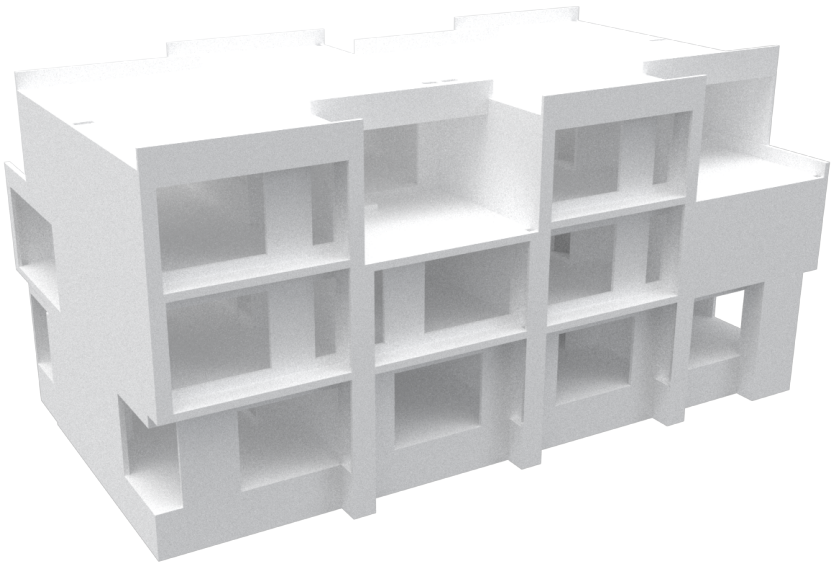

Figure 1.2: Reference structure.

The global building model will be analysed in the structural design software TimberTech (2013). A software specifically developed for analysis of timber structures in cross-laminated timber and timber frame construction. The calculation method implemented in the software, developed at the university of Trento, will further be referred to as method A and is explained in-depth in section 4.1. A selection of shear walls and their respective loads are then extracted from the global model to provide a clear basis for comparison between different modelling strategies. The structures has been chosen to highlight the behaviour of different modes of deformation and they will also function as a step wise increase of complexity in the shear wall model. These test structures are then analysed using 4 different stiffness assessment methods (methods B-D) described in chapter 4.

2

Shear wall construction

2.1 Timber frame construction

A standard timber frame shear wall is constructed of a wood frame with studs and a top and bottom member. The frame is then covered on one or both sides by a sheating-panel that is nailed or stapled to the wooden frame, see figure 2.1.

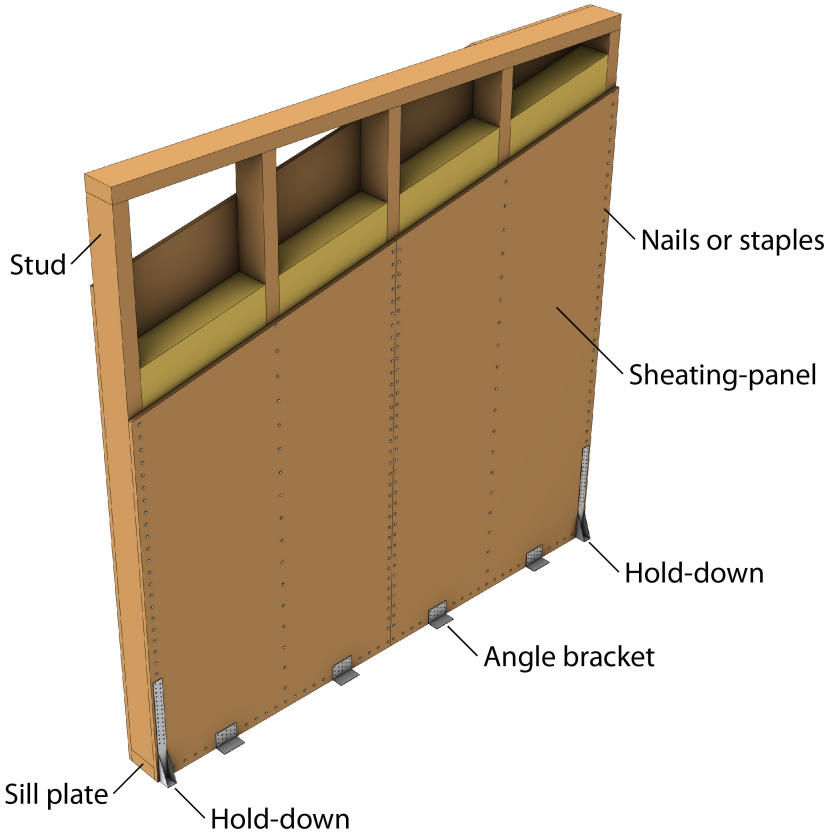

Figure 2.1: Typical timber frame shear wall construction.

2.2 Timber frame modes of deformation

The main modes of deformation of timber frame shear walls that are commonly considered in today's practice are presented in figure 2.2, Casagrande et al. (2015), Hummel et al. (2016).

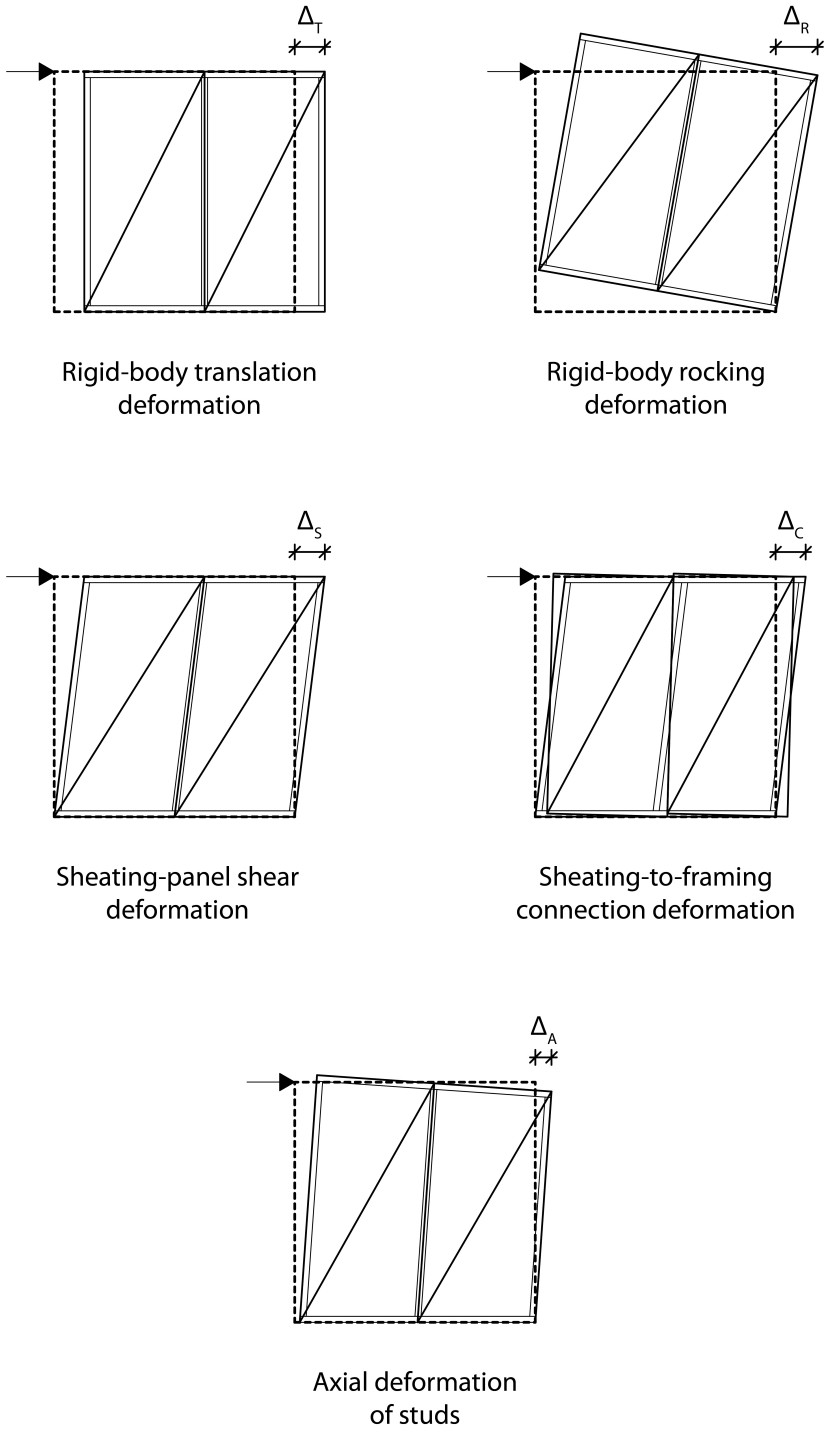

Figure 2.2: Modes of deformation for a timber frame shear wall.

The rocking deformation of the timber frame wall is in figure 2.2 referenced as rigid-body rocking. In comparison to the cross-laminated timber wall however a timber frame wall has much more ductility to account for. This means that the assumption that the timber frame wall will rotate as a rigid-body is further away from reality than it is for a generally more stiff cross-laminated timber wall, Hummel et al. (2016). Method A and B further explained in sections 4.1 and 4.2 views this in separate ways where method A assumes a rigid-body rotation in the same way as for a cross-laminated timber wall and method B calculates the horizontal deformation as a combination of compression perpendicular to grain in the sill plate caused by the vertical wall studs and elongation of the tension anchor, see figure 2.3. How this behaviour is modelled in an FE-software is discussed in chapter 5.

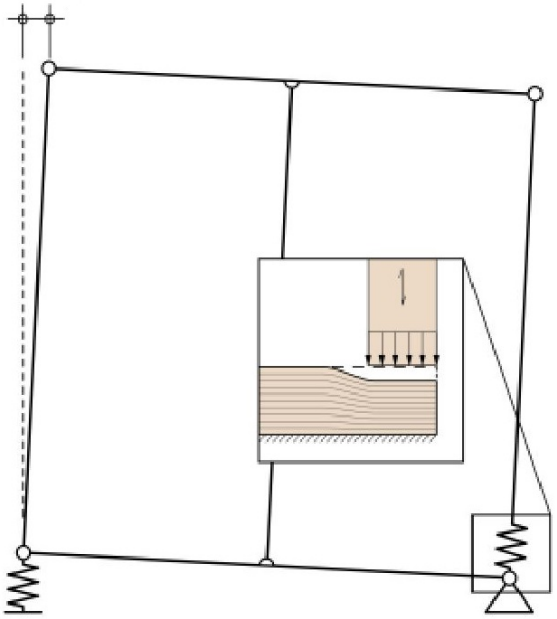

Figure 2.3: Compression perpendicular to grain in contact zone between stud and sill plate and slip of the tensile anchoring, Hummel et al. (2016).

2.3 Cross-laminated timber construction

Cross-laminated timber is a layered timber material with board layers glued together in alternating directions. As can be seen in Figure 2.4 both the number of layers and the angle of rotation between the layers can vary. Most common is however a 90° rotation angle and an odd number of layers in the range between 3 and 7 for the build-up. This is to make the fibres of the outer board layers align and thus provide a symmetric cross-section. The strength grade and thickness of the individual layers can also be different allowing for case specific optimizations. Cross-laminating the boards brings the benefits of a more orthotropic behaviour of the timber panel increasing both the in-plane and out-of-plane stiffness. The panel becomes more suitable for two-way action and the risk for splitting failure at connections is reduced, Popovski et al. (2019).

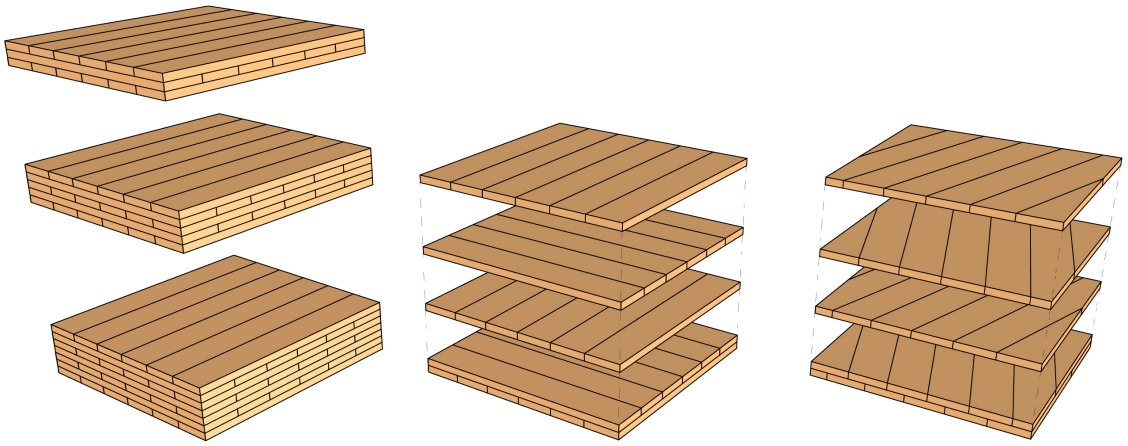

Figure 2.4: Cross-laminated timber build-ups with varying amounts of layers and different rotation angles.

Shear wall construction in cross-laminated timber is fairly straight forward as the wall panel is simply placed with it's main grain direction in vertical direction and is then connected to the ground and potentially neighbouring shear walls, see figure 2.5. The types of connectors used are further discussed in chapter 3.

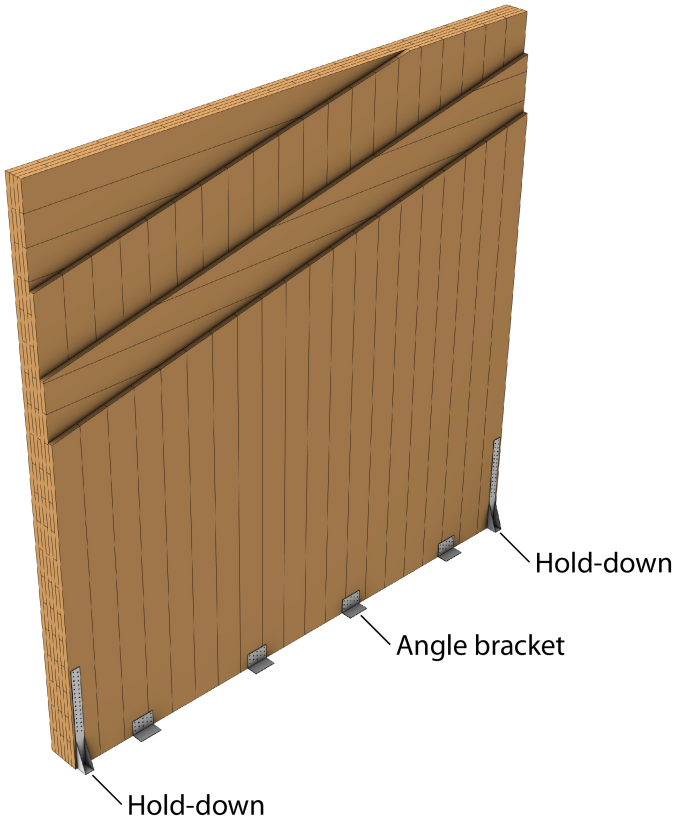

Figure 2.5: Typical cross-laminated timber shear wall construction.

2.4 Cross-laminated timber modes of deformation

A cross-laminated timber shear wall has four different modes of deformation that are commonly considered in modern practice, see figure 2.6. The most simplified assessment methods consider that the wall remains rigid through out the whole deformation and that all deformations comes from rigid-body translation and rigid-body rocking. The next commonly added contribution is the shear deformation. However, the need to include the bending deformation of the cross-laminated timber wall is debated due to it's relatively small magnitude, Gavric et al. (2015). The total top (or head) deflection is the sum of these contributions. It can be noted that the translation and rocking deformations depend on the characteristics and positions of the connectors as well as the friction and applied vertical force. While the shear and bending deformation besides the loading only depend on the characteristics of the cross-laminated timber element itself, Flatscher (2017).

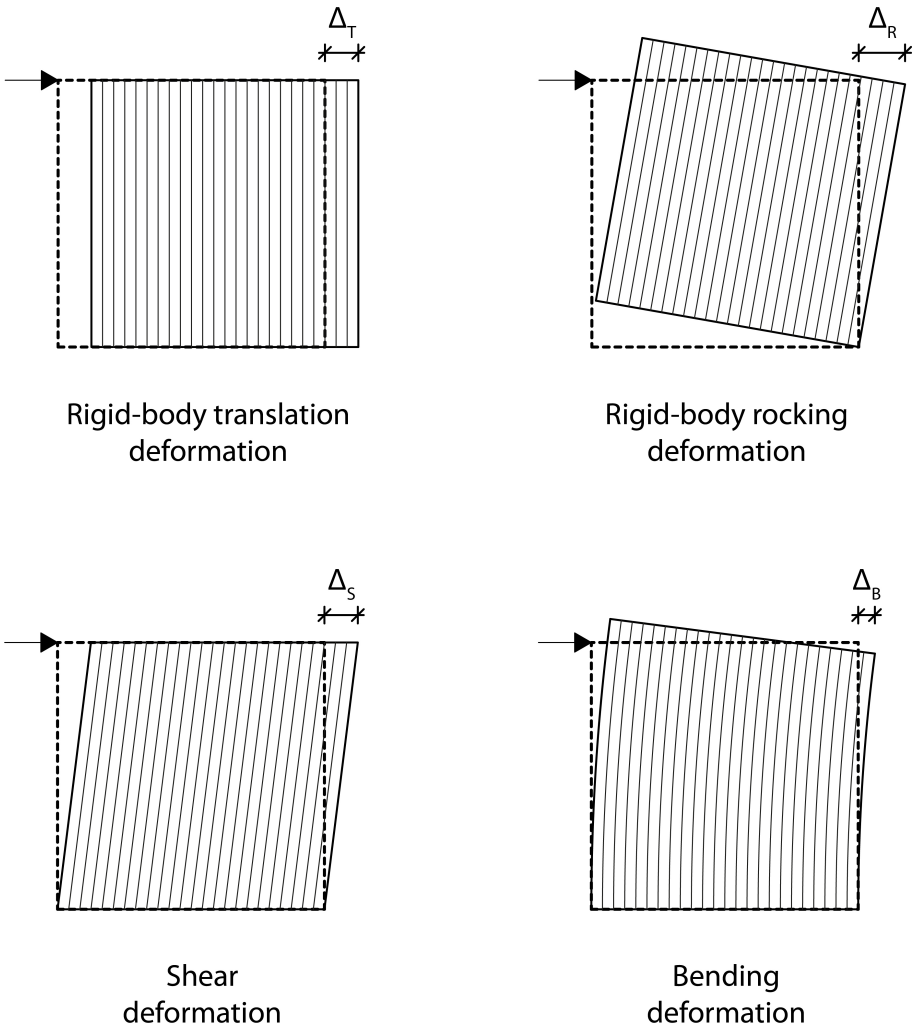

Figure 2.6: Modes of deformation for a cross-laminated timber shear wall.

2.5 Cross-laminated timber stiffness definition

To model the material of a cross-laminated timber wall in a finite-element software different methods can be used. Two common approaches for the material definition is to either create one orthotropic material representing the properties of the entire thickness of the element, the so called transformed section method. Or to define the material properties individually for each layer of the built-up section and then calculate the global stiffness. The two methods are similar in the sense that they both result in a single stiffness matrix for the cross-laminated timber panel. However, they differ a bit in their calculation methods and the second method is sometimes presented as a software package that allow for multi-layer/composite elements, Fragiacomo (2013). Although both methods essentially are capable of handling the same typology of structures. In the following two sections the two methods are described.

2.5.1 Transformed section method

As laid out by Aondio et al. (2020) the stiffness of an arbitrary linear elastic orthotropic volume can be described by three elasticity-moduli, three shear-moduli and six poisson ratios. For a cross-laminated timber element however, the needed information can be reduced to two elasticity-moduli and three shear-moduli. The out of plane young's modulus is neglected and the poisson ratios are set to zero. As is visualized in Figure 2.7 the shear-moduli G_{xy}, G_{yx} and G_{xz} and the young's moduli E_{xx} and E_{yy} are the only stiffness components needed to be defined. The main grain direction of the cross-laminated timber element is governed by the direction of the outer board layers and will in this section be set to the x-direction.

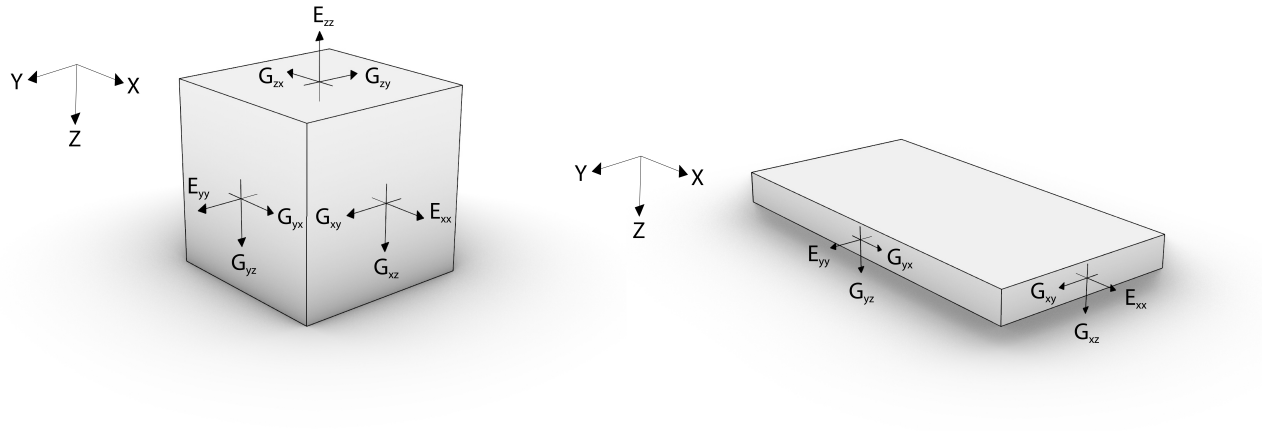

Figure 2.7: Stiffness components of an arbitrary volume (left) and the components considered for a cross-laminated timber surface element (right).

When modelling an orthotropic cross-laminated timber material Mindlin plate theory is often preferred as it takes into account the out-of-plane shear deformations. To form a stiffness matrix for an equivalent orthotropic Mindlin shell element the following input of equivalent bending and shear stiffnesses is required, E_{xx}, E_{yy}, G_{xy}, G_{yz}, and G_{xz} as well as the Poisson ratios ν_{xy} and ν_{yx}. In equation 2.1 we can see the different parts of the stiffness matrix. Red representing the flexural stiffness (bending and torsion), green the shear stiffness, blue the membrane stiffness and yellow the eccentricity. For strain and curvature definitions see figure 2.8.

$$\begin{Bmatrix} m_x \\ m_y \\ m_{xy} \\ v_x \\ v_y \\ n_x \\ n_y \\ n_{xy} \end{Bmatrix} = \begin{bmatrix} D_{11} & D_{12} & D_{13} & 0 & 0 & D_{16} & D_{17} & D_{18} \\ & D_{22} & D_{23} & 0 & 0 & & D_{27} & D_{28} \\ sym. & & D_{33} & 0 & 0 & sym. & & D_{38} \\ & & & D_{44} & D_{45} & 0 & 0 & 0 \\ & & & sym. & D_{55} & 0 & 0 & 0 \\ & & & & & D_{66} & D_{67} & D_{68} \\ & & & & & & D_{77} & D_{78} \\ & & sym. & & & sym. & & D_{88} \end{bmatrix} * \begin{Bmatrix} k_x \\ k_y \\ k_{xy} \\ \gamma_{xz} \\ \gamma_{yz} \\ \epsilon_x \\ \epsilon_y \\ \gamma_{xy} \end{Bmatrix} \tag{2.1}$$

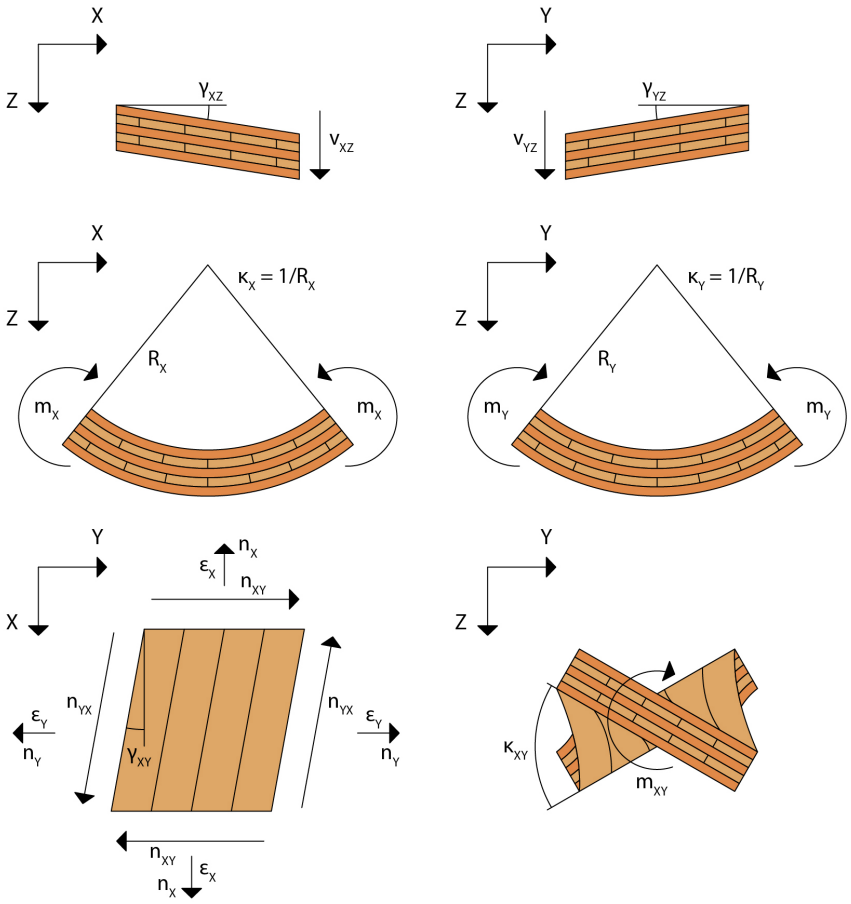

Figure 2.8: Strain and curvature definitions based on moments, shear and normal forces.

When the cross-laminated build up is symmetric and with 90° rotation angle between the board layers many of the elements can be set to zero, see equation 2.2. The remaining elements are calculated according to equations 2.3 - 2.12, Dlubal Software GmbH. (2016).

$$\begin{Bmatrix} m_x \\ m_y \\ m_{xy} \\ v_x \\ v_y \\ n_x \\ n_y \\ n_{xy} \end{Bmatrix} = \begin{bmatrix} D_{11} & D_{12} & 0 & 0 & 0 & 0 & 0 & 0 \\ & D_{22} & 0 & 0 & 0 & 0 & 0 & 0 \\ & & D_{33} & 0 & 0 & 0 & 0 & 0 \\ & & & D_{44} & 0 & 0 & 0 & 0 \\ & & & & D_{55} & 0 & 0 & 0 \\ & & & & & D_{66} & D_{67} & 0 \\ & & & & & & D_{77} & 0 \\ sym. & & & & & & & D_{88} \end{bmatrix} * \begin{pmatrix} \kappa_x \\ \kappa_y \\ \kappa_{xy} \\ \gamma_{xz} \\ \gamma_{yz} \\ \epsilon_x \\ \epsilon_y \\ \gamma_{xy} \end{pmatrix} \tag{2.2}$$

$$D_{11} = E_{xx} \frac{t^3}{12\left(1 - \nu_{xy}\nu_{yx}\right)} \tag{2.3}$$

$$D_{22} = E_{yy} \frac{t^3}{12\left(1 - \nu_{xy}\nu_{yx}\right)} \tag{2.4}$$

$$D_{12} = sgn\left(\nu_{xy}\right) \sqrt{\nu_{xy}\nu_{yx} D_{11} D_{22}} \tag{2.5}$$

$$D_{33} = G_{xy} \frac{t^3}{12} \tag{2.6}$$

$$D_{44} = G_{xz} \frac{5t}{6} \tag{2.7}$$

$$D_{55} = G_{yz} \frac{5t}{6} \tag{2.8}$$

$$D_{66} = E_{xx} \frac{t}{1 - \nu_{xy}\nu_{yx}} \tag{2.9}$$

$$D_{77} = E_{yy} \frac{t}{1 - \nu_{xy}\nu_{yx}} \tag{2.10}$$

$$D_{67} = sgn\left(\nu_{xy}\right) \sqrt{\nu_{xy}\nu_{yx} D_{66} D_{77}} \tag{2.11}$$

$$D_{88} = G_{xy} t \tag{2.12}$$

Further, if the Poisson ratios ν_{xy} and ν_{yx} are also set to zero as suggested by Aondio et al. (2020) the stiffness matrix can be simplified to equation 2.13 and the individual elements accordingly follows equations 2.14 - 2.21. This procedure is applicable since for wood materials the expansion/contraction influence of the Poisson ratio is

small in comparison to the rest of the deformation and the simplification of equations is prioritized.

$$\begin{Bmatrix} m_x \\ m_y \\ m_{xy} \\ v_x \\ v_y \\ n_x \\ n_y \\ n_{xy} \end{Bmatrix} = \begin{bmatrix} D_{11} & 0 & 0 & 0 & 0 & 0 & 0 & 0 \\ & D_{22} & 0 & 0 & 0 & 0 & 0 & 0 \\ & & D_{33} & 0 & 0 & 0 & 0 & 0 \\ & & & D_{44} & 0 & 0 & 0 & 0 \\ & & & & D_{55} & 0 & 0 & 0 \\ & & & & & D_{66} & 0 & 0 \\ & & & & & & D_{77} & 0 \\ sym. & & & & & & & D_{88} \end{bmatrix} * \begin{pmatrix} \kappa_x \\ \kappa_y \\ \kappa_{xy} \\ \gamma_{xz} \\ \gamma_{yz} \\ \epsilon_x \\ \epsilon_y \\ \gamma_{xy} \end{pmatrix} \tag{2.13}$$

$$D_{11} = E_{xx}\frac{t^3}{12} \tag{2.14}$$

$$D_{22} = E_{yy}\frac{t^3}{12} \tag{2.15}$$

$$D_{33} = G_{xy}\frac{t^3}{12} \tag{2.16}$$

$$D_{44} = G_{xz}\frac{5t}{6} \tag{2.17}$$

$$D_{55} = G_{yz}\frac{5t}{6} \tag{2.18}$$

$$D_{66} = E_{xx}t \tag{2.19}$$

$$D_{77} = E_{yy}t \tag{2.20}$$

$$D_{88} = G_{xy}t \tag{2.21}$$

Due to the alternating grain directions between the board layers equivalent bending and shear stiffnesses must now be calculated for the cross-laminated timber board as a whole. Aondio et al. (2020) suggest that the bending stiffnesses E_{xx} and E_{yy} can be calculated as the average elasticity of the board layers using the Steiner formula, see equations 2.22 and 2.23.

$$E_{xx} = \sum_{i=1}^{n} E_{xx,i}t_i z_i^2 + \sum_{i=1}^{n} E_{xx,i}\frac{t_i^3}{12} \tag{2.22}$$

$$E_{yy} = \sum_{i=1}^{n} E_{yy,i}t_i z_i^2 + \sum_{i=1}^{n} E_{yy,i}\frac{t_i^3}{12} \tag{2.23}$$

Where:

$E_{xx} = Bending\ stiffness\ in\ x-direction\ [MPa]$
$E_{yy} = Bending\ stiffness\ in\ y-direction\ [MPa]$
$t_i = Thickness\ of\ board\ layer\ [m]$
$z_i = Inner\ lever\ arm\ [m]$
$n = Number\ of\ board\ layers$

Another method is to average the stiffness using the inertia, see equations 2.24 and 2.25. This is a simplification of two methods called the gamma method and the shear analogy method. Popovski et al. (2019) points out that if the short edges of the boards are not glued together the orthogonal layers should be considered with zero stiffness. A fact that may have a relatively large impact on the stiffness magnitude.

In the shear wall situation the cross-laminated timber element is loaded in its plane which would motivate the use of the membrane stiffness for the orthotropic shell element. The difference is that the stiffness is averaged over the cross sectional area instead of the inertia, see equations 2.26 and 2.27, D'Arenzo et al. (2019).

$$E_{xx} = \frac{\sum_{i=1,3,...}^{n} E_0 I_i + \sum_{j=2,4,...}^{n-1} E_{90} I_j}{I_{tot}} \tag{2.24}$$

$$E_{yy} = \frac{\sum_{i=1,3,...}^{n} E_{90} I_i + \sum_{j=2,4,...}^{n-1} E_0 I_j}{I_{tot}} \tag{2.25}$$

$$E_{xx} = \frac{\sum_{i=1,3,...}^{n} E_0 A_i + \sum_{j=2,4,...}^{n-1} E_{90} A_j}{A_{tot}} \tag{2.26}$$

$$E_{yy} = \frac{\sum_{i=1,3,...}^{n} E_{90} A_i + \sum_{j=2,4,...}^{n-1} E_0 A_j}{A_{tot}} \tag{2.27}$$

Where:

$E_{xx} = Bending\ stiffness\ in\ x-direction\ [MPa]$
$E_{yy} = Bending\ stiffness\ in\ y-direction\ [MPa]$
$E_0 = Young's\ modulus\ in\ grain\ direction\ [MPa]$
$E_{90} = Young's\ modulus\ orthogonal\ to\ grain\ direction\ [MPa]$
$I = Moment\ of\ inertia\ of\ board\ layer\ [m^4]$
$A = Area\ of\ board\ layer\ [m^2]$
$i = Board\ layers\ in\ x-direction$
$j = Board\ layers\ in\ y-direction$
$n = Number\ of\ board\ layers$

For the equivalent shear stiffnesses there are different methods for the in-plane shear stiffness G_{xy} and the out-of plane shear stiffnesses G_{yz} and G_{xz}. Aondio et al. (2020) suggest that the in-plane shear stiffness element D_{33} is to be averaged over the board layers with equation 2.28.

$$D_{33} = \sum_{i=1}^{n} 2 * G_{xy,i} t_i z_i^2 + \sum_{i=1}^{n} G_{xy,i} \frac{t_i^3}{6} \tag{2.28}$$

Where:

$G_{xy,i} = In - plane\ shear\ stiffness\ of\ board\ layer\ [MPa]$
$t_i = Thickness\ of\ board\ layer\ [m]$
$z_i = Inner\ lever\ arm\ [m]$
$n = Number\ of\ board\ layers$

Two reduction factors are generally applied to the in-plane shear stiffness to account for imperfections such as splits and slits in the boards and whether the short edges of the boards are glued or not. First the torsional bending reduction factor k_{33} which is applied to D_{33}. It is defined by Gustafsson et al. (2019) according to equation 2.30 and by Aondio et al. (2020) according to equation 2.31. There is no consensus on which consideration that is to be used but the factors should not be combined. If torsional bending stiffness is considered important for the system at hand further investigation should be conducted.

$$D_{33} = G_{xy} \frac{t^3}{12} * k_{33} \tag{2.29}$$

$$k_{33} = \begin{cases} 0.65 & with\ splits\ or\ slits \\ 0.8 & without\ splits\ or\ slits \end{cases} \tag{2.30}$$

$$k_{33} = \begin{cases} 1 & with\ glued\ edges \\ 0 & without\ glued\ edges \end{cases} \tag{2.31}$$

Secondly, the membrane shear reduction factor k_{88} is applied to D_{88} and similarly the definition is debated. Gustafsson et al. (2019) defines it as a fixed value according to equation 2.33 while Aondio et al. (2020) relates it to the glued short edges according to equation 2.34.

$$D_{88} = G_{xy} t * k_{88} \tag{2.32}$$

$$k_{88} = 0.75 \tag{2.33}$$

$$k_{88} = \begin{cases} 1 & with\ glued\ edges \\ 0.25 & without\ glued\ edges \end{cases} \tag{2.34}$$

To determine the out-of-plane shear stiffnesses G_{yz} and G_{xz} the shear coupling between the different board layers has to be considered. Gustafsson et al. (2019) proposes a laminate shear correction factor κ, see equations 2.35 - 2.38. If G_{90} is not provided for the material at hand a good estimation is $(1/10) * G_0$, Gustafsson et al. (2019).

$$\kappa_x = \frac{\left(\sum\left(E_i I_i + E_i A_i z_i^2\right)\right)^2}{\sum G_i l t_i * \int_t \frac{S_i^2 E_i^2}{G_i l} dz} \tag{2.35}$$

$$\kappa_y = \frac{\left(\sum\left(E_i I_i + E_i A_i z_i^2\right)\right)^2}{\sum G_i h t_i * \int_t \frac{S_i^2 E_i^2}{G_i h} dz} \tag{2.36}$$

$$G_{xz} = \kappa_x * \frac{\sum_{i=1,3,\ldots}^{n} G_{90} t_i + \sum_{j=2,4,\ldots}^{n-1} G_0 t_j}{t_{tot}} \tag{2.37}$$

$$G_{yz} = \kappa_y * \frac{\sum_{i=1,3,\ldots}^{n} G_0 t_i + \sum_{j=2,4,\ldots}^{n-1} G_{90} t_j}{t_{tot}} \tag{2.38}$$

Where:

$\kappa_x = Shear\ reduction\ factor\ in\ major\ direction$
$\kappa_y = Shear\ reduction\ factor\ in\ minor\ direction$
$E_i = Young's\ modulus\ of\ layer\ [MPa]$
$I_i = Moment\ of\ inertia\ of\ layer\ [m^4]$
$A_i = Area\ of\ layer\ [m^2]$
$z_i = Inner\ lever\ arm\ of\ layer\ [m]$
$G_i = Shear\ modulus\ of\ layer\ [MPa]$
$l = Length\ of\ wall\ [m]$
$h = Height\ of\ wall\ [m]$
$t = Thickness\ of\ wall\ [m]$
$t_i = Thickness\ of\ layer\ [m]$
$S_i = Static\ moment\ of\ layer\ [m^3]$
$G_{xz} = Out-of-plane\ shear\ stiffness\ in\ major\ direction\ [MPa]$
$G_{yz} = Out-of-plane\ shear\ stiffness\ in\ minor\ direction\ [MPa]$
$G_0 = Shear\ modulus\ of\ layer\ in\ grain\ direction\ [MPa]$
$G_{90} = Shear\ modulus\ of\ layer\ orthogonal\ to\ grain\ direction\ [MPa]$
$n = Number\ of\ board\ layers$

2.5.2 Multi-layer/composite element

To describe a layered material modelling technique the method used by the commercial software *Dlubal RFEM* is here explained. Dlubal Software GmbH. (2016) provides the add-on *RF-LAMINATE*. A tool for modelling of multi-layer/composite elements where each layer has different mechanical properties. The program supports non-symmetric cross-sections and with the use of transformations the applied method can be used for arbitrary rotation angles between the board layers. One can also choose whether shear coupling should be considered or not. In this section the calculation method for a symmetric build-up with 90° rotation angle and considered shear coupling will be presented.

The software considers a plate of n layers of a generally orthotropic material, see figure 2.9. With the elastic and shear modulus of each layer, individual stiffness matrices is then formed according to equation 2.39 using Kirchhoff plate theory, Dlubal Software Gmbh. (2016).

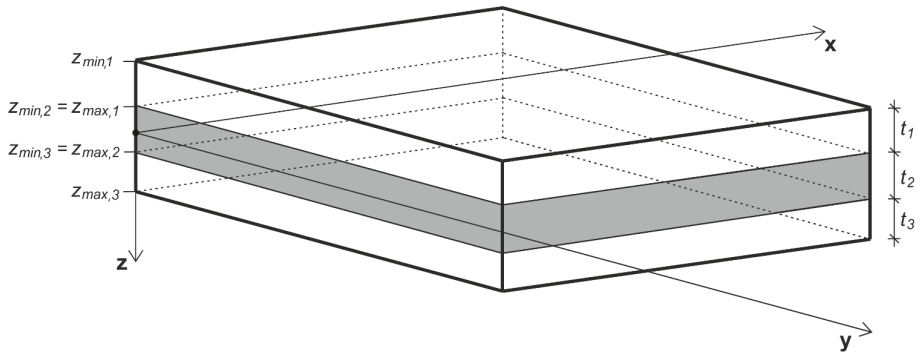

Figure 2.9: Layered plate geometry as considered in *RF-LAMINATE*, Dlubal Software GmbH. (2016).

$$d_i = \begin{bmatrix} d_{11,i} & d_{12,i} & 0 \\ & d_{22,i} & 0 \\ sym. & & d_{33,i} \end{bmatrix} = \begin{bmatrix} \frac{E_{xx,i}}{1-\nu_{xy,i}^2 \frac{E_{yy,i}}{E_{xx,i}}} & \frac{\nu_{xy,i} E_{yy,i}}{1-\nu_{xy,i}^2 \frac{E_{yy,i}}{E_{xx,i}}} & 0 \\ & \frac{E_{yy,i}}{1-\nu_{xy,i}^2 \frac{E_{yy,i}}{E_{xx,i}}} & 0 \\ sym. & & G_{xy,i} \end{bmatrix} \quad (2.39)$$

Where:

$E_{xx,i} = Young's\ modulus\ of\ layer\ in\ x-direction\ [MPa]$
$E_{yy,i} = Young's\ modulus\ of\ layer\ in\ y-direction\ [MPa]$
$G_{xy,i} = In-plane\ shear\ modulus\ of\ layer\ [MPa]$
$\nu_{xy,i} = Poisson\ ratio\ of\ layer$

Due to the symmetry of the cross-section the eccentricity elements of the global stiffness matrix is equal to zero, see equation 2.40. The non-zero elements can be calculated accordingly; flexural stiffness using equation 2.41, membrane stiffness using equation 2.42 and shear stiffness using equations 2.43 - 2.48.

$$\begin{Bmatrix} m_x \\ m_y \\ m_{xy} \\ v_x \\ v_y \\ n_x \\ n_y \\ n_{xy} \end{Bmatrix} = \begin{bmatrix} D_{11} & D_{12} & 0 & 0 & 0 & 0 & 0 & 0 \\ & D_{22} & 0 & 0 & 0 & 0 & 0 & 0 \\ & & D_{33} & 0 & 0 & 0 & 0 & 0 \\ & & & D_{44} & 0 & 0 & 0 & 0 \\ & & & & D_{55} & 0 & 0 & 0 \\ & & & & & D_{66} & D_{67} & 0 \\ & & & & & & D_{77} & 0 \\ sym. & & & & & & & D_{88} \end{bmatrix} * \begin{pmatrix} \kappa_x \\ \kappa_y \\ \kappa_{xy} \\ \gamma_{xz} \\ \gamma_{yz} \\ \epsilon_x \\ \epsilon_y \\ \gamma_{xy} \end{pmatrix} \tag{2.40}$$

$$D_j = \sum_{i=1}^{n} \frac{z_{max,i}^3 - z_{min,i}^3}{3} d_{j,i} \qquad j = 11, 12, 22, 33 \tag{2.41}$$

$$D_{j+55} = \sum_{i=1}^{n} t_i d_{j,i} \qquad j = 11, 12, 22, 33 \tag{2.42}$$

$$D_{44} = max\left(D_{44,calc,1}\ ; D_{44,calc,2}\right) \tag{2.43}$$

$$D_{44,calc,1} = \frac{\int_{-t/2}^{t/2} E_{xx}(z) z dz}{\int_{-t/2}^{t/2} E_{xx}(z) dz} \tag{2.44}$$

$$D_{44,calc,2} = \frac{48}{5 * min(l\ ;\ h)^2} * \frac{1}{\frac{1}{\sum_{i=1}^{n} E_{xx,i} \frac{t_i^3}{12}} - \frac{1}{\sum_{i=1}^{n} E_{xx,i} \frac{z_{max,i}^3 - z_{min,i}^3}{3}}} \tag{2.45}$$

$$D_{55} = max\left(D_{55,calc,1}\ ; D_{55,calc,2}\right) \tag{2.46}$$

$$D_{55,calc,1} = \frac{\int_{-t/2}^{t/2} E_{yy}(z) z dz}{\int_{-t/2}^{t/2} E_{yy}(z) dz} \tag{2.47}$$

$$D_{55,calc,2} = \frac{48}{5 * min(l\ ;\ h)^2} * \frac{1}{\frac{1}{\sum_{i=1}^{n} E_{yy,i} \frac{t_i^3}{12}} - \frac{1}{\sum_{i=1}^{n} E_{yy,i} \frac{z_{max,i}^3 - z_{min,i}^3}{3}}} \tag{2.48}$$

Where:

$z_{max,i} = Maximum\ z - coodinate\ of\ layer\ [m]$
$z_{min,i} = Minimum\ z - coodinate\ of\ layer\ [m]$

$z = Inner\ lever\ arm\ [m]$
$t_i = Thickness\ of\ layer\ [m]$
$l = Wall\ length\ [m]$
$h = Wall\ height\ [m]$
$E_{xx,i} = Young's\ modulus\ of\ layer\ in\ x - direction\ [MPa]$
$E_{yy,i} = Young's\ modulus\ of\ layer\ in\ y - direction\ [MPa]$
$n = Number\ of\ board\ layers$

3

Connections

As the cross-laminated timber generally is much more rigid than its anchorage system the global stiffness of a CLT wall is largely dependant on its connections, Gavric (2012). The connection behaviour also becomes increasingly more important when the structure is subjected to high loads such as earthquakes or heavy winds. As they are then not just responsible for load-carrying capacity but are also a source of ductility and load-dissipation, Flatscher (2017). There are many types of connectors and the development of new products is constantly ongoing. Within this report two common wall-to-floor/wall-to-foundation connectors will be discussed; angle brackets and hold-downs. As well as screwed intermediate wall-to-wall connections for parallel walls. In general these connections does not support rotation and can therefore be simplified to 2-degree-of-freedom springs supporting the wall in translation. Further this can either be done with springs at the position of each connector or with so called lumped springs where a smaller amount of springs holds the properties of multiple connectors combined, Fragiacomo (2013).

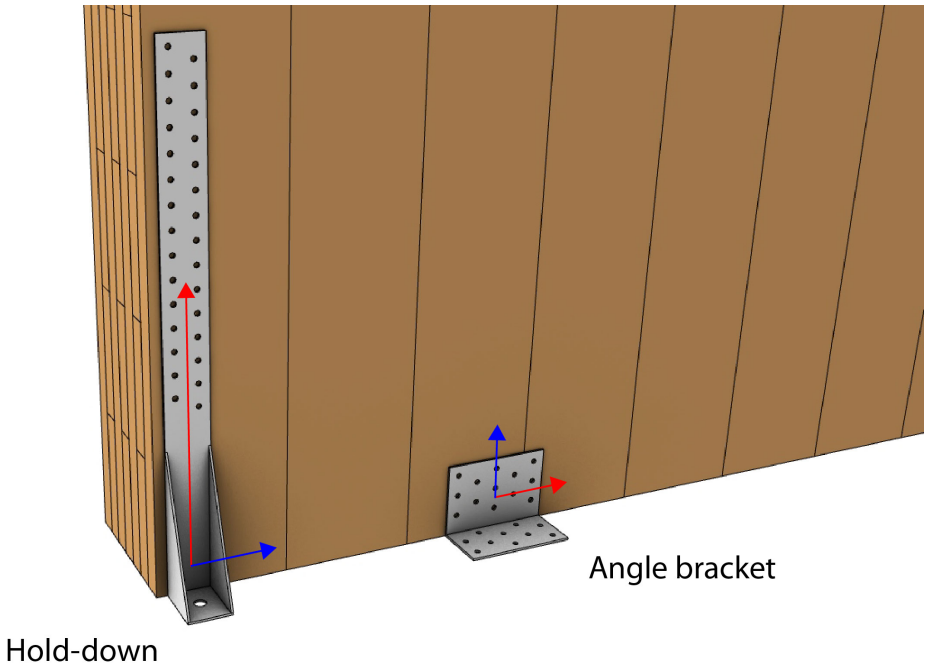

Figure 3.1: Connector types hold-down and angle bracket with their strong axis (red) and weak axis (blue).

Hold-downs are placed at the outermost corners of the shear wall and are primarily designed to act in tension to prevent uplift of the wall. The stiffness of the hold-downs will thus have a large impact on the rocking deformation of the shear wall. The angle brackets are placed along the wall base and are designed to primarily act in shear to prevent sliding of the wall. The translation deformation of the shear wall as whole will consequently have a direct correlation to the stiffness of the angle brackets. Although these connectors are design to carry load in one direction methods D and E takes the weak axis stiffnesses of the hold-downs and angle brackets into consideration to account for the total stiffness capacity. This is also further discussed in chapter 6.

3.1 Horizontal connection

When modelling the wall to foundation connection considerations are needed on where the wall has its center of rotation. An incorrect position could lead to both under- and overestimations of the rigid-body rocking deformation. The neutral axis of the wall can be calculated using the hold down forces. The force distribution in the compression zone can thereafter be considered in different ways. Either with a linear distribution such as proposed by Casagrande et al. (2015) (see figure 4.1) or with the formation of a stress block as in the approaches by Tomasi (2013) (see figure 3.2 and equation 3.1) and Wallner-Novak et al. (2013) (see figure 3.3 and equation 3.2). The stress block methods differ in their assumption of the width of the compression zone as either a function of the neutral axis position or as a fixed fraction of the wall length. When a linear distribution is assumed the wall is considered as a rigid body. The stress block methods however imply that the wall deforms in the compression zone and hence moves the center of rotation. The hold-downs and angle brackets are generally modelled as springs but with a stress block approach the pressure contact condition to the foundation also needs to be taken into account. FE-modelling techniques for this purpose are further discussed in chapter 6.

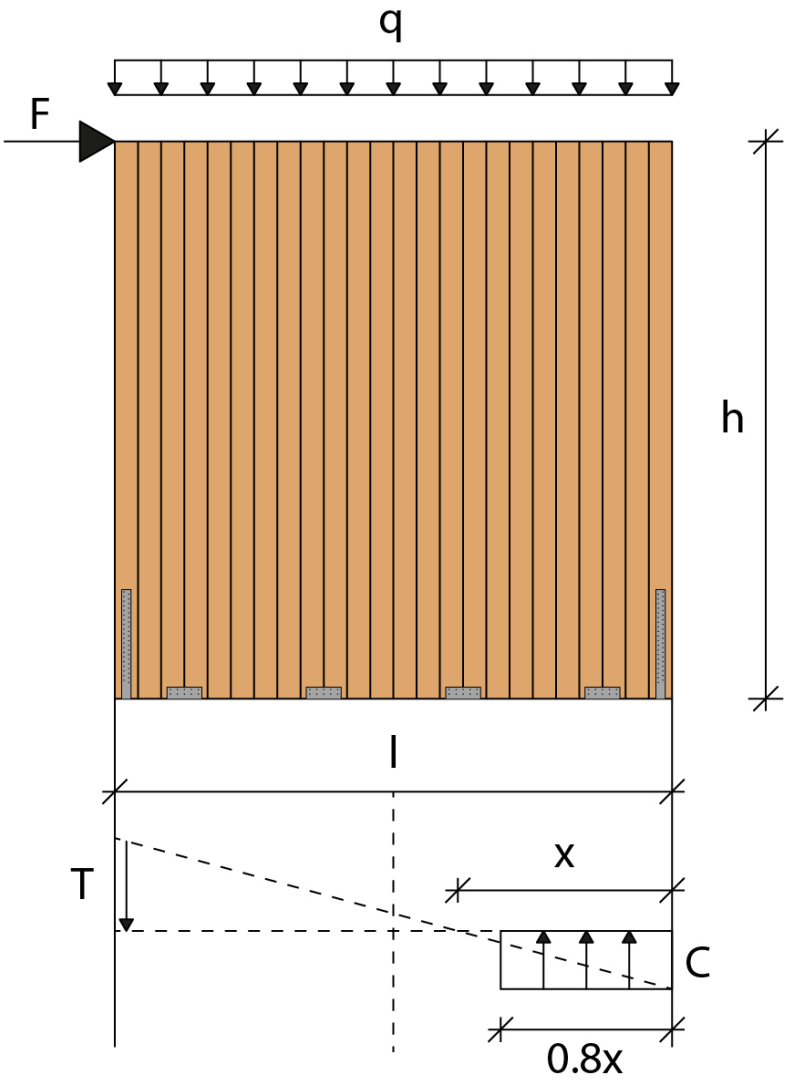

Figure 3.2: Compression zone force distribution by Tomasi (2013).

$$x = \frac{q * l + T}{0.8 * f_{c,k} * t_{ef}} \qquad 0 < x \leq \frac{l}{2} \tag{3.1}$$

Where:

$x = Position\ of\ neutral\ axis\ [m]$
$l = Wall\ length\ [m]$
$q = Evenly\ distributed\ vertical\ force\ [kN/m]$
$T = Tension\ force\ in\ hold - down\ [kN]$
$f_{c,0,k} = Characteristic\ timber\ compression\ strength\ in\ grain\ direction\ [MPa]$
$t_{ef} = Total\ thickness\ of\ vertical\ layers\ [m]$

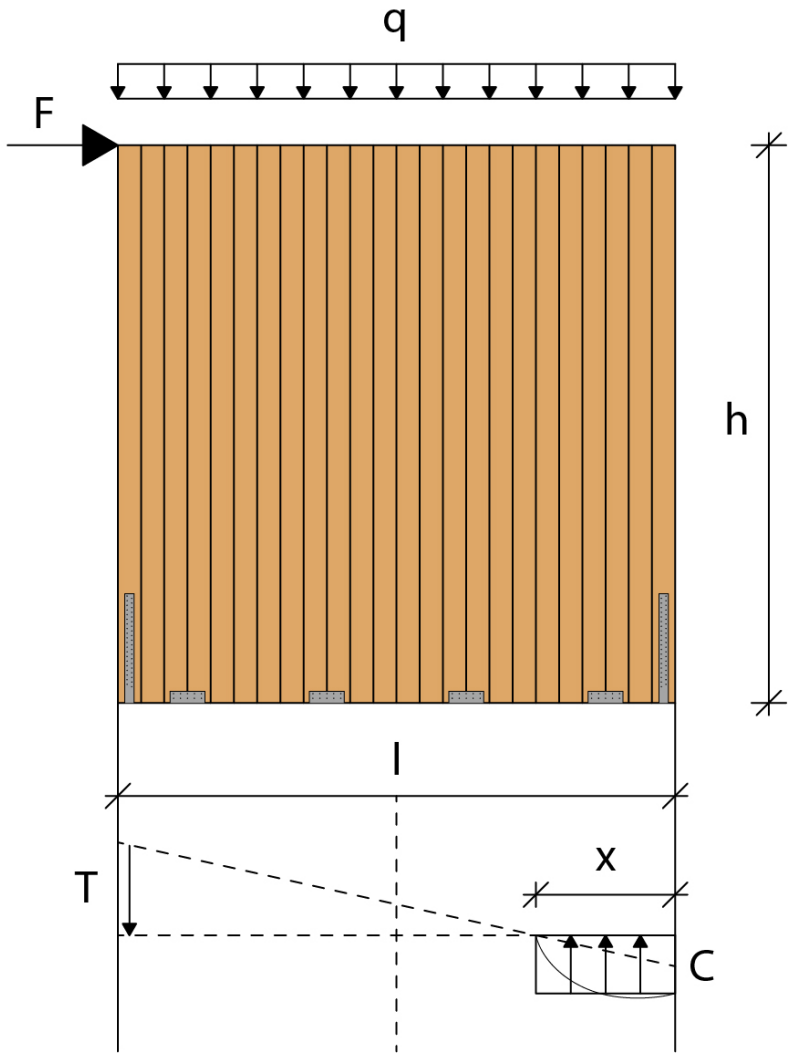

Figure 3.3: Compression zone force distribution by Wallner-Novak et al. (2013).

$$x = \frac{l}{4} \tag{3.2}$$

Where:

$x = Position\ of\ neutral\ axis\ [m]$
$l = Wall\ length\ [m]$

Regardless of the force distribution across the length of the wall Shickhofer et al. (2010) points out that in practical cases a significant part of the shear force may be transmitted via friction to the foundation. This phenomena is further developed by Gavric et al. (2015) in method D and Flatscher (2017) in method E where the friction force is introduced in the equation for rigid-body translation deformation.

3.2 Vertical connection

When placing several shear walls in series the type of parallel wall to wall connection needs to be considered to achieve the correct stiffness of the joint. Understandably the type and amount of fasteners will have a direct impact on the connection stiffness. But internal or surface splines/strips, half-lapped joints or various tube connection systems have different ways to transfer the in-plane shear forces and the out-of-plane bending between the panels. For ease of use in this report only screwed connections representing either a one-sided or a double-sided hinge condition will be considered in the test structures, see figure 3.4. The stiffness of typical timber-to-timber screwed connections can be calculated using empirical formulas such as those presented in Eurocode 5, DIN EN 1995-1-1. For the stiffness assessment of more complex connection systems reference should be made to the specific supplier.

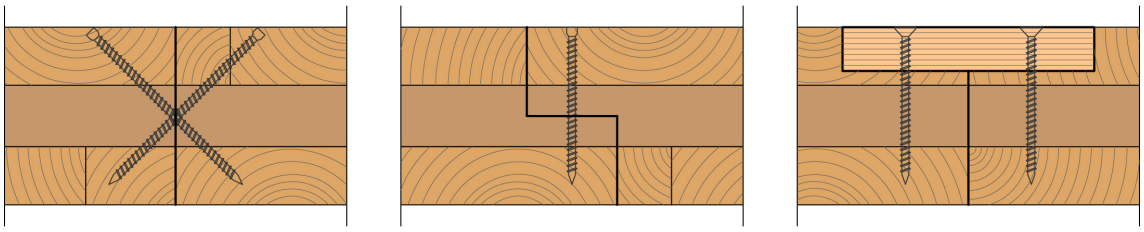

Figure 3.4: Examples of vertical joints. From left; butt joint (one-sided hinge), half-lap joint (one-sided hinge) and one-sided spline joint (double-sided hinge).

4

Stiffness Assessment Methods

The following chapter presents 5 methods to calculate the horizontal deformation of a wall element under vertical and horizontal loading. To then capture all of the considered modes of deformation in the finite-element model each deformation needs to be converted into a stiffness. The deformations can be separated into two categories; connector based deformation and material based deformation. As mentioned in section 2.4 the translation and rocking is independent from the material properties of the wall and are instead solely dependent on the wall geometry, the loads and the connector stiffness. Hence these modes of deformation are connector based. Further the shear and bending deformations are dependent on the geometry, loading and the material characteristics and are therefore material based. In table 4.1 an overview of the included modes of deformation in the stiffness assessment methods is presented.

Table 4.1: Considered modes of deformation in stiffness assessment methods A-E.

	Method				
	A	**B**	**C**	**D**	**E**
Timber frame					
Rigid-body translation	X	X			
Rigid-body rocking	X	X			
Sheating-panel shear deformation	X	X			
Sheating-panel connection deformation	X	X			
Axial deformation of studs		X			
CLT					
Rigid-body translation	X	X	X	X	X
Rigid-body rocking	X	X	X	X	X
Shear deformation	X	X	X	X	X
Bending deformation		X	X	X	X

When it comes to cross-laminated timber the methods have further differences when it comes to how detailed the boundary conditions are considered. In table 4.2 these differences are presented. It should however be noted that these considerations are not included for timber frame walls.

Table 4.2: Differences in consideration of boundary conditions in stiffness assessment methods A-E.

	Method				
	A	**B**	**C**	**D**	**E**
CLT					
Type of foundation		X	X		
Friction				X	X
Weak axis stiffness of connectors				X	X

4.1 Method A - Casagrande et al.

Stiffness assessment method A, also called the UNITN method, has been established at the university of Trento, Italy by Casagrande et al. (2015). The method is aimed to determine the elastic stiffness and horizontal displacement of timber shear-walls under horizontal and vertical load. As seen in figure 4.1 the model assumes a linear elastic and continuous behaviour of the bottom joint.
For timber frame walls the total deformation includes:

- **Rigid-body translation**
- **Rigid-body rocking**
- **Sheating-panel shear deformation**
- **Sheating-to-framing connection deformation**

For cross-laminated timber walls the total deformation includes:

- **Rigid-body translation**
- **Rigid-body rocking**
- **Shear deformation**

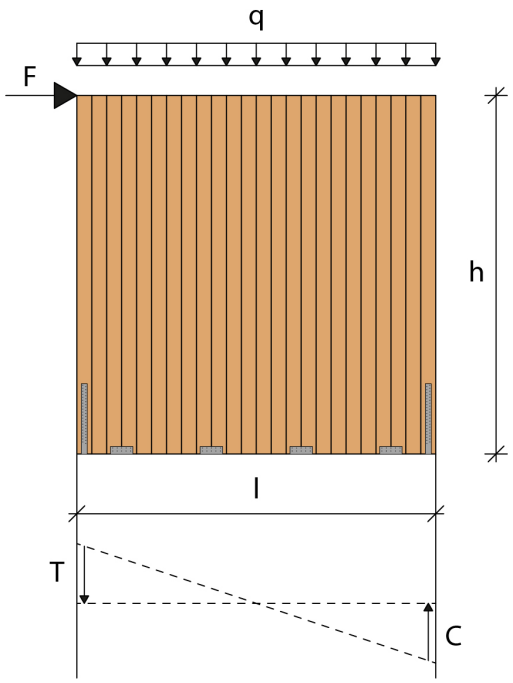

Figure 4.1: Stiffness assessment method A by Casagrande et al. (2015).

4.1.1 Rigid-body translation

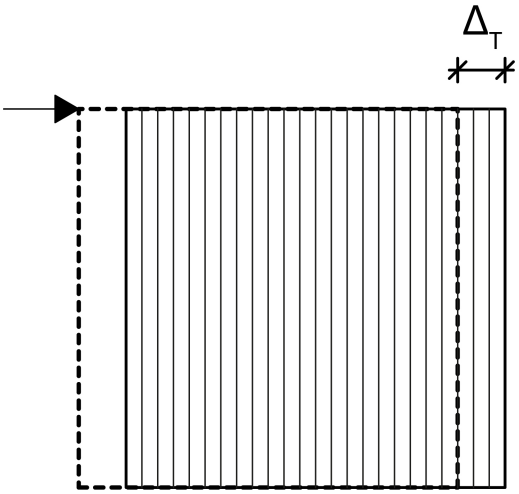

Figure 4.2: Rigid-body translation.

In method A Casagrande et al. (2015) considers the deformation caused by rigid-body translation (Figure 4.2) in the same way for both timber frame walls and cross-laminated timber walls. The deformation is simply governed by the stiffness and position of the angle-brackets or screws used to connect the wall to the foundation. The deformation can be calculated using either equation 4.1 or 4.2. Where 4.1 uses a fixed number of fasteners and 4.2 a fixed spacing between the fasteners.

$$\Delta_T = \frac{F}{k_a * n_a} \tag{4.1}$$

$$\Delta_T = \frac{F * i_a}{k_a * l} \tag{4.2}$$

Where:

$\Delta_T = Rigid - body\ translation\ [m]$
$F = Horizontal\ point\ load\ [kN]$
$k_a = Angle - bracket\ or\ screw\ stiffness\ [kN/m]$
$n_a = Number\ of\ angle - brackets\ or\ screws$
$i_a = Fastener\ spacing\ [m]$
$l = Wall\ length\ [m]$

4.1.2 Rigid-body rocking

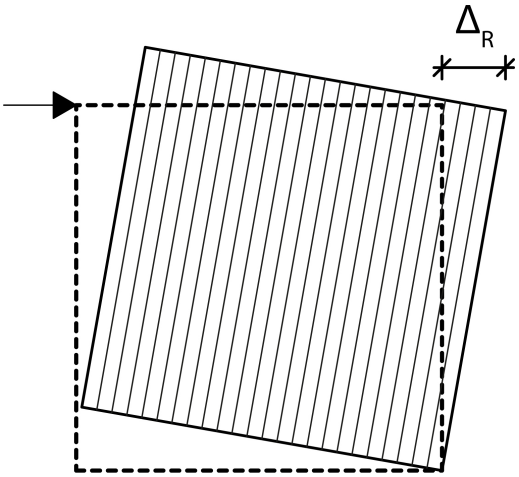

Figure 4.3: Rigid-body rocking.

The rigid-body rocking deformation (Figure 4.3) differs from the other modes due to it's binary behaviour. When a hold-down is in compression the stiffness contribution from this hold-down must not be accounted for in the total wall stiffness. However, when the overturning moment from the horizontal force becomes larger than the stabilizing moment from the vertical force, the hold-down is set in tension. In this state the stiffness contribution should be accounted for in the total wall stiffness. The rigid-body rocking mode could thereby be seen as having two states; inactive (hold-down in compression) and active (hold-down in tension). Within method A the same rocking behaviour is assumed for both timber frame walls and cross-laminated timber walls, Casagrande et al. (2015).

$$F_q = \frac{\tau * q * l^2}{2 * h} \tag{4.3}$$

$$\Delta_R = \begin{cases} 0 & F \leq F_q \\ \frac{h}{\tau * l * k_h} * \left(\frac{F * h}{\tau * l} - \frac{q * l}{2} \right) & F > F_q \end{cases} \tag{4.4}$$

Where:

$\Delta_R = Rigid - body\ rocking\ deformation\ [m]$
$F = Horizontal\ point\ load\ [kN]$
$F_q = Horizontal\ point\ load\ at\ which\ hold - down\ force\ equals\ 0\ [kN]$
$\tau = Multiplier\ for\ internal\ lever\ arm\ between\ hold - downs\ (usually\ 0.95 - 1)$
$l = Wall\ length\ [m]$
$k_h = Hold - down\ stiffness\ [kN/m]$
$q = Evenly\ distributed\ vertical\ load\ [kN/m]$

4.1.3 Sheating-panel shear deformation

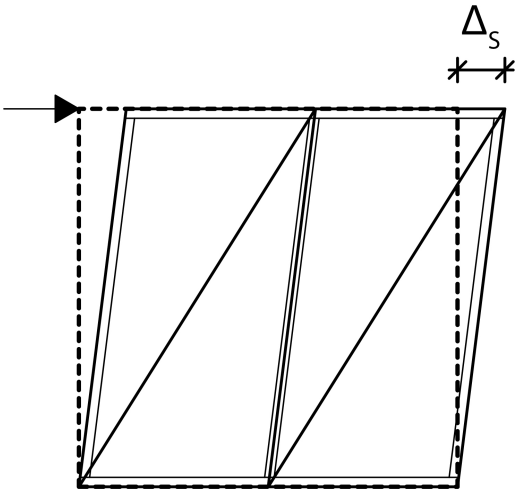

Figure 4.4: Sheating-panel shear deformation.

For timber frame walls the contribution from the shear deformation of the sheating-panel (Figure 4.4) is based on the shear modulus and shear area of the sheating panels and can be calculated according to equation 4.5. The equation also takes into account whether the wall is braced with panels on one or both sides. In the case that panels of the same type, thickness and width is used on both sides of the wall, equation 4.5 can be simplified to equation 4.6, Casagrande et al. (2015).

$$\Delta_S = F * h * \left(\sum_{j=1}^{n_p,side1} \frac{1}{G_{p,j} * t_{p,j} * b_j} + \sum_{j=1}^{n_p,side2} \frac{1}{G_{p,j} * t_{p,j} * b_j} \right) \tag{4.5}$$

$$\Delta_S = \frac{F * h}{G_p * t_p * l * n_{bs}} \tag{4.6}$$

Where:

$\Delta_p = Sheating - panel\ shear\ deformation\ [m]$
$F = Horizontal\ point\ load\ [kN]$
$h = Panel\ height\ [m]$
$G_p = Sheating - panel\ shear\ modulus\ [MPa]$
$t_p = Sheating - panel\ thickness\ [m]$
$b = Sheating - panel\ width\ [m]$
$l = Wall\ length\ [m]$
$n_{bs} = Number\ of\ braced\ sides\ of\ the\ wall$

4.1.4 Shear deformation

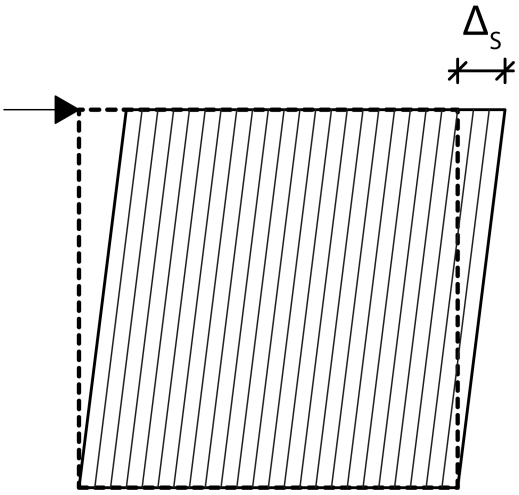

Figure 4.5: Shear deformation.

Within method A the shear deformation of a cross-laminated timber wall (Figure 4.5) is calculated using equation 4.7. Which is an alteration of equation 4.6 using the shear-modulus and thickness of the entire cross-laminated timber wall instead of the sheating-panels as for timber frame walls, Casagrande et al. (2015).

$$\Delta_S = \frac{F * h}{G_{CLT} * t_{CLT} * l} \tag{4.7}$$

Where:

$\Delta_S = CLT - wall\ shear\ deformation\ [m]$
$F = Horizontal\ point\ load\ [kN]$
$h = Panel\ height\ [m]$
$G_{CLT} = CLT - wall\ shear\ modulus\ [MPa]$
$t_{CLT} = CLT - wall\ total\ thickness\ [m]$
$l = Wall\ length\ [m]$

4.1.5 Sheating-to-framing connection deformation

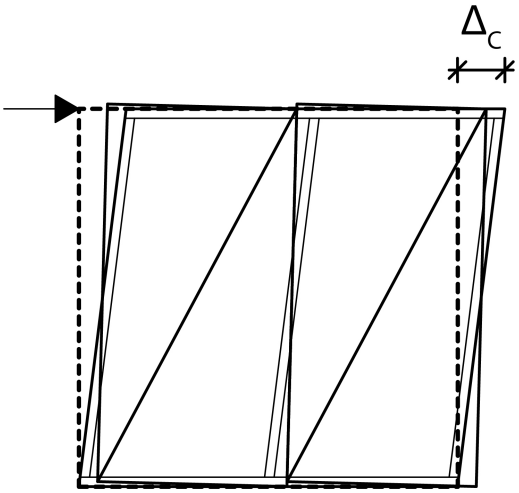

Figure 4.6: Sheating-to-framing connection deformation.

The sheating-to-framing connection deformation of a timber frame wall (Figure 4.6) is calculated using the stiffness and lever arm of each individual fastener between the sheating-panel and the timber frame, see equation 4.8. The magnitude is thereby largely dependent on the shape of the panel. For timber frame walls with sheating-panels on both sides of the wall the fasteners for each side is considered separately, doubling the stiffness, Casagrande et al. (2015).

$$\Delta_C = \frac{F * h^2}{k_c} * \left[\frac{1}{\sum_{i=1}^{n} x_i^2} + \frac{1}{\sum_{i=1}^{n} y_i^2} \right] \tag{4.8}$$

Where:

$\Delta_C = Sheating - to - framing\ connection\ deformation\ [m]$
$F = Horizontal\ point\ load\ [kN]$
$h = Panel\ height\ [m]$
$k_c = Individual\ fastener\ stiffness\ [kN/m]$
$x_i = x - coordinate\ of\ fastener\ i,\ relative\ to\ panel\ center$
$y_i = y - coordinate\ of\ fastener\ i,\ relative\ to\ panel\ center$

4.2 Method B - Hummel et al.

In method B Hummel et al. (2016) proposes a method similar to method A with the addition of the bending deformation of the wall. While for cross-laminated timber walls the derivation of a bending stiffness is more straight forward the corresponding deformation of the timber frame wall is viewed as an axial deformation of the frame studs. For cross-laminated timber walls the rigid-body rocking also takes into account the rigidity of the foundation where two types are identified; a rigid foundation such as a concrete slab and an elastic foundation such as an intermediate timber floor or an elastic intermediate layer.

For timber frame walls the total deformation includes:

- **Rigid-body translation**
- **Rigid-body rocking**
- **Sheating-panel shear deformation**
- **Sheating-to-framing connection deformation**
- **Axial deformation of studs**

For cross-laminated timber walls the total deformation includes:

- **Rigid-body translation**
- **Rigid-body rocking**
- **Shear deformation**
- **Bending deformation**

The rigid-body translation is viewed in method B by Hummel et al. (2016) in the same way as by Casagrande et al. (2015) in method A. Where the horizontal force is divided by the stiffness of the fasteners used to connect the wall to the foundation, see equations 4.1 and 4.2. The equations are the same for both timber frame walls and cross-laminated timber walls.

Likewise, the timber frame sheating-panel shear deformation is calculated by Hummel et al. (2016) in the exact same way as by Casagrande et al. (2015) in method A. See equations 4.5 and 4.6 for timber frame walls.

4.2.1 Rigid-body rocking

In method B considering a timber frame wall, the horizontal displacement due to rocking is calculated based on compression perpendicular to grain in the frame sill plate and the slip of the tensile anchorage. Hummel et al. (2016) presents equations 4.9 and 4.10 where the overturning moment from the horizontal force is checked against the stabilizing moment from the vertical force through a maximum-statement. The displacement due to deformation of the sill plate in compression perpendicular to grain is hence independent from the resulting moment and the displacement contribution from the tensile anchorage is set to 0 if there is no uplifting force.

$$\Delta_R = \frac{h}{l-2*e} * \left(\frac{\nu_{90} * F_{c,90}/A_{ef}}{1{,}2 * k_{c,90} * f_{c,90}} + \frac{max\left(F * \frac{h}{l-2*e} - \frac{q*l}{2} \ ; \ 0\right)}{n_h * n_n * k_n} \right) \tag{4.9}$$

$$F_{c,90} \approx \frac{h}{l} * F + \frac{a_s}{2} * q \tag{4.10}$$

Where:

$\Delta_R = Rigid-body\ rocking\ [m]$
$F = Horizontal\ point\ load\ [kN]$
$q = Evenly\ distributed\ vertical\ load\ [kN/m]$
$h = Wall\ height\ [m]$
$l = Wall\ length\ [m]$
$a_s = Stud\ spacing\ [m]$
$e = Distance\ from\ wall\ edge\ to\ hold-down\ [m]$
$n_h = Number\ of\ hold-downs$
$n_n = Number\ of\ fasteners\ per\ hold-down$
$k_n = Fastener\ stiffness\ [kN/m]$
$\nu_{90} = Allowed\ deformation\ of\ the\ sill\ plate\ [m]$
$F_{c,90} = Force\ in\ edge\ stud\ acting\ perpendicular\ to\ grain\ on\ the\ sill\ plate\ [kN]$
$A_{ef} = Effective\ contact\ area\ in\ compression\ perpendicular\ to\ grain\ [m^2]$
$k_{c,90} = Lateral\ pressure\ coefficient\ (1.25\ for\ structural\ softwood\ timber)$
$f_{c,90} = Strength\ in\ compression\ perpendicular\ to\ grain\ of\ the\ sleeper\ [MPa]$

When considering rigid-body rocking for cross-laminated timber walls Hummel et al. (2016) takes into account whether the foundation is rigid or elastic. For a rigid foundation equation 4.11 is used and for a foundation with an elastic intermediate layer equation 4.12 is used. In equation 4.12 the length of the compressed zone is needed. In section 3.1 two different methods for determining the compression zone length are presented.

$$\Delta_{R,Rigid} = \frac{h}{l-2*e} * \frac{max\left(F * \frac{h}{l-2*e} - \frac{q*l}{2} \ ; \ 0\right)}{n_h * n_n * k_n} \tag{4.11}$$

$$\Delta_{R,Elastic} = \frac{h^2}{l - e - \frac{l_c}{3}} * \frac{2 * F}{\frac{E_s * b_s}{t_s} * l_c^2} \tag{4.12}$$

Where:

$\Delta_{R,Rigid} = Rigid - body\ rocking\ in\ case\ of\ rigid\ foundation\ [m]$
$\Delta_{R,Elastic} = Rigid - body\ rocking\ in\ case\ of\ elastic\ foundation\ [m]$
$F = Horizontal\ point\ load\ [kN]$
$q = Evenly\ distributed\ vertical\ load\ [kN/m]$
$h = Wall\ height\ [m]$
$l = Wall\ length\ [m]$
$l_c = Length\ of\ compressed\ zone\ [m]$
$e = Distance\ from\ wall\ edge\ to\ hold - down\ [m]$
$n_h = Number\ of\ hold - downs\ per\ wall\ edge$
$n_n = Number\ of\ fasteners\ per\ hold - down$
$k_n = Fastener\ stiffness\ [kN/m]$
$E_s = Young's\ modulus\ of\ elastic\ intermediate\ layer\ [MPa]$
$b_s = Width\ of\ elastic\ intermediate\ layer\ [m]$
$t_s = Thickness\ of\ elastic\ intermediate\ layer\ [m]$

4.2.2 Sheating-to-framing connection deformation

The timber frame wall sheating-to framing connection deformation is calculated in method B using equation 4.13, Hummel et al. (2016).

$$\Delta_C = \frac{1}{n_{bs}} * (2 * l + 2 * n_{sp} * h) * \frac{a_n * F}{k_n * l^2} \tag{4.13}$$

Where:

$\Delta_C = Sheating - to - framing\ connection\ deformation\ [m]$
$F = Horizontal\ point\ load\ [kN]$
$h = Wall\ height\ [m]$
$l = Wall\ length\ [m]$
$n_{bs} = Number\ of\ braced\ sides\ of\ the\ wall$
$n_{sp} = Number\ of\ sheating - panels\ per\ side\ of\ the\ wall$
$a_n = Fastener\ spacing\ [m]$
$k_n = Fastener\ stiffness\ [kN/m]$

4.2.3 Shear deformation

For cross-laminated timber walls Hummel et al. (2016) consideres a reduced effective shear-modulus, see equation 4.14 and 4.15.

$$\Delta_S = \frac{F * h}{G_{ef} * t * l} \tag{4.14}$$

$$G_{ef} = \frac{G}{1 + 6 * \left(0.32 * \left(\frac{t_a}{a_a}\right)^{-0.77}\right) * \left(\frac{t_a}{a_a}\right)^2} \tag{4.15}$$

Where:

$\Delta_S = Shear\ deformation\ [m]$
$F = Horizontal\ point\ load\ [kN]$
$h = Wall\ height\ [m]$
$l = Wall\ length\ [m]$
$t = Wall\ thickness\ [m]$
$G = Shear - modulus\ of\ board\ layers\ [MPa]$
$t_a = Average\ board\ layer\ thickness\ [m]$
$a_a = Average\ board\ width\ within\ board\ layers\ [m]$

4.2.4 Axial deformation of studs

In method B Hummel et al. (2016) uses equation 4.16 to calculate the axial deformation of the studs in a timber frame wall, see figure 2.3.

$$\Delta_A = \frac{2}{3} * \frac{F}{E_0 * A} * \left(l + \frac{h^3}{l^2}\right) \tag{4.16}$$

Where:

$\Delta_A = Axial\ deformation\ of\ studs\ [m]$
$F = Horizontal\ point\ load\ [kN]$
$h = Wall\ height\ [m]$
$l = Wall\ length\ [m]$
$A = Cross - sectional\ area\ of\ timber\ frame\ studs\ [m^2]$
$E_0 = Young's\ modulus\ in\ grain\ direction\ of\ timber\ frame\ studs\ [MPa]$

4.2.5 Bending deformation

For a cross-laminated timber wall Hummel et al. (2016) calculates the bending deformation using the bending stiffness of the vertical board layers, see equation 4.17 and 4.18.

$$\Delta_B = \frac{F * h^3}{3 * EI_{ef}} \tag{4.17}$$

$$EI_{ef} = E_0 * t_{ef} * \frac{l^3}{12} \tag{4.18}$$

Where:

$\Delta_B = Bending\ deformation\ [m]$
$F = Horizontal\ point\ load\ [kN]$
$h = Wall\ height\ [m]$
$l = Wall\ length\ [m]$
$t_{ef} = Total\ thickness\ of\ vertical\ board\ layers\ [m]$
$E_0 = Young's\ modulus\ in\ grain\ direction\ of\ vertical\ board\ layers\ [MPa]$

4.3 Method C - Wallner-Novak et al.

Method C by Wallner-Novak et al. (2013) is designed for cross-laminated timber walls and is largely similar to method B by Hummel et al. (2016). The only difference is the reduction of the effective shear modulus used to calculate the shear deformation.

The total deformation includes:

- **Rigid-body translation**
- **Rigid-body rocking**
- **Shear deformation**
- **Bending deformation**

4.3.1 Shear deformation

The shear deformation in method C is calculated using equation 4.19 and 4.20 where the effective shear modulus is reduced with 25%.

$$\Delta_S = \frac{F * h}{G_{ef} * t * l} \tag{4.19}$$

$$G_{ef} = 0.75 * G \tag{4.20}$$

Where:

$\Delta_S = Shear\ deformation\ [m]$
$F = Horizontal\ point\ load\ [kN]$
$h = Wall\ height\ [m]$
$l = Wall\ length\ [m]$
$t = Wall\ thickness\ [m]$
$G = Shear - modulus\ of\ board\ layers\ [MPa]$

4.4 Method D - Gavric et al.

In Method D Gavric et al. (2015) suggest that previous assessment methods have failed to account for the full stiffness potential of the shear wall connectors. As hold-downs and angle brackets usually are assumed to only act in their strong direction and are neglected in their weak direction. Method D instead includes the vertical tensile stiffness of angle brackets, introduces a friction coefficient to reduce translation as well as a shape reduction factor for the shear deformation. The method is developed for cross-laminated timber walls.

For cross-laminated timber walls the total deformation includes:

- **Rigid-body translation**
- **Rigid-body rocking**
- **Shear deformation**
- **Bending deformation**

Gavric et al. (2015) calculates the bending deformation in method D in the same way as Hummel et al. (2016) in method B, see equation 4.17 and 4.18.

4.4.1 Rigid-body translation

Gavric et al. (2015) does in principle consider the translation in a similar way as in the previous methods, see equations 4.21 and 4.22. The exception is that the horizontal force is reduced with the static friction force calculated from the vertical force and a friction coefficient of 0.3. Further the fastener stiffness is summed up from all connectors to the foundation in the horizontal direction. Including both the angle brackets acting in their strong direction and hold-downs acting in their weaker direction.

$$\Delta_T = \frac{F - F_{fr}}{\sum k_i} \tag{4.21}$$

$$F_{fr} = k_{fr} * q * l \tag{4.22}$$

Where:

$\Delta_T = Rigid - body\ translation\ [m]$
$F = Horizontal\ point\ load\ [kN]$
$F_{fr} = Static\ friction\ force\ [kN]$
$k_i = Stiffness\ of\ fastener\ in\ horizontal\ direction\ [kN/m]$
$k_{fr} = Friction\ coefficient\ (0.3)$
$q = Evenly\ distributed\ vertical\ load\ [kN/m]$

$l = Wall\ length\ [m]$

4.4.2 Rigid-body rocking

Similar to how the rigid-body translation takes into account the horizontal stiffness of the hold-downs the rigid-body rocking deformation in method D includes the vertical tensile capacity of both the angle brackets and the hold-downs, see equation 4.23. Gavric et al. (2015) also extends the expression to walls in series where three different behaviours are discussed; single wall behaviour, coupled wall behaviour and single-coupled wall behaviour. Equation 4.23 represents the single wall behaviour which naturally occurs for stand-alone walls but also in the extreme condition where two adjacent walls are coupled with enough stiffness so that no slip occurs in the vertical joint. The two extreme cases for coupled wall behaviour is when there is no vertical connection between two adjacent walls and when the windward wall is on the limit to complete uplift of the entire wall panel. For coupled behaviour equation 4.24 is used. The single-coupled wall behaviour is then all cases in between single and coupled behaviour. One wall is completely lifted from the foundation but there is still vertical slip occurring between the adjacent wall panels due to the elasticity of the vertical joint. For single-coupled behaviour equation 4.25 is used.

$$\Delta_{R,sing} = \frac{\left(F*h-\frac{q*l^2}{2}\right)*h}{\sum k_i*l_i^2} \tag{4.23}$$

$$\Delta_{R,coup} = \frac{\left(F*h-\frac{q*l^2}{4}\right)*h}{\sum k_{1,i}*\left(l_{1,i}-\frac{l}{2}\right)^2+\sum k_{2,i}*l_{2,i}^2+k_v*\left(\frac{l}{2}\right)^2} \tag{4.24}$$

$$\Delta_{R,sing-coup} = \frac{\left(F*h-\frac{q*l^2}{2}+\frac{\frac{q*l^2}{2}*\sum k_i*l_i}{\sum k_{1,i}+k_v}\right)*h}{\sum k_i*l_i^2-\frac{\left(\sum k_{1,i}*l_{1,i}\right)^2}{\sum k_{1,i}+k_v}} \tag{4.25}$$

Where:

$\Delta_R = Rigid-body\ rocking\ deformation\ [m]$
$F = Horizontal\ point\ load\ [kN]$
$h = Wall\ height\ [m]$
$l = Wall\ length\ [m]$
$q = Evenly\ distributed\ vertical\ load\ [kN/m]$
$k_i = Stiffness\ of\ fastener\ in\ vertical\ direction\ [kN/m]$
$k_{1,i} = Stiffness\ of\ fastener\ of\ wall\ 1\ in\ vertical\ direction\ [kN/m]$
$k_{2,i} = Stiffness\ of\ fastener\ of\ wall\ 2\ in\ vertical\ direction\ [kN/m]$
$k_v = Stiffness\ of\ vertical\ joint\ between\ adjacent\ walls\ 1\ and\ 2\ [kN/m]$

$l_i = Lever\ arm\ from\ fastener\ to\ center\ of\ rotation\ [m]$
$l_{1,i} = Lever\ arm\ from\ fastener\ of\ wall\ 1\ to\ center\ of\ rotation\ [m]$
$l_{2,i} = Lever\ arm\ from\ fastener\ of\ wall\ 2\ to\ center\ of\ rotation\ [m]$

4.4.3 Shear deformation

When calculating the shear deformation in method D Gavric et al. (2015) adds a shape reduction factor of 1.2, see equation 4.26. The shear-modulus is then multiplied with the effective area of only the vertical board layers.

$$\Delta_S = \frac{1.2 * F * h}{G * t_{ef} * l} \tag{4.26}$$

Where:

$\Delta_S = Shear\ deformation\ [m]$
$F = Horizontal\ point\ load\ [kN]$
$h = Wall\ height\ [m]$
$l = Wall\ length\ [m]$
$t_{ef} = Total\ thickness\ of\ vertical\ board\ layers\ [m]$
$G = Shear - modulus\ of\ vertical\ board\ layers\ [MPa]$

4.5 Method E - Flatscher & Schickhofer

Flatscher (2017) takes an alternative approach to the stiffness assessment and instead of using a force-based method, method E is developed based on displacement. The main idea is that the deformation is divided between connection deformation and panel deformation. In this sense the connection deformation can be studied under the assumption that the wall panel is rigid. Likewise, the shear and bending contributions, similarly as in the previously discussed methods, are treated decoupled from connection properties. Flatscher (2017) references the calculation of elastic CLT deformations to Schickhofer et al. (2010).

The total deformation includes:

- **Rigid-body translation**
- **Rigid-body rocking**
- **Shear deformation**
- **Bending deformation**

The calculation procedure consists of the following steps:

1. The **connection based deformations**, translation and rocking, are estimated with a share parameter p, see equations 4.27 and 4.28.

$$\Delta_T = p * \Delta_{con} \tag{4.27}$$

$$\Delta_R = (1 - p) * \Delta_{con} \tag{4.28}$$

Where:

$\Delta_T = Rigid - body\ translation\ deformation\ [m]$
$\Delta_R = Rigid - body\ rocking\ deformation\ [m]$
$\Delta_{con} = Connection\ based\ deformation\ [m]$
$p = Share\ parameter\ (0 \leq p \leq 1)$

2. The lateral and vertical displacements of each connector is then calculated using equations 4.29 and 4.30.

$$\Delta_{con,x,i} = p * \Delta_{con,i} \tag{4.29}$$

$$\Delta_{con,y,i} = x_i * \frac{(1 - p) * \Delta_{con,i}}{h} \tag{4.30}$$

Where:

$\Delta_{con,x,i} = Lateral\ displacement\ of\ connector\ i\ [m]$
$\Delta_{con,y,i} = Vertical\ displacement\ of\ connector\ i\ [m]$
$\Delta_{con,i} = Connection\ based\ deformation\ of\ connector\ i\ [m]$
$p = Share\ parameter\ (0 \leq p \leq 1)$
$x_i = Distance\ from\ connector\ to\ center\ of\ rotation\ [m]$
$h = Wall\ height\ [m]$

3. The lateral and vertical force acting on each connector is calculated based on the connector stiffness using equations 4.31 and 4.32.

$$F_{con,x,i} = k_{H,i} * \Delta_{con,x,i} \tag{4.31}$$

$$F_{con,y,i} = k_{V,i} * \Delta_{con,y,i} \tag{4.32}$$

Where:

$F_{con,x,i} = Lateral\ force\ acting\ on\ connector\ i\ [N]$
$F_{con,y,i} = Vertical\ force\ acting\ on\ connector\ i\ [N]$
$k_{H,i} = Horizontal\ stiffness\ of\ connector\ i\ [N/m]$
$k_{V,i} = Vertical\ stiffness\ of\ connector\ i\ [N/m]$

4. The total lateral load acting on the wall based on translation and rocking respectively is calculated with equations 4.33 and 4.34.

$$F_T = \sum F_{con,x,i} + \left(\sum F_{con,y,i} + q * l\right) * \mu \tag{4.33}$$

$$F_R = \frac{1}{h} * \left(\sum \left(F_{con,y,i} * x_i\right) + \frac{q * l^2}{2}\right) \tag{4.34}$$

Where:

$F_T = Total\ lateral\ load\ based\ on\ translation\ [N]$
$F_R = Total\ lateral\ load\ based\ on\ rocking\ [N]$
$F_{con,x,i} = Lateral\ force\ acting\ on\ connector\ i\ [N]$
$F_{con,y,i} = Vertical\ force\ acting\ on\ connector\ i\ [N]$
$q = Evenly\ distributed\ vertical\ force\ [N/m]$
$x_i = Distance\ from\ connector\ to\ center\ of\ rotation\ [m]$
$h = Wall\ height\ [m]$
$l = Wall\ length\ [m]$
$\mu = Friction\ coefficient\ (optional,\ can\ be\ set\ to\ 0\ to\ not\ include\ friction)$

5. Since only one lateral force can act on the structure at the same time an update of the share parameter p has to be iterated until equation 4.35 is fulfilled.

$$F = F_T = F_R \tag{4.35}$$

Where:

$F = Lateral\ load\ acting\ on\ the\ wall\ [N]$
$F_T = Total\ lateral\ load\ based\ on\ translation\ [N]$
$F_R = Total\ lateral\ load\ based\ on\ rocking\ [N]$

6. When equation 4.35 is fulfilled p is assumed correct and the elastic CLT deformations can be calculated accordingly. Shear deformation with equations 4.36 and 4.37 and bending deformation with equation 4.38.

$$\Delta_S = \frac{F * h}{G_{eff} * t * l} \tag{4.36}$$

$$G_{eff} = \frac{G_{mean}}{1 + 6 * p_s * \left(\frac{t_{max}}{a}\right)^{1.24}} \tag{4.37}$$

Where:

$\Delta_S = Shear\ deformation\ [m]$
$F = Lateral\ load\ acting\ on\ the\ wall\ [N]$
$G_{mean} = Average\ shear-modulus\ of\ board\ layers\ [MPa]$
$G_{eff} = Effective\ shear-modulus\ [MPa]$
$h = Wall\ height\ [m]$
$l = Wall\ length\ [m]$
$t = Wall\ thickness\ [m]$
$t_{max} = Maximum\ board\ layer\ thickness\ [m]$
$a = Single\ board\ width\ or\ maximum\ distance\ between\ cracks\ [m]$
$p_s = Parameter\ based\ on\ number\ of\ board\ layers\ (0.53\ for\ 3\ layers,\ 0.43\ for\ 5\ layers\ or\ more)$

$$\Delta_B = \frac{4 * F * h^3}{E_0 * l^3 * t_{eff}} \tag{4.38}$$

Where:

$\Delta_B = Bending\ deformation\ [m]$
$F = Lateral\ load\ acting\ on\ the\ wall\ [N]$
$E_0 = Young's\ modulus\ in\ the\ grain\ direction\ [MPa]$
$h = Wall\ height\ [m]$
$l = Wall\ length\ [m]$
$t_{eff} = Total\ thickness\ of\ the\ vertical\ board\ layers\ [m]$

5

Finite-Element Modelling Techniques

Fragiacomo (2013) shows through cyclic tests of cross-laminated timber wall sub-assemblies that the modelling of the shear wall connectors is crucial to the model behaviour. Whereas the cross-laminated timber panel itself can be modelled as linear-elastic or even rigid unless openings are present. He discusses three different modelling techniques for the cross-laminated timber wall; rigid elements, a rigid pinned frame with diagonal springs and 2D plane stress shell elements. The three methods simplifies the shear wall model to various degrees and thereby allow for different types of deformation. Modelling the wall as a rigid element will only allow for rigid-body deformations (translation and rotation), leaving out the shear and bending deformation. The diagonal spring method will allow the wall to deform in translation, rotation and shear but not in bending. Unless the spring stiffness is calibrated by imposing the horizontal deformation from shear wall test data. The 2D plane stress elements are the least simplified and will deform in both translation, rotation, shear and bending.

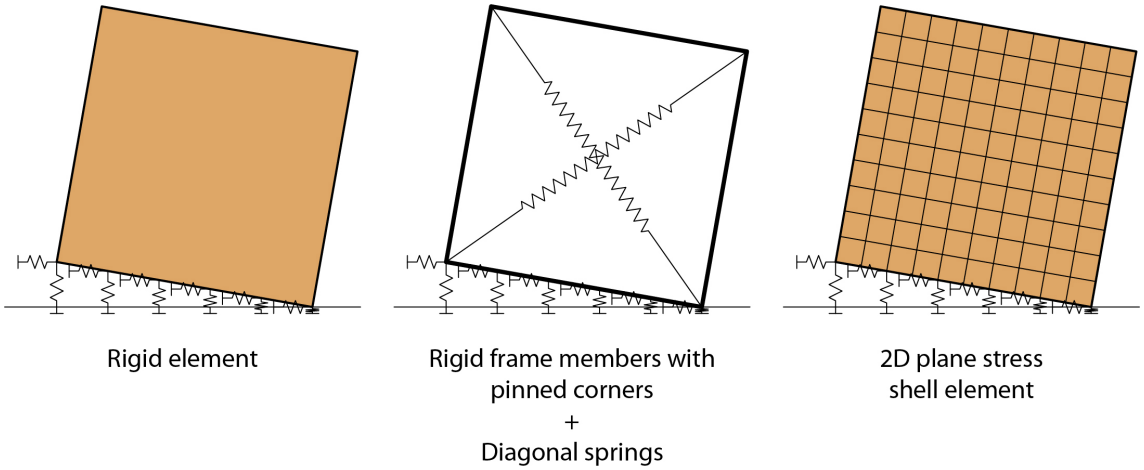

Figure 5.1: Cross-laminated timber modelling techniques, Fragiacomo (2013).

5.1 2 degree-of-freedom nodes

The stiffness assessment methods presented in the previous section calculates the displacement in relation to each mode of deformation. In order to create a finite-

element model with the same behaviour each deformation needs to be converted to a stiffness. Either as a material property or as springs representing connectors, individually or grouped in so called lumped springs. Fragiacomo (2013) suggests that since the typical shear wall connectors (hold-downs and angle brackets) does not support rotations the system can be constructed with 2 degrees-of-freedom at each node. Thus separating every mode of deformation in horizontal and vertical components. Method A by Casagrande et al. (2015) does in fact propose its own system with 2 degree-of-freedom nodes based on the deformation assumptions made in the calculations, see figure 5.2 and equations 5.1 - 5.4. The method can also be extended to systems of shear walls as seen in figure 5.3.

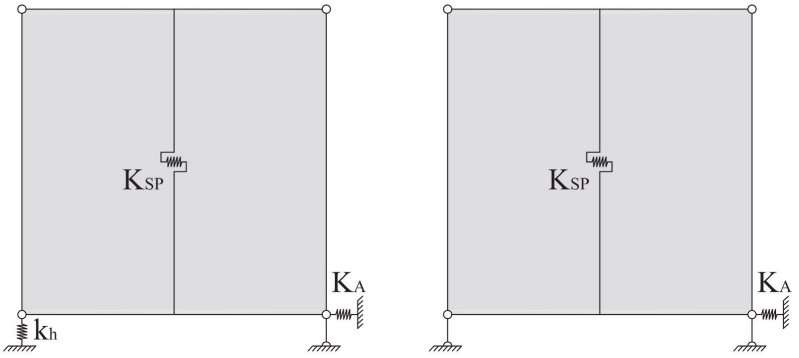

Figure 5.2: Shear wall modelling system with 2D degree-of-freedom nodes by Casagrande et al. (2015). Activated hold-down (left) and deactivated hold-down (right).

$$K_{SH} = \frac{n_{bs} * k_c * l}{\lambda * s_c} \tag{5.1}$$

$$K_P = \frac{G_p * n_{bs} * t_p * l}{h} \tag{5.2}$$

$$K_{SP} = \begin{cases} \frac{K_P * K_{SH}}{K_P + K_{SH}} & for\ timber\ frame\ walls \\ K_P & for\ CLT\ walls \end{cases} \tag{5.3}$$

$$K_A = \frac{k_a * l}{i_a} \tag{5.4}$$

Where:

$K_{SH} = Sheating - to - framing\ connection\ stiffness\ [kN/m]$
$K_P = Sheating - panel\ shear\ stiffness/CLT - panel\ shear\ stiffness\ [kN/m]$
$K_{SP} = Horizontal\ linear\ spring\ stiffness\ [kN/m]$
$K_A = Rigid - body\ translation\ stiffness\ [kN/m]$
$K_h = Hold - down\ tensional\ stiffness\ [kN/m]$

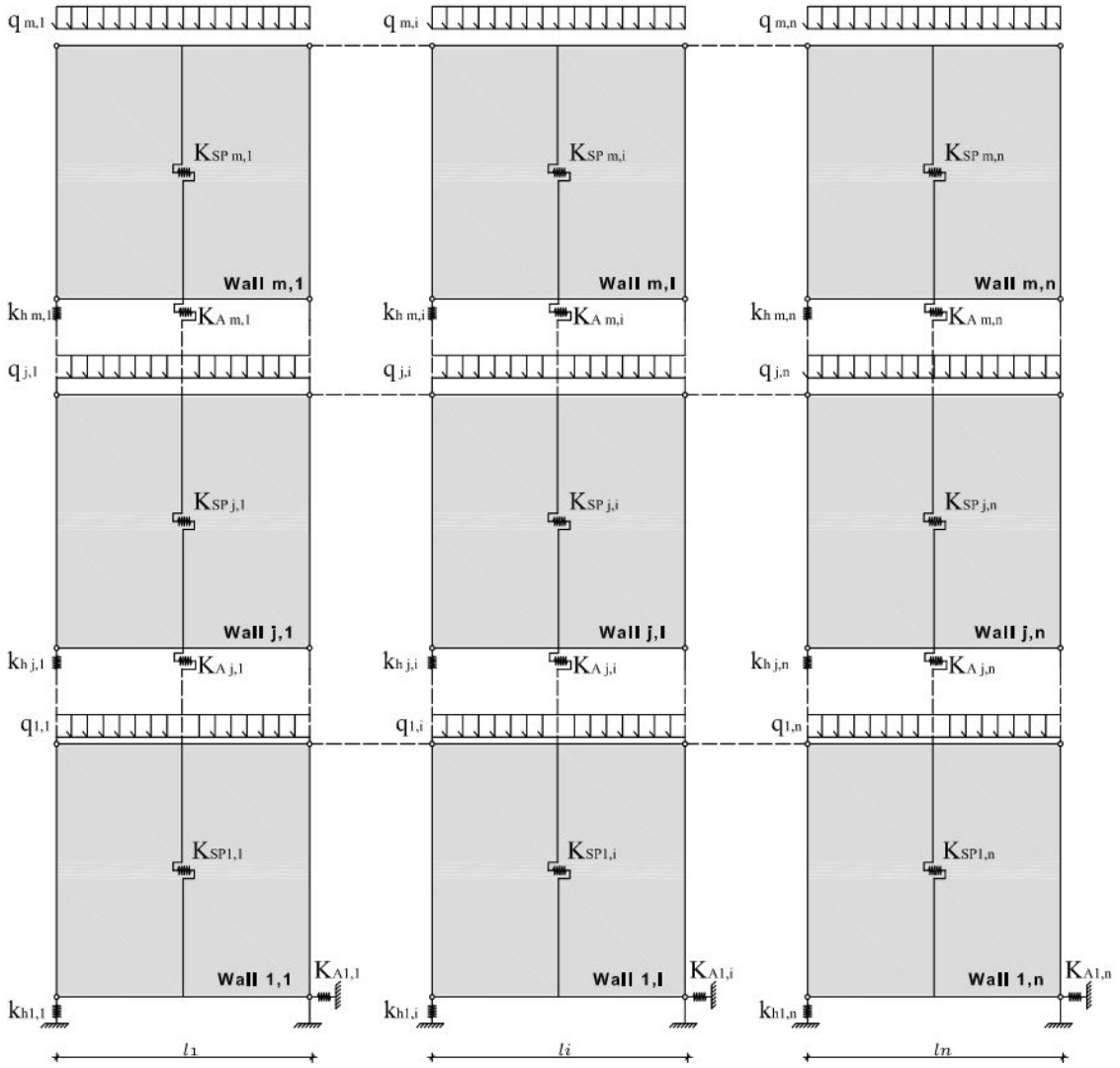

Figure 5.3: System of m x n shear walls modelling a full-scale building, Casagrande et al. (2015).

The 2 degree-of-freedom node system by Casagrande et al. (2015) works well for shear walls modelled as rigid elements where, as in method A, the center of rotation can be pinned supported. However, when multiple non-rigid walls are placed in series the vertical wall-to-wall connections must be included in the model more detailed. As the stiffness of the connection can vary the rigid-body rocking approach by Gavric et al. (2015) in method D becomes applicable, see figure 5.4. In the regime of single wall behaviour the 2 degree-of-freedom system by Casagrande et al. (2015) is naturally valid in its current form considering the two wall panels as one. Similarly for the coupled behaviour the approach is also valid since both panels have their center of rotation in contact with the foundation, thus making a pinned connection per panel possible. The intermediate connection just needs to be added along the vertical joint. For the combined single-coupled behaviour the center of rotation for the individual windward side panel can no longer be pinned to the foundation. In this situation where the vertical joint is sufficiently stiff to lift the entire windward side panel from its foundation considerations can be made as

to weather a hold down is actually motivated at the intermediate corner. Either the intermediate hold-downs can be made stiffer to keep the walls in the coupled state or they can be discarded and thus move the center of rotation to the outermost corner of the entire wall length.

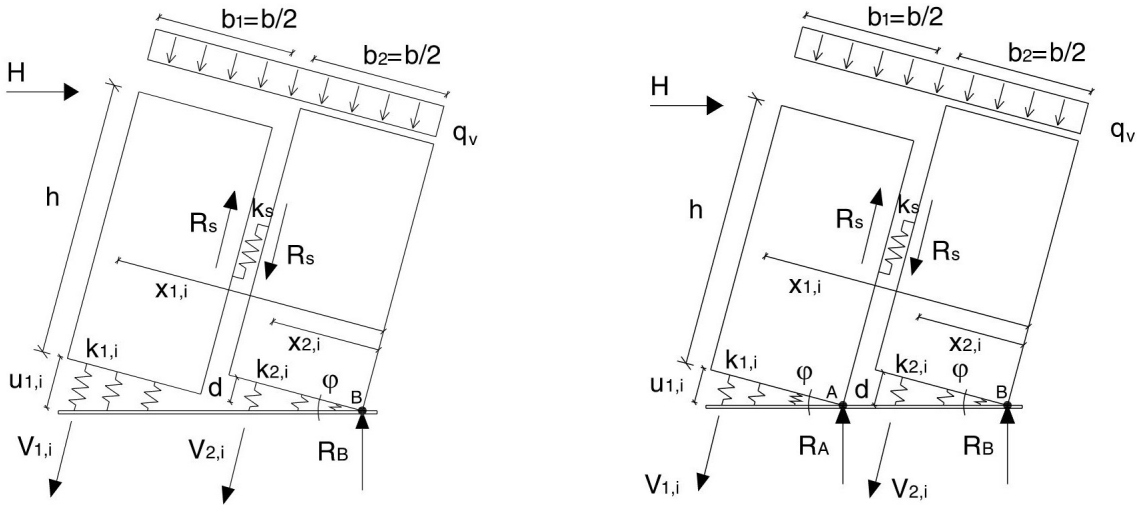

Figure 5.4: Single-coupled wall behaviour (left) and coupled wall behaviour (right), Gavric et al. (2015).

5.2 Surface end releases and hinges

In certain FE-softwares linear releases and hinges can be constructed along surface edges. A surface edge can thereby be assigned a linear condition relative to an adjacent surface edge or line. This behavior is sought after when considering for example the vertical joint between two wall panels as well as the horizontal shear connection between stacked walls. Simply connecting the wall panels to each other rather than having a support relative to a certain point in space. The linear hinge is used to consider elasticity and decoupling between surfaces (see figure 5.5) while the linear release allows for decoupling of objects connected to a line (see figure 5.6). Both methods make use of what is called the double-node technology where for each node along the connection double nodes are created and connected to each other with a spring. The line release however extends its use further since it allows for non-linearities such as pressure contact to be assigned to this spring. An alignment based on either deformation or force is then adapted using the so called penalty method, Kuhn (2018).

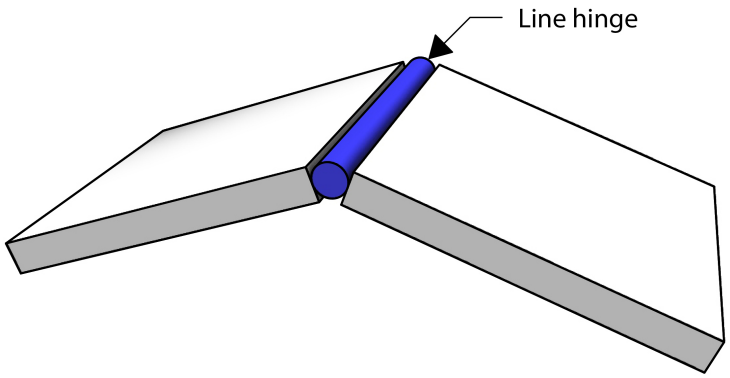

Figure 5.5: Visual representation of a line hinge.

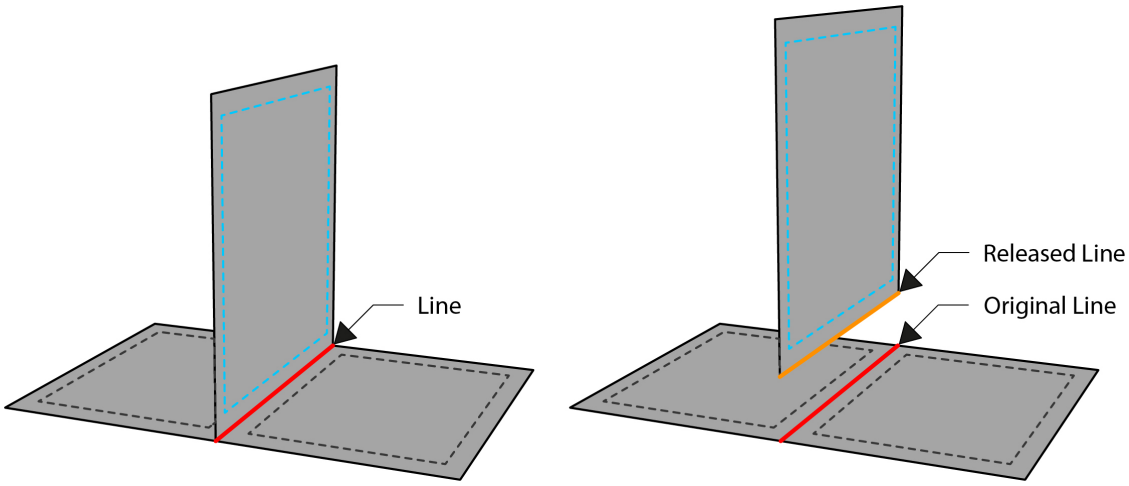

Figure 5.6: Visualisation of a line release in relation to its original line.

It should be noted that the assignment of line hinges needs to correspond well with the actual conditions of the connection. For example a vertical wall-to-wall connection using a single row of fasteners represents a one sided line hinge while for example a cover-plate connection or the connection between two sheating-panels of a timber frame wall has two rows of fasteners and thereby represents double sided line hinges, Kuhn (2018).

5.3 Friction

As Schickhofer et al. (2010) discusses that a significant part of the shear force may be transmitted to the foundation via friction and both method D and E includes this behaviour in the stiffness assessment. A method to consider the friction in a shear wall finite-element model is needed. To include the friction force to the underlying structure as an increased stiffness of the horizontal connectors is in principle a straight forward procedure. However the friction force depends on the normal force acting on the friction surface, see figure 5.7. Thereby making the increased stiffness

dependent on the current load case. Meaning that a specific friction force dependent on the vertical force needs to be added to each load case.

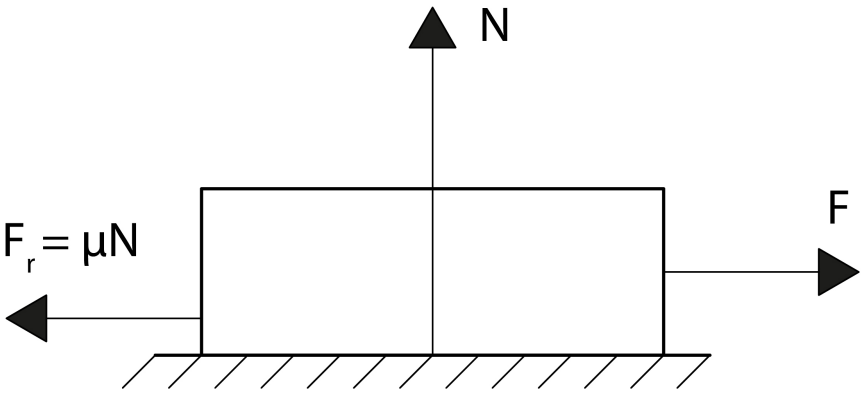

Figure 5.7: Alternative timber frame shear wall construction with cut sill plates and vertically connected studs, Jung (2013).

5.4 Local force distribution at nodal supports

When modelling nodal support conditions in an FE-software the distribution of forces in the immediate vicinity of the node must be studied with caution. If the supported structure is rigid this is of course not an issue, but if the structure is ductile the risk of over-stressing might be exaggerated due to coarse meshing. For detailed studies of the connections a mesh convergence study should therefore be performed. Many software provide local mesh refinement procedures to increase the integration points around geometric singularities. In a single shear wall model the this might be a good solution to get an better overview of the extreme forces in the wall. For a global building model however, mesh refinements would make the calculation heavier. To reduce the risk of overestimating the stresses and at the same time not rely on mesh refinements a general middle ground approach is to model for example the hold-downs as line elements connecting two nodes further into the mesh. This would prevent over-stressing at the corner points and distribute the reaction force in a manor more close to the actual behaviour of the hold-down.

5.5 Deformation of timber frame sill plate

In equation 4.9 of method B Hummel et al. (2016) takes into consideration the allowed deformation of the sill plate in compression perpendicular to grain. In principle this is something that easily can be calculated knowing the strength parameters of the sill plate, the effective area under compression and the axial force in the timber frame stud. Modelling this behaviour in a finite-element software however raises the level of detail quite extensively. A workaround discussed by Jung (2013) is to simply construct the timber frame with the sill plate cut before the stud and connect the studs vertically along the building height, see figure 5.8. Essentially taking away the compression perpendicular to grain, reducing the rocking deformation and

stiffening the vertical load path throughout the shear wall.

Figure 5.8: Alternative timber frame shear wall construction with cut sill plates and vertically connected studs, Jung (2013).

If the choice is still made to model the connection between stud and sill plate in detail in a finite-element environment both of these methods can be modelled using an axial offset of the sill plate in relation to the stud (or vice versa). Certain softwares allows for direct input of axial eccentricity while in others this would need to be modelled explicitly with a cut of the sill plate and a rigid link from the end node to the stud, see figure 5.9, Dlubal Software GmbH. (2016).

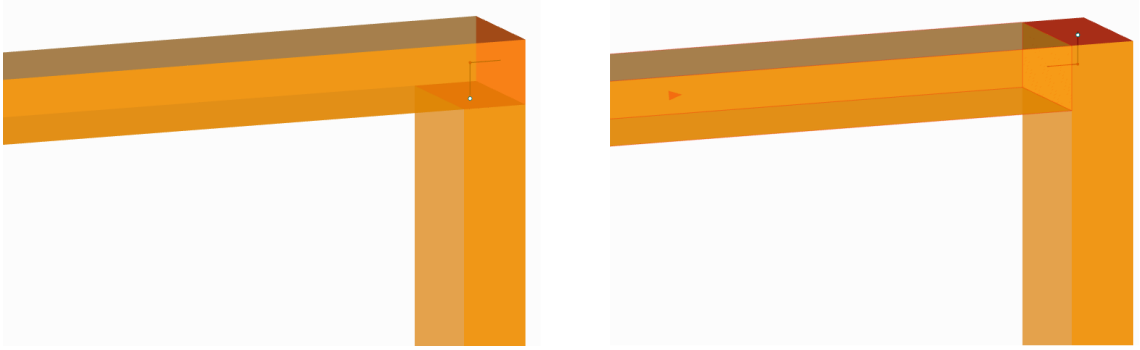

Figure 5.9: FE-modelling of axial offset with a rigid link from the cut stud to the sill plate (left) and from the cut sill plate to the vertically continuous stud (right).

5.6 Non-linear - Linear conversion

As pointed out by Fragiacomo (2013) in linear static analysis of simple structures such as stand alone shear walls the sign of the axial force in the connectors can often be predicted. However, in a linear dynamic analysis such as modal spectrum analysis the building is subjected to vibrations and the connectors hence faces both tension and compression forces. This demands that an equivalent axial stiffness k_{eq} is determined for the connectors. The finite-element software Acord (2022) implements such a technique calculating an equivalent spring stiffness given a certain load case and a set of non-linear springs, see figure 5.10. The procedure needs a first iteration where the forces in each of the springs are calculated non-linearly. Based on the forces in each spring the method is then based on equilibrium equations making it possible to analytically find the rotation θ. A linearly distributed stiffness k_{eq} is then derived to give the same rotation θ with a fully linear model. It should be noted that this procedure moves the center-of-rotation of the wall to the center of the wall base edge. When calculated non-linearly the length of the compression zone will vary depending on the resulting moment and the foundation rigidity, Acord (2020).

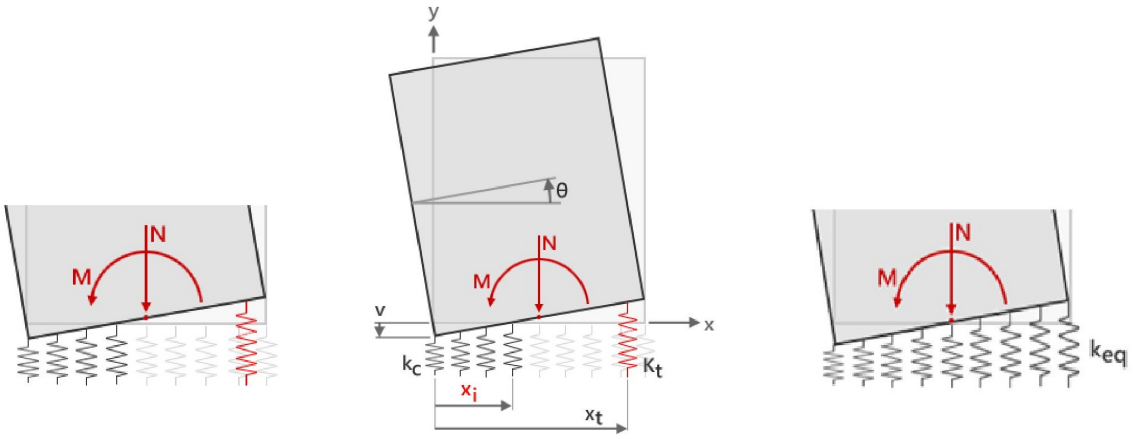

Figure 5.10: Visualization of the linearization procedure implemented in the finite-element software Acord.

5.6.1 Linearization test

Apart from the previously mentioned example none of the other commercially available finite-element softwares studied provides any guidance on how their software linearizes a non-linear work law in a linear dynamic analysis. To understand how a certain finite-element software treats a non-linear spring in a linear dynamic analysis a simple test can be conducted. The setup consist of a single axially loaded spring according to figure 5.11. The spring is assigned a bi-linear stiffness (see figure 7.17) and a linear dynamic analysis, so called modal analysis, is then performed. The resulting force and displacement is recorded and the stiffness calculated. Running the analysis with a series of bi-linear stiffness alterations will then give a picture of how the software linearizes the spring stiffness.

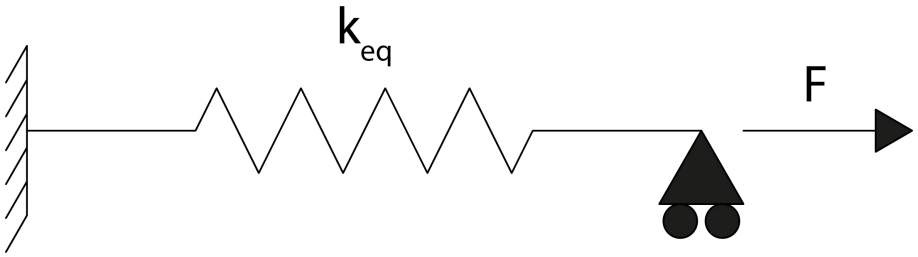

Figure 5.11: Linear dynamic analysis non-linear spring linearization test setup.

6

Proposed Finite-Element Modelling Strategies

In the following chapter finite-element modelling strategies are proposed for timber frame shear walls and cross-laminated timber shear walls. The strategies are developed with the knowledge base from the former chapters and have been optimized to include the applicable modes of deformation and allow for scaleability to global building models. The developed finite-element modelling strategy will further on be referred to as the "proposed strategy".

6.1 Material definition

In general the consideration is made that the material based stiffness should be accounted for through an adequate material definition instead of a conversion to a rigid plate or frame with calibrated springs. The connector based deformations are modelled with the use of linear hinges, linear releases and springs.

When it comes to the material definitions for the timber frame shear wall the modelling choices are more or less straight forward. Considering the philosophy that the material based deformation should be handled by the material itself the frame is modelled as beam elements and the sheating-panels as 2D plane stress shell elements, both with unaltered properties of the specified materials.

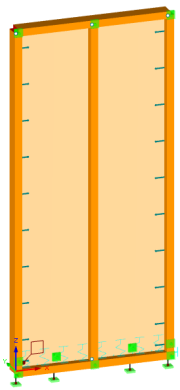

Figure 6.1: Visualization of a timber frame shear wall modelled with the proposed finite-element modelling strategy, method F.

The cross-laminated timber shear wall can as described in section 2.5 be considered as either an orthotropic or a layered material. In principle the choice of material definition should not influence the final stiffness. It can rather be viewed as different methods for reaching at least very similar stiffness matrices for the wall cross-section as a whole. Precautions should however be taken on how reduction factors are applied within the finite-element software at hand so that reduction factors are not duplicated or left out. The following modelling strategy will be based on the assumption that a reliable stiffness matrix is produced by either one of the material definition methods. Then considering the need for capturing the material based deformations it is chosen to model the wall as a 2D plane stress shell element and apply said defined material.

Once the material is defined and the wall itself is modelled the connections and support conditions comes next. Meaning the hold-downs, angle brackets at the horizontal joints and the screwed wall-to-wall connections at the vertical joints as well as out-of-plane supports and pressure contact conditions where applicable.

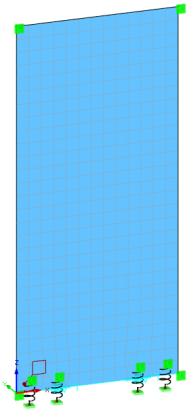

Figure 6.2: Visualization of a cross-laminated shear wall modelled with the proposed finite-element modelling strategy, method F.

6.2 Pressure contact

The contact surfaces at the wall-to-foundation and wall-to-floor positions are modelled with a so called pressure contact condition. This means a non-linear behaviour where the foundation/floor is prevented to deform under compression while uplift of the wall due to tension is fully released, see force-displacement diagram in figure 6.3. This condition essentially keeps the walls from intersecting each other and the foundation/floor which thereby allows for more natural deformation distributions between elements. As the pressure contact naturally applies along the full length of the surface it is modelled using a linear release where the non-linearity is applied between the set of duplicated nodes described in section 5.2. This modelling technique together with the choice of an elastic material definition will allow the wall to find its center-of-rotation independently. Compared to for instance setting

a pinned connection at the corner point as in the 2-degree-of-freedom-nodes system by Casagrande et al. (2015) described in section 5.1.

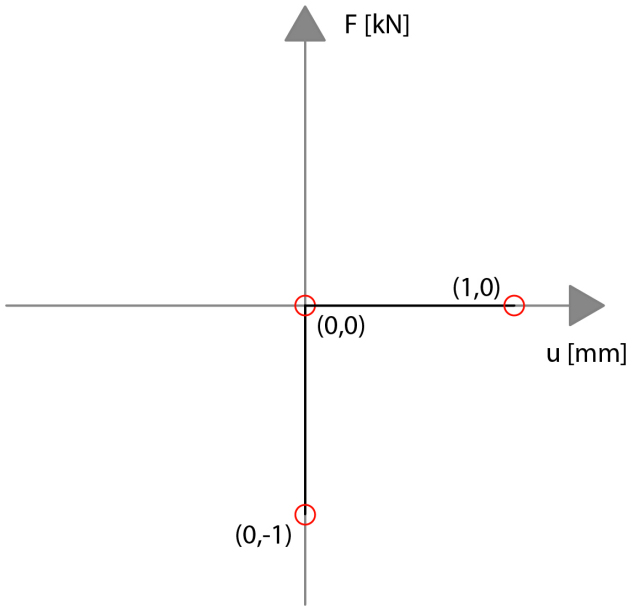

Figure 6.3: Bi-linear work law with pressure contact condition applied to the linear release. For higher or lower loads the diagram is linearly extrapolated from the assigned data points.

6.3 Modelling angle brackets

The horizontal shear connectors can either be modelled at their discrete positions or as a "smeared" stiffness along the edge of the wall-surface. Due to the significant amount of angle brackets in a large scale model it is proposed to average the stiffness over the wall-length and assign it to a linear release. If the weak axis stiffness of the hold-downs should be considered they are to be treated in the same way as the angle brackets but with its own stiffness magnitude. The horizontal stiffnesses are then simply summed up and divided by the wall length. The average stiffness per meter can then be assigned to the axial direction of the linear release created for the pressure contact.

6.4 Modelling hold-downs

Due to the binary behaviour of the hold-downs as described by Casagrande et al. (2015) in section 4.1.2 the hold-downs are modelled as non-linear springs. Since there are generally only one hold-down at each wall end discrete positions are used instead of "smearing" the stiffness over the entire wall length as a linear release. In order to prevent over-stressing at the corner points and distribute the reaction force in a position more close to the actual behaviour of the hold-down, two nodes further into the mesh are connected (see figures 6.5 and 6.6). The two nodes are

connected with a tension-only spring mimicking the hold-down behaviour in tension and without any stiffness in compression (see figure 6.4). Thus allowing the pressure contact condition of the line release between the wall panel surfaces to handle the compression independently. If the tensional capacity of the angle brackets are to be considered the same procedure could be applied with tension-only springs connecting two nodes at the discrete positions of the angle brackets. This would however quickly increase the modelling effort and instead adding a vertical stiffness averaged over the wall length to the linear release created for the pressure contact could be considered viable. A consideration should be made based on the angle bracket stiffness and spacing.

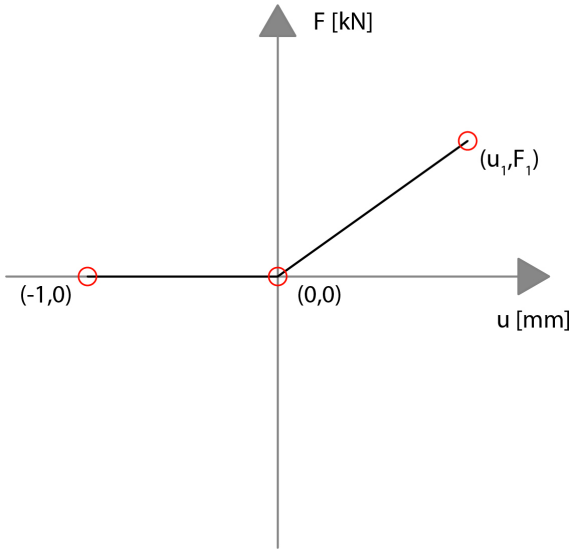

Figure 6.4: Bi-linear work law with tension-only condition applied to the hold-down spring. For higher or lower loads the diagram is linearly extrapolated from the assigned data points.

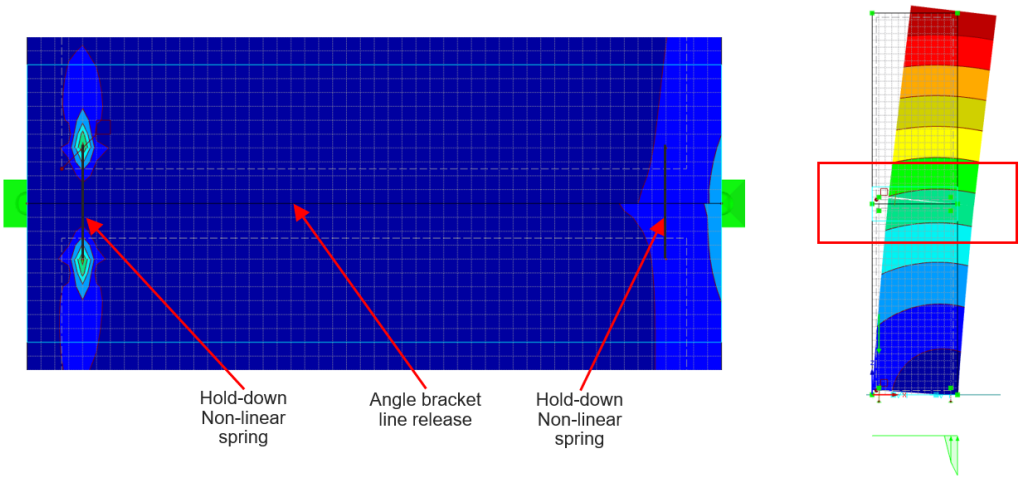

Figure 6.5: Shear force distribution of a CLT wall-to-wall connection with hold-downs modelled as spring elements between two internal surface nodes.

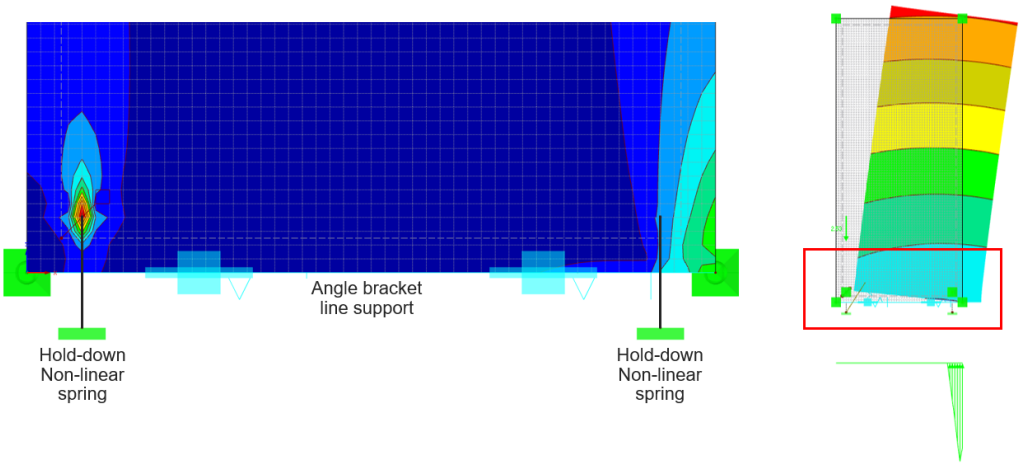

Figure 6.6: Shear force distribution of a CLT wall-to-foundation connection with hold-downs modelled as spring elements between an internal surface node and an external rigid support.

6.5 Vertical joint of cross-laminated timber walls

Looking at the vertical joint between adjacent cross-laminated timber walls the vertical and horizontal stiffness is concentrated to one set of connectors. In general the vertical stiffness component is combined with a pressure contact condition between the wall panels. Unless the direction of the resulting moment is known however, the pressure contact condition has to be valid in two directions (pressure and suction). This becomes an issue in the FE-model since duplicate releases between adjacent surfaces leads to the intermediate line being completely uncoupled leaving the model unstable. To propose a modelling strategy the horizontal deformation will be studied for two different cases in relation to a pressure contact condition with known direction of the resulting moment. Firstly with the horizontal stiffness set to zero and secondly with a horizontal stiffness equal to the vertical stiffness of the screwed connection, see section 7.7.

6.6 Vertical joint of timber frame walls

The vertical joint in a timber frame wall differs from the condition of the cross-laminated timber. As the sheating-panels are nailed or stapled around their perimeter the linear hinge condition can be used to create the double sided hinge condition that occurs with two rows of fasteners. That the stud positioned at the vertical joint connects to both of the adjacent sheating-panels also means that the need for a pressure contact condition in the vertical joint is removed.

7

Results

7.1 Material properties of reference building

The shear walls of the reference building are modelled with the material properties presented in table 7.1. The strength and stiffnesses of the material is presented in table 7.2.

Table 7.1: Material properties of modelled shear wall cross-sections.

	Wall-section		
	1	**2**	**3**
Timber frame			
Frame member cross-section [mm]	60x120		
Frame member strength grade	C24		
Sheating-panel thickness [mm]	18		
Sheating-panel strength grade	OSB/3		
Number of braced sides	2		
CLT			
Number of board layers		5	5
Board layer thicknesses [mm]		20-20-20-20-20	40-20-40-20-40
Board layer strength grade		C24	C24
Board width [mm]		120	120
Glued short-edges		Yes	Yes
Slits or splits in boards		No	No

Table 7.2: Characteristic strength and stiffness properties in MPa for used structural timber materials according to DIN EN 338:2016.

	$f_{m,k}$	$f_{t,0,k}$	$f_{t,90,k}$	$f_{c,0,k}$	$f_{c,90,k}$	$f_{v,k}$	$E_{0.05}$	$E_{0,mean}$	$E_{90,mean}$	G_{mean}
C24	24	14.5	0.4	21	2.5	4.0	7400	11000	370	690

The connectors used along the horizontal edge of the shear walls are angle-brackets and hold-downs, further discussed in section 3.1. Both connectors have two types, one for timber-to-concrete connections and one for timber-to-timber connections. As the reference building has a concrete foundation and cross-laminated timber floors this can be interpreted as one variant for wall-to-foundation connections and one for wall-to-floor connections. The stiffness properties in tension and shear for each connector are presented in table 7.3 and 7.4.

Table 7.3: Timber to concrete connector stiffness properties in tension and shear based on cyclic tests performed by Gavric et al. (2014).

	Timber to concrete			
	Tension		**Shear**	
Hold-down WHT540	$\bar{x}$	COV[%]	$\bar{x}$	COV[%]
F_y [kN]	40.46	8.11	3.61	35.59
ν_y [mm]	8.81	21.76	1.13	42.30
K_{el} [kN/mm]	4.51	14.31	3.40	33.25
Angle-bracket BMF 90x116x48x3	$\bar{x}$	COV[%]	$\bar{x}$	COV[%]
F_y [kN]	19.22	2.73	22.98	5.19
ν_y [mm]	7.26	9.04	11.74	5.87
K_{el} [kN/mm]	2.53	9.72	2.09	16.41

Table 7.4: Timber to timber connector stiffness properties in tension and shear based on cyclic tests performed by Gavric et al. (2014).

	Timber to timber			
	Tension		**Shear**	
Hold-down WHT440	$\bar{x}$	COV[%]	$\bar{x}$	COV[%]
F_y [kN]	32.21	4.52	2.72	28.13
ν_y [mm]	11.91	19.83	1.71	17.23
K_{el} [kN/mm]	2.65	19.27	1.56	16.20
Angle-bracket BMF 100x100x90x3	$\bar{x}$	COV[%]	$\bar{x}$	COV[%]
F_y [kN]	11.12	9.69	16.61	7.46
ν_y [mm]	3.97	28.12	13.73	7.27
K_{el} [kN/mm]	2.98	22.05	1.10	12.34

The connection along the vertical joint of the shear walls is a butt joint, see figure 3.4. The connection is a skewed screw connection using 8x120mm fully threaded screws with a single fastener stiffness K_{ser} of 2182 kN/m assuming that the minimum edge and end distances are fulfilled.

7.2 Timber frame stiffness

In figure 7.1 the distribution of deformation between the different deformation modes has been calculated for a timber frame wall with properties corresponding to wall-section 1 as laid out in section 1.3.1. Figure 7.2 shows the respective load-displacement relations for the stiffness assessment methods compared to the proposed modelling strategy in chapter 6 under a 1kN/m evenly distributed vertical load. The calculations follows the equations laid out in sections 4.1 and 4.2.

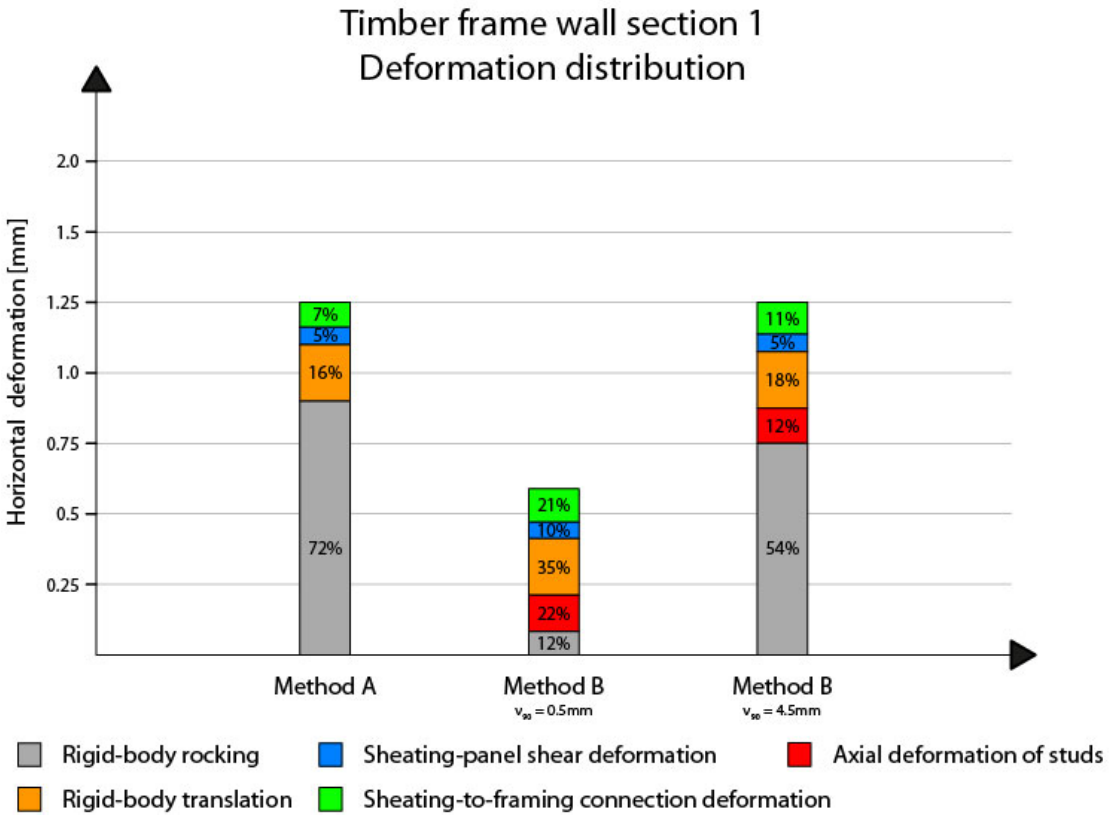

Figure 7.1: Deformation distribution between modes of deformation for timber frame wall-section 1 under vertical and horizontal unit loads calculated with method A and B.

Looking at figure 7.1 we can see large differences in the deformation distribution between method A and B. This has to do with the different assumptions made regarding the rocking deformation of the wall, see sections 2.2, 4.1 and 4.2. More particularly the decisive parameter for the large difference in total deformation as seen in figure 7.2 is the allowed deformation of the sill plate ν_{90} as accounted for in equation 4.9 of method B. The allowed deformation of 0.5mm has been calculated

from the strength of the sill plate. However, for comparison of the deformation distribution ν_{90} has also been altered so that method B shows the same total deformation as method A.

The sheating-panel shear deformation and rigid-body translation is calculated identically in the two methods. The difference in sheating-to-framing connection deformation depends on the fact that method A accounts for the fasteners along the internal stud while method B only considers the fasteners along the sheating-panel perimeter.

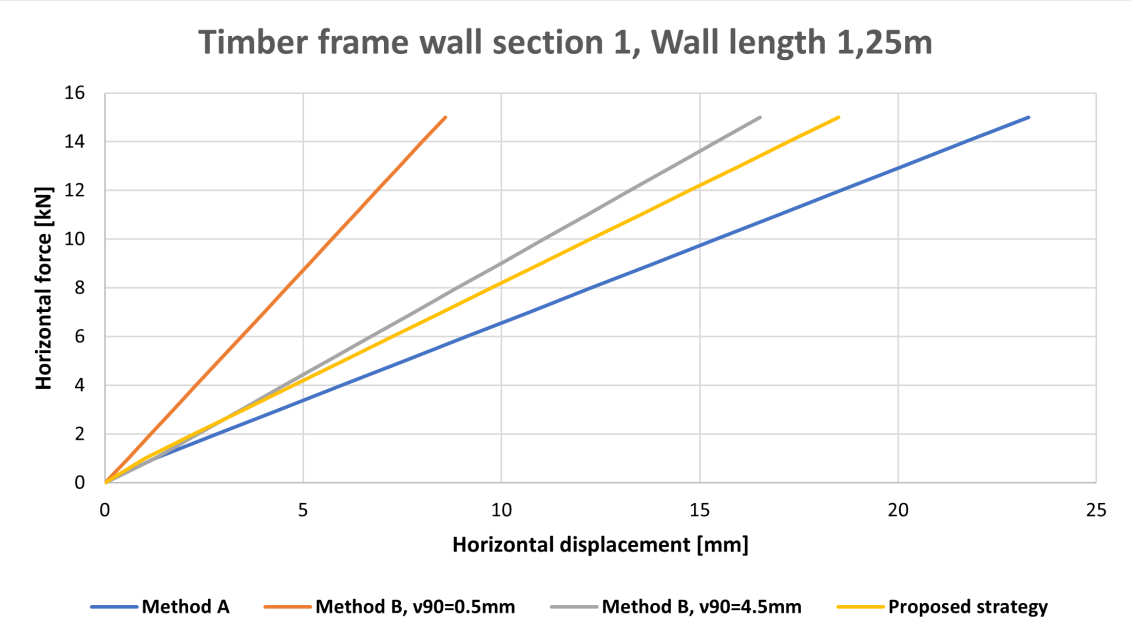

Figure 7.2: Load-displacement relation for timber frame wall-section 1 under 1kN/m evenly distributed vertical load calculated with method A and B compared to the proposed modelling strategy.

In figure 7.2 it can be seen that method B calculates a higher stiffness than both method A and the proposed strategy. The alteration of the allowed sill plate deformation does however become some what arbitrary due to the inevitable discrepancy between the allowed deformation and the actual deformation. That the proposed method is stiffer than method A is reasonable due to the consideration of friction and weak axis capacities of the connectors, see section 7.4.

7.3 Cross-laminated timber stiffness

Figure 7.3 shows the deformation distribution for CLT-wall-section 2 with properties as described in section 1.3.1. In figure 7.4 the load-displacement relations under 1kN/m evenly distributed vertical load is shown. Further, in figure 7.5 the deformation distribution for CLT-wall-section 3 is shown and in figure 7.6 is the corresponding load-displacement diagram. The calculations follows the equations in chapter 4. In both figure 7.4 and 7.5 the stiffness assessment methods are compared to the proposed modelling strategy in chapter 6 modelled with a laminate stiffness definition.

Wall-sections 2 and 3 are constructed so that wall-section 3 has a more uneven relation between the stiffness in x- and y-direction. More specifically the vertical board layers of section 3 has double the thickness of the horizontal layers. The parameters concerning the connections has been left unchanged between the two sections. Comparing figure 7.3 and 7.5 we can see that the stiffer wall-section 3 generates less material based deformations (shear and bending) than wall-section 2. However, the changes in magnitude of the total deformation is generally very small as can be seen in the load-displacement diagrams in figure 7.4 and 7.6. It can also be noted in the load-displacement diagrams that method D and E are stiffer than the other methods. This can be explained by their consideration of weak axis capacities of hold-downs and angle brackets and their inclusion of friction in the calculation of rigid-body translation. Which is further shown in the deformation distribution where method D and E show a significantly lower share of translation deformation.

The authors of the stiffness assessment methods have different opinions on which layers of the cross-laminated timber build-up to consider for the shear deformation. Gavric et al. (2015) assumes in method D that only the vertical board layers will contribute while the other methods calculates using the full wall thickness. In methods B, C and E the shear modulus is instead reduced with individual approaches as can be seen in table 7.5. Methods A and D makes no reductions and simply uses the shear modulus averaged over the wall thickness.

Table 7.5: Comparison of effective shear modulus calculated for wall section 2 with stiffness assessment methods A-E. Where wall-section 2 has an average shear modulus of 690MPa.

Stiffness assessment method	**Effective shear modulus [MPa]**	**Reduction [%]**
Method A	690	0
Method B	574	-16.8
Method C	518	-24.9
Method D	690	0
Method E	539	-21.9

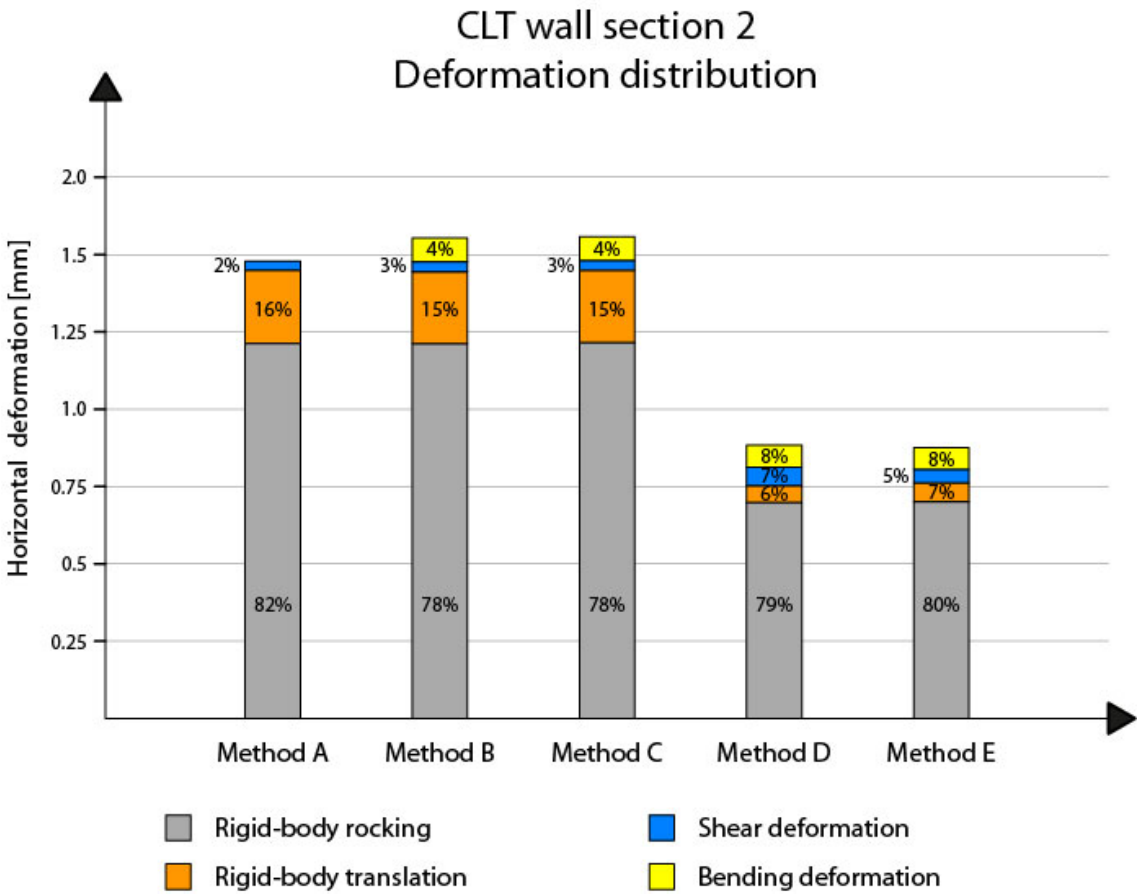

Figure 7.3: Deformation distribution between modes of deformation for CLT-wall-section 2 under vertical and horizontal unit loads calculated with methods A-E.

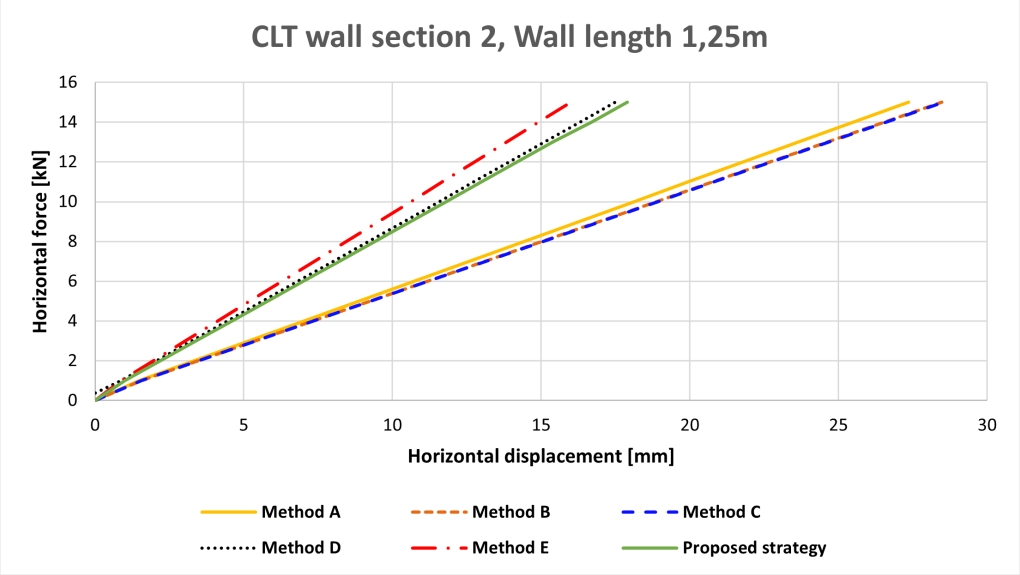

Figure 7.4: Load-displacement relation for CLT-wall-section 2 under 1kN/m evenly distributed vertical load calculated with methods A-E compared to the proposed modelling strategy.

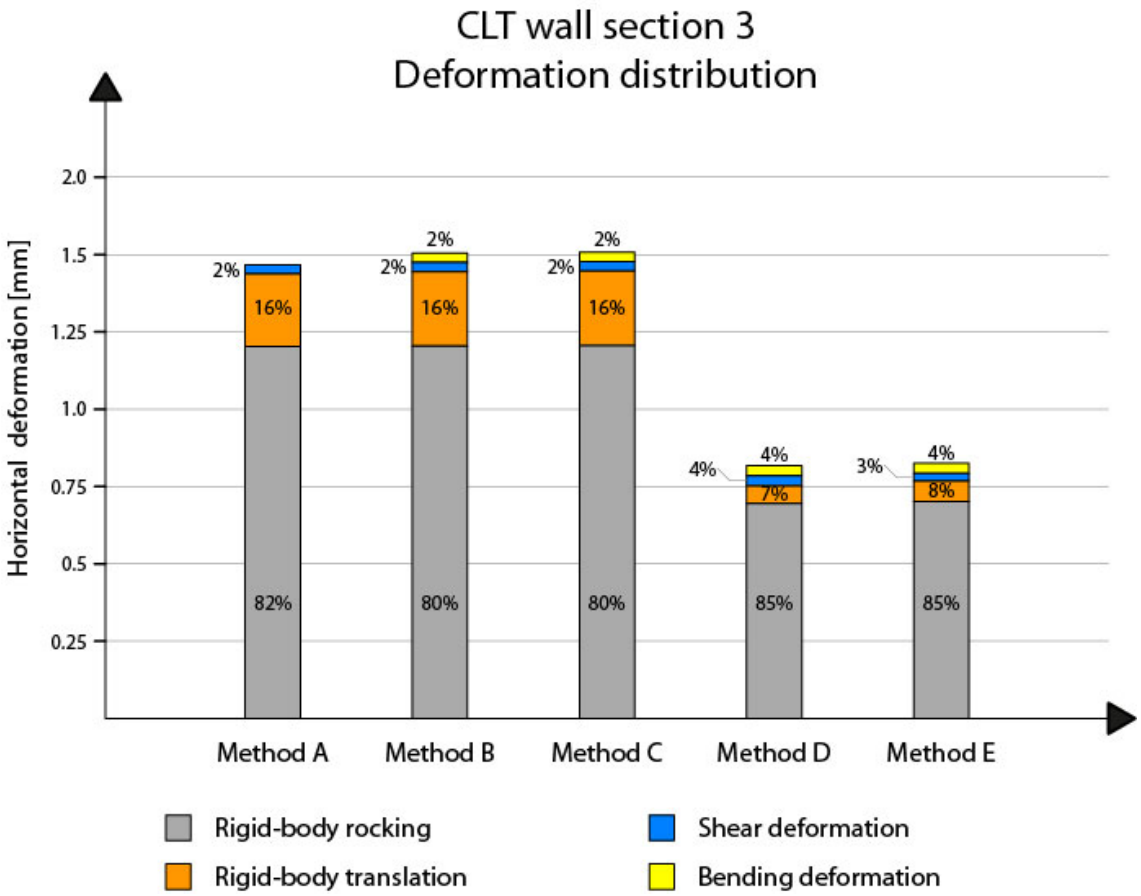

Figure 7.5: Deformation distribution between modes of deformation for CLT-wall-section 3 under vertical and horizontal unit loads calculated with methods A-E.

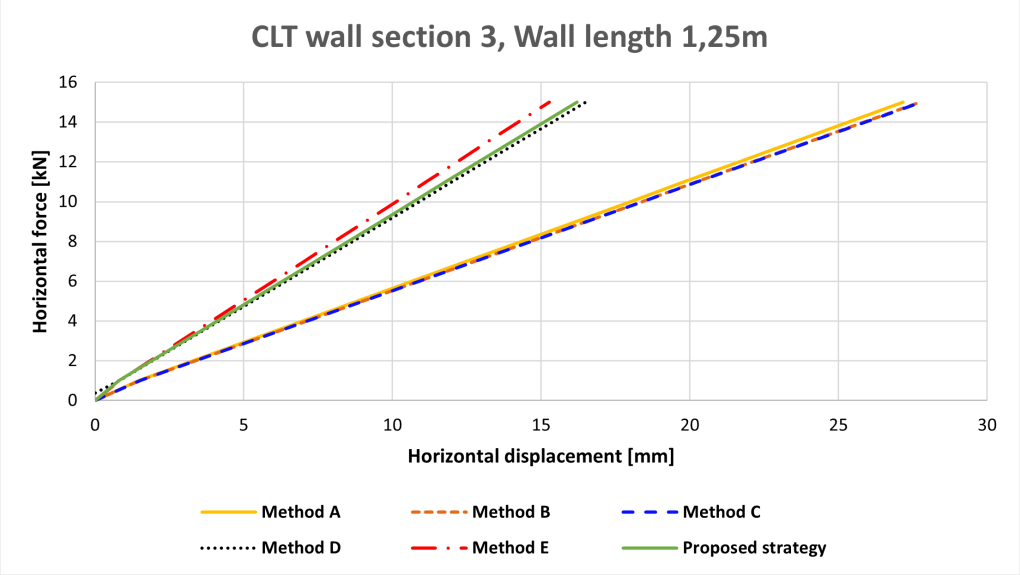

Figure 7.6: Load-displacement relation for CLT-wall-section 3 under 1kN/m evenly distributed vertical load calculated with methods A-E compared to the proposed modelling strategy.

7.3.1 Wall length influence on deformation distribution

In this section a comparison is made between the deformation distribution of a 1.25m and 3.5m long wall. Both walls has a height of 2.8m and identical properties according to wall-section 2. In figure 7.7 and 7.8 the load displacement diagrams can be seen and figure 7.9 visualizes the changes in deformation distribution between the two wall lengths.

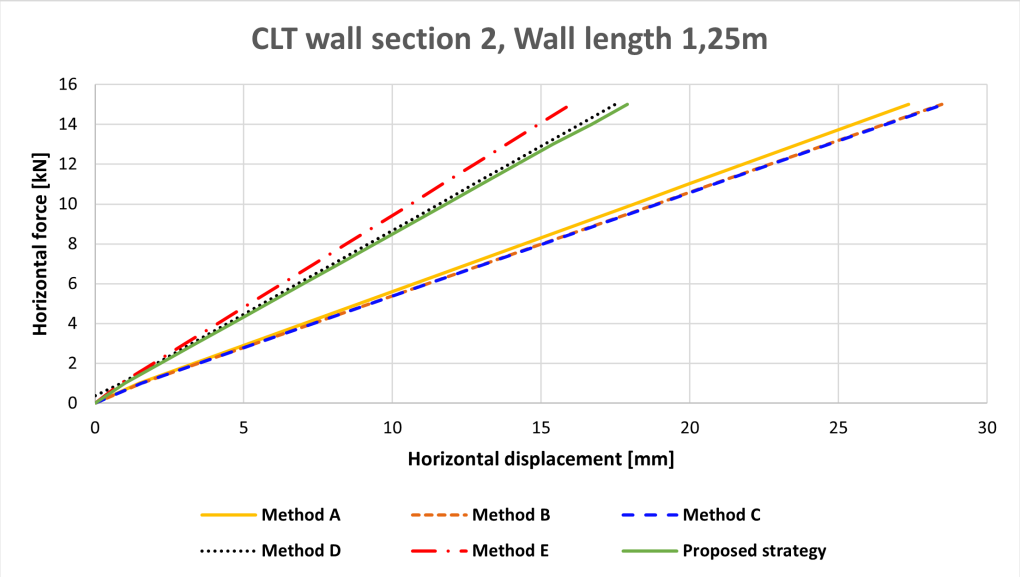

Figure 7.7: Load-displacement relation for a 1,25m long cross-laminated timber wall with wall-section 2 under 1kN/m evenly distributed vertical load calculated with methods A-E compared to the proposed modelling strategy.

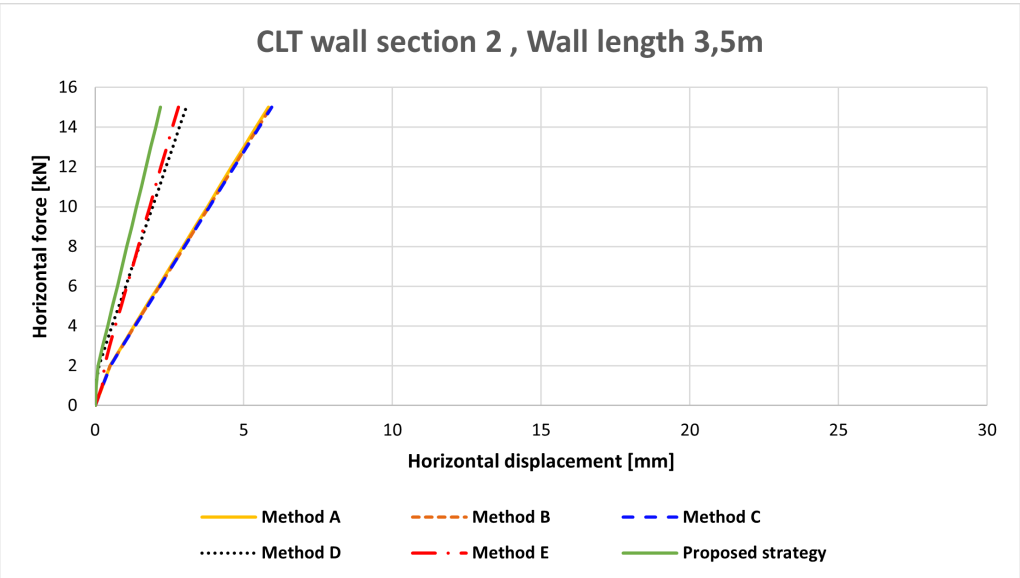

Figure 7.8: Load-displacement relation for a 3,5m long cross-laminated timber wall with wall-section 2 under 1kN/m evenly distributed vertical load calculated with methods A-E compared to the proposed modelling strategy.

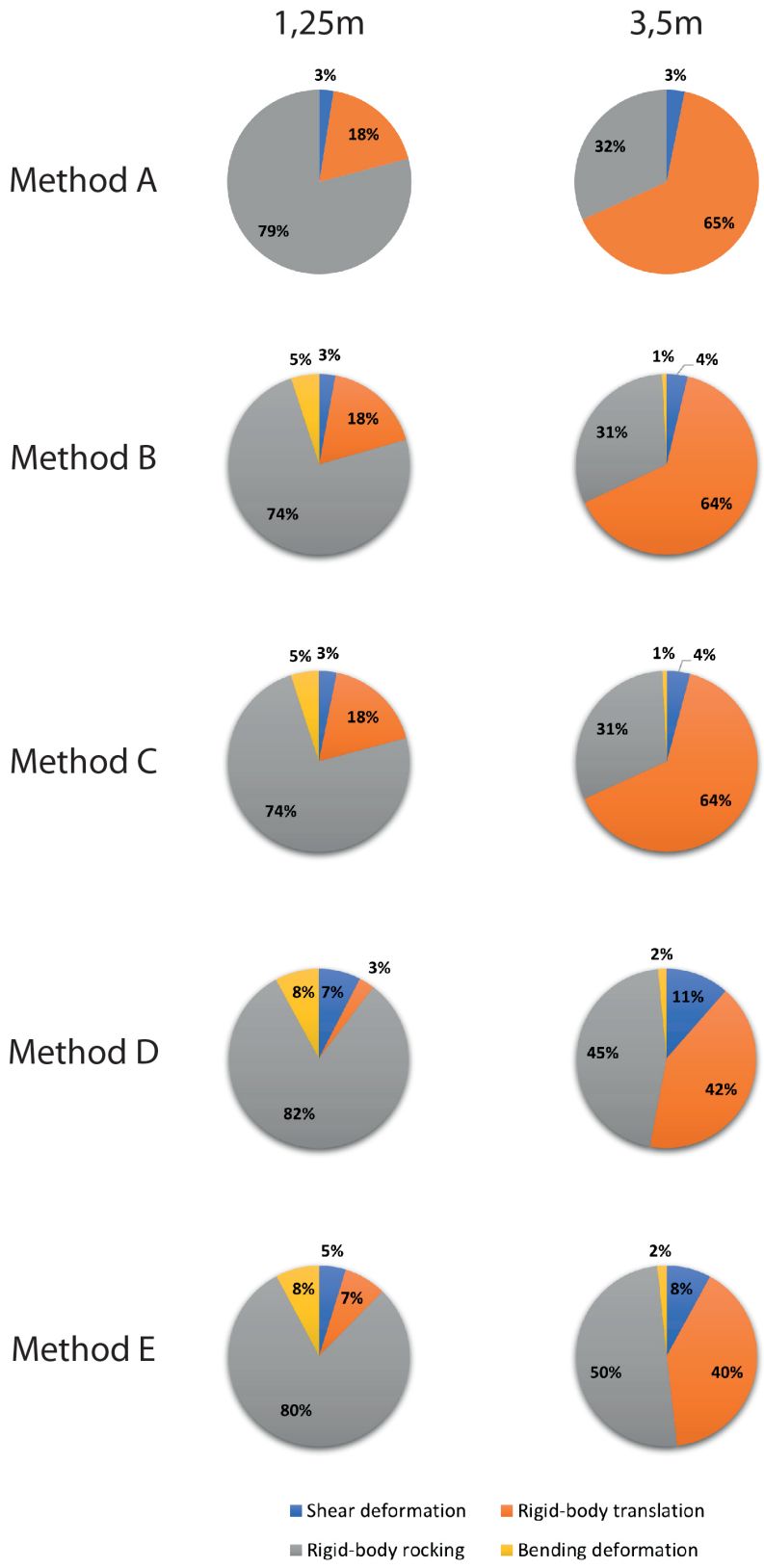

Figure 7.9: Comparison of deformation distribution for a 1.25m and 3.5m long cross-laminated timber wall calculated with methods A-E. The horizontal load is individually calibrated to achieve the same total deformation for all methods.

The horizontal displacements at 15kN horizontal load has been extracted from the load displacement diagrams in figures 7.7 and 7.8 and are summarized in table 7.6 to showcase the significant increase of stiffness with an increased wall length. As seen in figure 7.9 the deformation distribution also changes when the wall length increases. Most notable is the shift in connector based deformation from rocking deformation to translation deformation. An intuitive shift since the longer wall will need much more for force to reach uplift. The material based deformations shear and bending holds a fairly equal share of the distribution as the increased sectional properties of longer wall reduces their deformation.

Table 7.6: Change in horizontal deformation between a 1,25 and 3,5m long cross-laminated timber shear wall with wall-section 2 under 1kN/m evenly distributed vertical load. Calculated with methods A-E and compared with the proposed strategy.

	1,25m wall, horizontal displacement [mm]	**3,5m wall, horizontal displacement [mm]**	**Diff. [%]**
Method A	27.36	5.83	-78.70
Method B	28.48	5.91	-79.25
Method C	28.54	5.93	-79.21
Method D	17.49	3.01	-82.46
Method E	16.00	2.80	-82.52
Proposed strategy	17.90	2.20	-87.71

7.3.2 Material definition

The stiffness matrices of wall section 2 and 3 has been calculated using the transformed section method and the multi-layer composite method described in sections 2.5.1 and 2.5.2. In table 7.7 and 7.8 comparisons of the stiffness matrix elements are presented for each wall section.

Table 7.7: Stiffness matrix elements for wall section 2. Comparison between the transformed section method and the multi-layer composite method by Dlubal Software GmbH. (2016).

Stiffness matrix element	**Transformed section method**	**Multi-layer composite method**	**Diff. [%]**
D_{11} **[kNm]**	562.3	732.4	+30.25
D_{22} **[kNm]**	385.2	215.1	-44.16
D_{33} **[kNm]**	57.5	57.5	0
D_{44} **[kN/m]**	7139.2	10731.3	+50.32
D_{55} **[kN/m]**	4020.4	6594.8	+64.03
D_{66} **[kN/m]**	674800.0	674800.0	0
D_{77} **[kN/m]**	462200.0	462200.0	0
D_{88} **[kN/m]**	69000.0	69000.0	0

Table 7.8: Stiffness matrix elements for wall section 3. Comparison between the transformed section method and the multi-layer composite method by Dlubal Software GmbH. (2016).

Stiffness matrix element	**Transformed section method**	**Multi-layer composite method**	**Diff. [%]**
D_{11} **[kNm]**	2847.6	3357.8	+17.92
D_{22} **[kNm]**	1033.4	523.1	-49.38
D_{33} **[kNm]**	235.5	235.5	0
D_{44} **[kN/m]**	15614.7	23232.5	+48.79
D_{55} **[kN/m]**	4395.3	7885.3	+79.40
D_{66} **[kN/m]**	1334800	1334800	0
D_{77} **[kN/m]**	484400	484400	0
D_{88} **[kN/m]**	110400	110400	0

To investigate the influence of the material definition on the horizontal displacement 4 test configurations are set up (see figure 7.10) and tests are performed combining the two wall sections with the two material definitions and the four test configurations. The walls are subjected to 1kN/m evenly distributed vertical and horizontal load on the top edge of each wall panel. Further the properties and assumptions presented in table 7.1 has been applied. The global maximum horizontal displacements are presented in table 7.9.

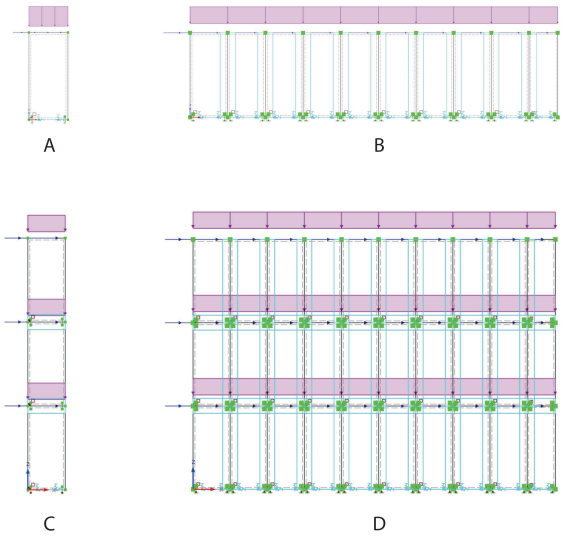

Figure 7.10: Test configurations A-D extracted from the reference structure for material definition influence investigation.

Table 7.9: Comparison of horizontal displacement of test configurations A-D between the transformed section method and the multi-layer composite method by Dlubal Software GmbH. (2016).

Wall section	**Test configuration**	**Orthotropic horizontal displacement [mm]**	**Laminate horizontal displacement [mm]**
2	A	0.5	0.5
3	A	0.5	0.5
2	B	0.5	0.5
3	B	0.4	0.4
2	C	15.4	15.4
3	C	13.6	13.6
2	D	5.4	5.4
3	D	5.1	5.1

The result shows that the material definitions influence on the horizontal deformation is negligible when studying a shear wall subjected to in-plane loading. Further, it shows that scaling the structure to a system of $3x1$, $1x10$ or $3x10$ walls does not alter the influence.

7.4 Friction and weak axis capacities

As described in section 5.3, including the frictional force in a large scale building model implies load case specific calculations of the force magnitude. The influence on the horizontal deformation of a cross-laminated timber shear wall from implementation of the friction force is therefore studied to clarify if the calculations should be justified. As the friction coefficient depends on the two materials sliding against each other, the friction coefficient used for the wall-to-foundation connection is 0.6 (assumed as a concrete slab), Aira et al. (2014). In the FE-model the friction is considered as an added stiffness in the axial direction of the linear release between foundation/floor and the wall panel. The studied wall has the properties of wall section 2 and is modelled with the proposed modelling strategy described in chapter 6. Further, it is loaded with 1kN/m evenly distributed load vertically along the upper wall edge. The resulting load-displacement diagram from the test is presented in figure 7.12 and a stiffness comparison in table 7.10.

In figure 7.11, 7.12 and table 7.10 the influence on the horizontal and vertical deformation from consideration of the weak axis strength capacitites of hold-downs and angle brackets is also presented. The vertical stiffness components is modelled with springs at the discrete positions of the connectors and the horizontal stiffness is averaged over the wall length and modelled with a line support.

Table 7.10: Influence on horizontal and vertical deformation of a cross-laminated timber shear wall from consideration of friction force and weak axis capacities of connectors.

Consideration	**Total horizontal deformation reduction** [%]	**Total vertical deformation reduction** [%]
Friction	-11.1	0
Weak axis strength	-22.2	-27.2

The results in figures 7.11, 7.12 and table 7.10 show that both the friction force and the weak axis capacities increase the stiffness of the wall. The larger increase being the added strength capacity from the weak axis of the connectors which is significant in both horizontal and vertical direction.

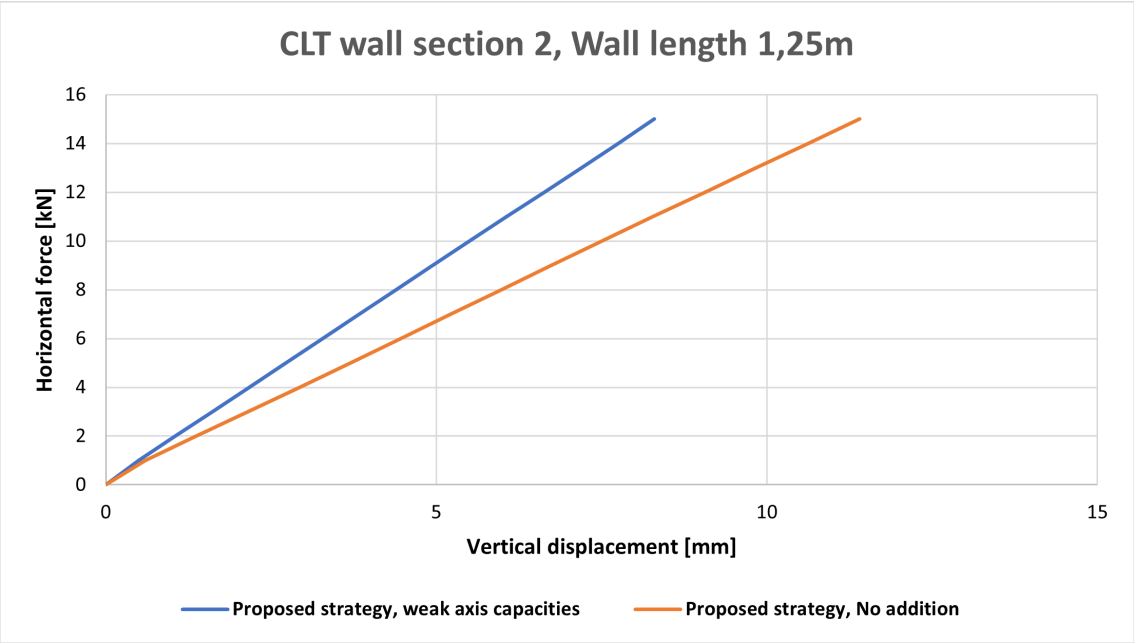

Figure 7.11: Load-displacement diagram showing the influence of consideration of weak axis capacities on the vertical displacement of a cross-laminated timber shear wall.

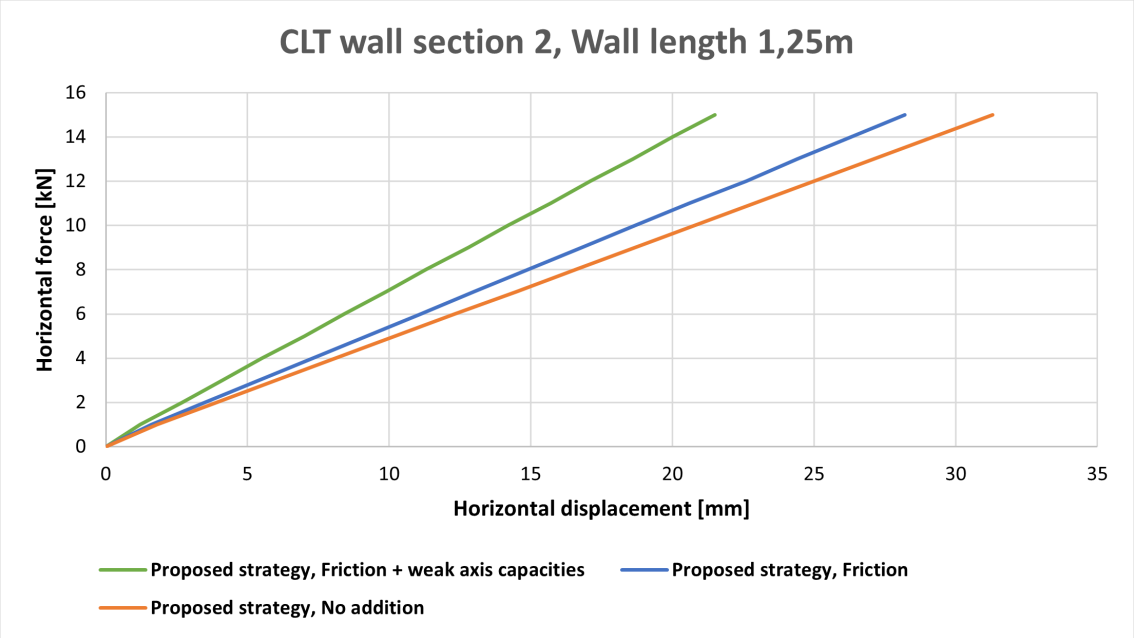

Figure 7.12: Load-displacement diagram showing the influence of friction and consideration of weak axis capacities on the horizontal displacement of a cross-laminated timber shear wall.

7.5 Foundation rigidity

Method B and C takes into account the rigidity of the shear walls underlying structure. To investigate the influence of this parameter on the horizontal deformation a cross-laminated timber shear wall has been modelled with three different types of foundation. Firstly a rigid foundation as would be the assumption for a concrete slab. Secondly an elastic foundation mimicking an upper-level cross-laminated timber floor with $E_{90,mean} = 370$MPa. Thirdly an elastic foundation with the Young's modulus E_{xx} of the wall section at hand. Thus mimicking the situation where the walls are placed directly upon each other and the floor is attached externally instead of sandwiched in between the wall panels. The shear wall is loaded with 1kN/m evenly distributed load vertically and horizontally along the upper wall edge. The results from the test are presented in table 7.11.

Table 7.11: Influence of foundation rigidity on the horizontal displacement of cross-laminated timber shear walls.

Foundation rigidity	**Global horizontal displacement [mm]**	**Diff. [%]**	**Global vertical displacement [mm]**	**Diff. [%]**
Wall section 2				
Rigid Concrete slab	0.739		0.170	
Elastic Timber floor	0.877	+18.7	0.187	+10.0
Elastic Timber wall	0.739	0.0	0.170	0.0
Wall section 3				
Rigid Concrete slab	0.440		0.153	
Elastic Timber floor	0.590	+34.1	0.171	+11.8
Elastic Timber wall	0.440	0.0	0.153	0.0

The results in table 7.11 shows that the foundation rigidity has a large impact on the displacement both vertically and horizontally. Wall section 3, being stiffer than wall section 2, shows a larger increase in horizontal displacement while the increase in vertical displacement is similar between the wall sections. Further the major axis in-plane Young's modulus of both wall sections provide enough stiffness to behave as rigid.

7.6 Stacked walls

To evaluate the behaviour of the wall-to-floor connection and how the global rocking deformation accumulates for each added floor level. A study has been made on the magnitude of the rocking deformation as a result of the position of the shear walls center-of-rotation. In figure 7.13 twelve storeys of stacked shear walls are subjected to a unit rotation and a unit vertical and horizontal load respectively. The resulting difference in deformation between having the center-of-rotation at the middle of the wall base and the corner point of the wall base is then presented in figures 7.14 and 7.15.

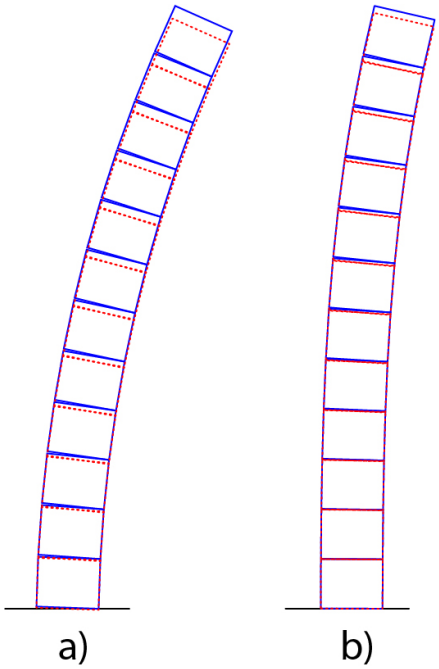

Figure 7.13: Rocking deformation of a 12-storey shear wall with center-of-rotation at the middle point of the wall base (red) and at the right corner point (blue). a) each storey is subjected to a unit rotation. b) each storey is subjected to a unit vertical and horizontal load.

The results in figure 7.14 shows that with an equal rotation of each floor level the horizontal deformation with rotation around the corner point of the wall base lies between 0.2-2% per degree of rotation higher than with rotation around the middle point of the wall base. The magnitude depends on the amount of floors and the length of the wall. Where a longer wall and more floors equals a larger difference. This is however a highly theoretical case since the vertical load transfer in a building would accumulate higher forces in the lower floors and thus lead to less rotation. In figure 7.13 case b), instead of an imposed unit rotation, the 12-storey shear wall is subjected to a unit vertical and horizontal load per floor. It can be seen in figure 7.15 that this leads to more similar results for the two methods with a difference between 0.1-1.5%. However with further added floors the difference would increase rapidly.

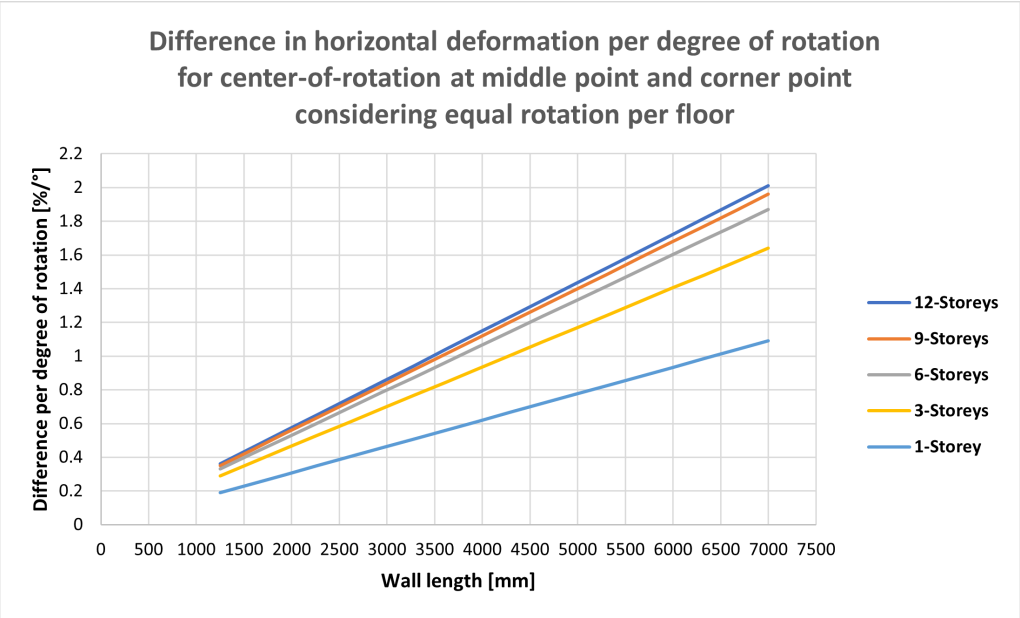

Figure 7.14: Difference in horizontal rocking deformation per degree of rotation for 2.8m high shear walls in various storeys with center-of-rotation at the wall base middle point compared to center-of-rotation at the wall base corner point (presented as a percentage of the total deformation with center-of-rotation at the corner point). All storeys subjected to a unit rotation.

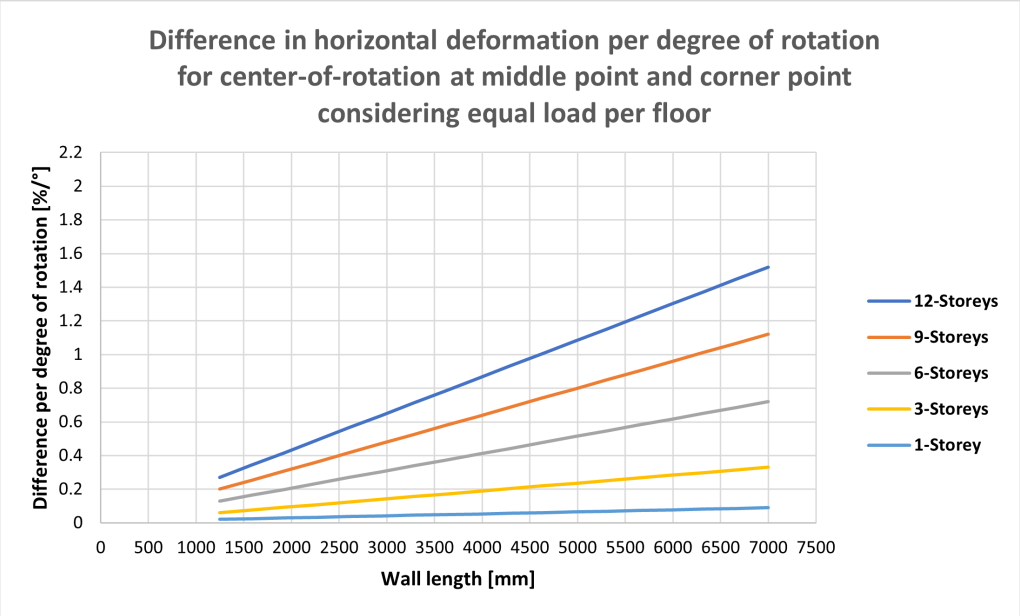

Figure 7.15: Difference in horizontal rocking deformation per degree of rotation for 2.8m high shear walls in various storeys with center-of-rotation at the wall base middle point compared to center-of-rotation at the wall base corner point (presented as a percentage of the total deformation with center-of-rotation at the corner point). All storeys subjected to a unit vertical and horizontal load.

7.7 Vertical joint

To understand the deformation behaviour of the vertical joint between two parallel adjacent wall panels a close study was made on the influence of a horizontal stiffness component along the vertical joint in combination with the more intuitive vertical stiffness component representing the connector stiffness. The study comprises of two adjacent walls loaded with a 1kN/m evenly distributed vertical load and a 1kN/m horizontal load along the top horizontal edge, see figure 7.16. The vertical joint is then modelled with a vertical stiffness and three different conditions for the horizontal stiffness; with horizontal stiffness set to zero, with horizontal stiffness equal to the vertical stiffness and with a pressure contact condition between the wall panels. The horizontal displacement is then studied both globally and locally at the top of the vertical joint. The results are presented in table 7.12 and shows that the horizontal stiffness component of the vertical joint has a relatively small influence on the global horizontal displacement.

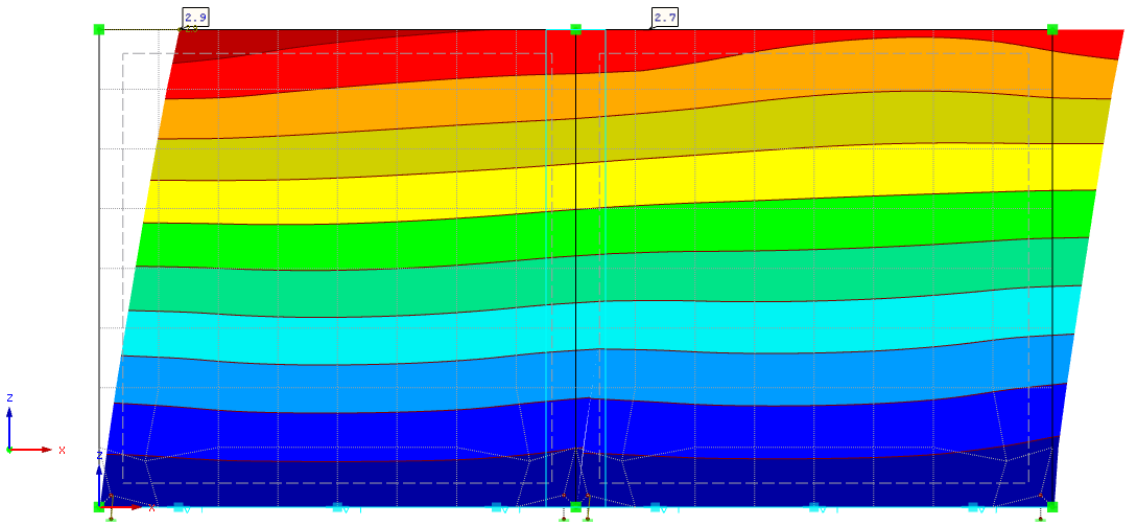

Figure 7.16: Horizontal displacement of two cross-laminated timber shear walls connected with horizontal pressure contact in the vertical joint.

Table 7.12: Impact of the horizontal stiffness in the vertical joint on the horizontal displacement of cross-laminated timber shear walls.

Horizontal stiffness	**Global horizontal displacement [mm]**	**Diff. [%]**	**Local horizontal displacement [mm]**	**Diff. [%]**
Pressure contact	2.93		2.70	
Equal to vertical stiffness	3.08	+5.1	2.90	+7.4
No stiffness	3.17	+8.2	3.10	+14.8

7.8 Automatic linearization

To showcase the need for precautions in modal analysis of timber shear walls, tests on how non-linear springs are linearized in linear dynamic analysis has been conducted for two commercially available finite-element softwares; SOFiSTiK (2020) and Dlubal Software GmbH (2016). The test procedure is described in section 5.6. In table 7.13 the inserted bi-linear work laws and the resulting linear stiffnesses k_{ef} from the linear dynamic analysis are presented. Figure 7.17 visualizes the parameters in table 7.13.

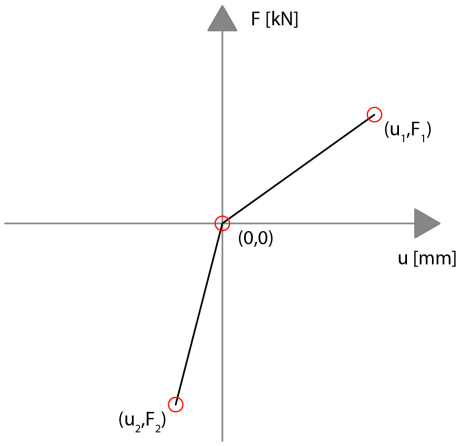

Figure 7.17: Parameter visualization of the bi-linear stiffness work laws applied to the springs in the linear dynamic analysis test. A positive force indicates tension and a negative compression.

Table 7.13: Linearization of non-linear springs in linear dynamic analysis calculated in SOFiSTiK (2020) and Dlubal Software GmbH (2016). Forces are given in kN, displacements in mm and stiffness in kN/mm.

	Stiffness parameters				**Applied force**	**Displacement**	**Equivalent stiffness**
	u_1	F_1	u_2	F_2	F	u	k_{eq}
SOFiSTiK							
1	1	2	-1	-1	1	0.5	2
2	1	2	-1	-1	-1	-0.5	2
3	1	1	-1	-2	1	0.5	2
4	1	1	-1	-2	-1	-0.5	2
Dlubal							
1	1	2	-1	-1	1	0.5	1
2	1	2	-1	-1	-1	-0.5	1
3	1	1	-1	-2	1	0.5	1
4	1	1	-1	-2	-1	-0.5	1

The results from the linearization test shown in table 7.13 points out the issue where different finite-element softwares treat the same task differently. Where SOFiSTiK takes the largest stiffness value of the two branches and Dlubal takes the smallest one and applies as a linear stiffness.

7.9 Equivalent linear stiffness

In figure 7.18 a cross-laminate timber shear wall modelled with the proposed method F is linearized with the procedure used by the software Acord, described in section 5.6. The top wall edge is loaded with 1kN/m in vertical and horizontal direction. As seen in the distribution of the support forces the elastic material definition, pressure contact condition and modelling of discrete hold-downs of the left model generates a center-of-rotation at about 20% of the wall length from the leeward corner. While the linearized model has its center-of-rotation originating at the middle point of the wall base which is then offset slightly to the windward corner due to the vertical load. The horizontal displacement as seen in figure 7.19 becomes the same for the two models. Vertically however, the displacement is the same but shifted downward in the global coordinate system due to the altered center-of-rotation, see figure 7.20.

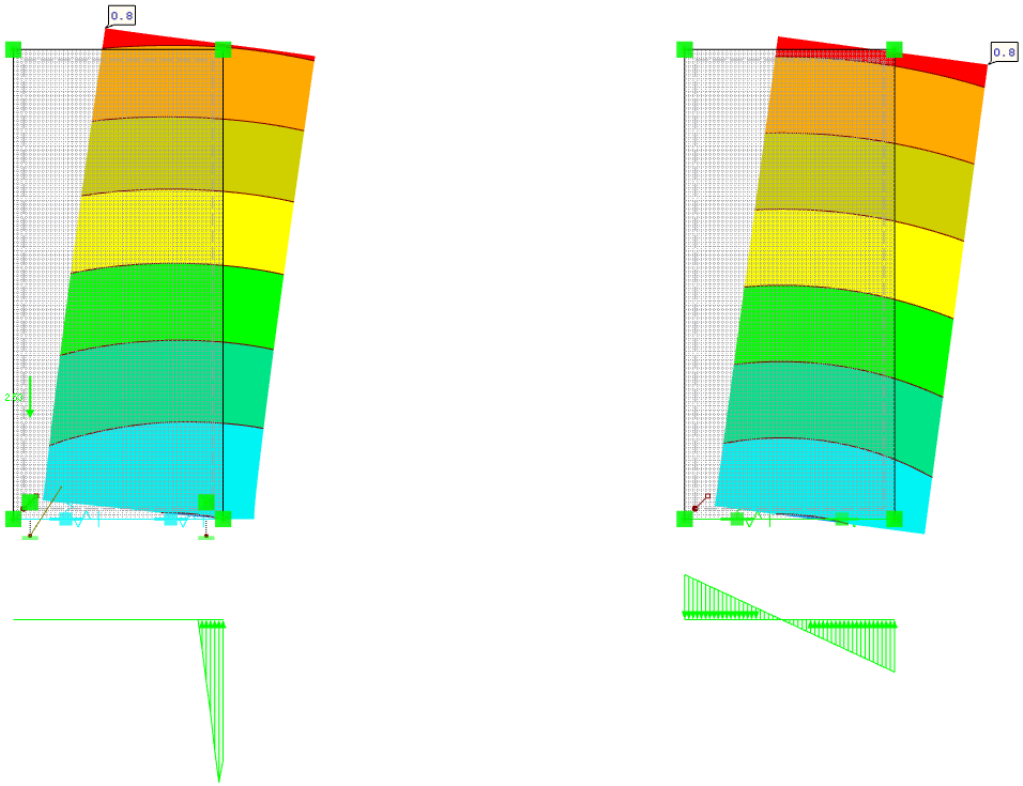

Figure 7.18: Global displacement of a cross-laminated timber wall modelled with the proposed method F (left) and a rigid body on calibrated equivalent linear stiffness springs (right).

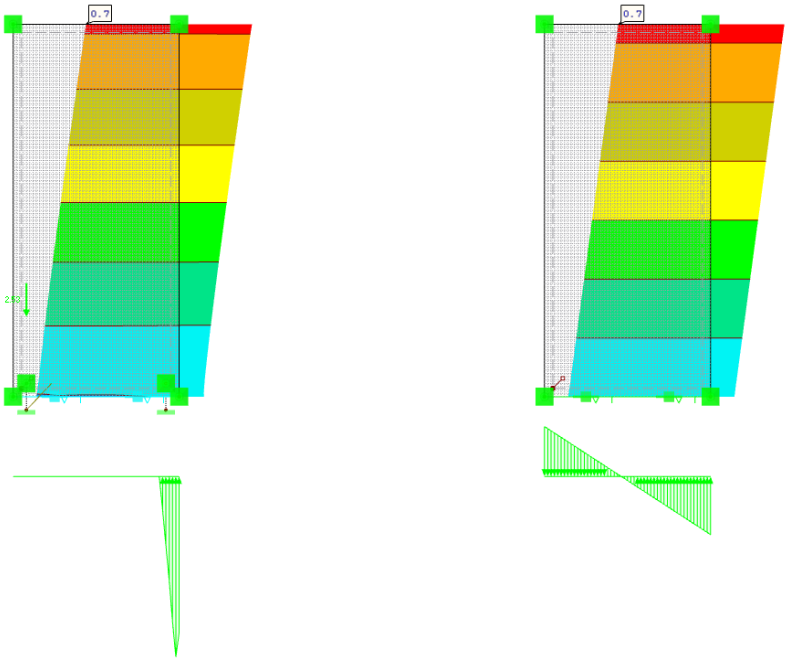

Figure 7.19: Horizontal displacement of a cross-laminated timber wall modelled with the proposed method F (left) and a rigid body on calibrated equivalent linear stiffness springs (right).

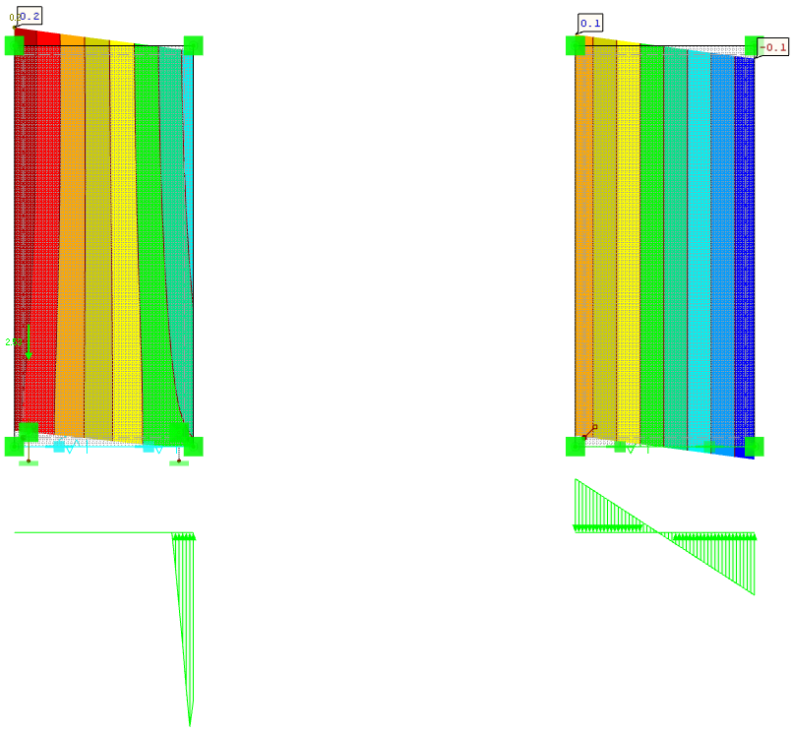

Figure 7.20: Vertical displacement of a cross-laminated timber wall modelled with the proposed method F (left) and a rigid body on calibrated equivalent linear stiffness springs (right).

8

Conclusions

8.1 Proposed finite-element modelling strategies

The finite-element modelling strategy proposed in chapter 6 is in many ways a straight forward method. The material definition is premiered to resemble the real world properties of the wall and handle the material based deformations. While the behaviour of the connectors are simplified to a system of 2-degree-of-freedom nodes. From there each connector is separated into its vertical and horizontal stiffness which then is modelled in separate elements. Further, when several stiffnesses align they are lumped together in linear releases/hinges or line supports. The important part is that although the modelling is simplistic, it does not reduce the possibility to read out results in each direction of each connector and member as well as across wall surfaces and at their boundaries. Within the conducted tests of cross-laminated timber shear walls it is shown that the proposed modelling strategy has a stiffness similar to that of stiffness assessment methods D and E. This is reasonable since they share the consideration of friction and weak axis strength capacities of the connectors. For timber frame shear walls the proposed modelling strategy is shown to be stiffer than method A which is deemed expected due to the consideration of friction and weak axis strength capacities. The results from method B for timber frame shear walls is however more unreliable due to the influence of the allowed sill plate deformation. With a strict limitation of the allowed sill plate deformation method B shows a lot higher stiffness than both method A and the proposed strategy but further investigations of the actual rocking deformation is needed to assess the viability of method B concerning timber frame shear walls.

8.2 Stiffness reduction factors

Since there is no consensus in the definition of the reduction factors k_{33}, k_{44}, k_{55} and k_{88} special thought needs to be put into the design. If the wall at hand will face particular loads more conservative reduction factors could be viable. The application of the reduction factors will vary depending on the used finite-element software but in general caution should be taken if the program applies factors "under the hood" based on settings such as consideration of shear coupling or whether the short edges of the cross-laminated timber are glued. If the user reduces the input stiffness and the program then applies further reductions the stiffness could be largely underestimated.

8.3 Wall length influence

Due to the high stiffness of cross-laminated timber a general behaviour is that the connection based deformations accounts for the larger part of the total wall deformation. For a shorter wall most of the deformation comes from rocking of the wall. What is noted in section 7.3.1 is that when the wall length is increased the deformation distribution changes. Considering the material based deformations (shear and bending) they naturally decrease when the wall becomes longer due to the increased section. However, the major change in behaviour is the reduction of the rocking deformation and increase of translation deformation. This transformation can be beneficial to keep in mind when designing as for instance a longer wall at a lower floor could reduce the total rocking behaviour of tall building significantly.

8.4 Stacked walls

As shown in section 7.6 the stacking of walls entails an accumulation of potential over- or under-estimations of the rocking behaviour if the center-of-rotation is not correct. The actual position of the center-of-rotation is load and stiffness dependent and can essentially be anywhere along the the wall base. With the proposed modelling strategy this uncertainty is minimized since the center-of-rotation is governed by the wall elasticity.

8.5 Horizontal stiffness in vertical joint

Since the studied walls always are supported along the full length of their wall base the linear release imposing the pressure contact condition between stacked walls only has to be one-sided (keeping the higher floor from displacing into the lower floor). Looking at the vertical joint between adjacent panels the pressure contact condition has to be valid in two directions unless the direction of the resulting moment is known beforehand. This becomes an issue in the FE-model since duplicate line releases between adjacent surfaces leads to the intermediate line being completely uncoupled and the model being unstable. The test conducted in section 7.7 shows that the influence on the horizontal deformation based on a horizontal stiffness in the vertical joint is within reasonable magnitudes from the pressure contact condition. Within the literature studied for this thesis it has not been proposed to include a horizontal stiffness at the vertical joint but rather only have the walls connected vertically. The motivation to add this horizontal stiffness to the proposed method is based on the fact that a screw connection essentially would have the same stiffness capacity in the horizontal direction. Especially when the shear-plane is in the plane of the wall such as for a half-lapped joint or spline joint. Even if the windward wall is deflecting more without the pressure contact condition it should be noted that setting a horizontal spring stiffness instead of a pressure contact condition will reduce the transfer of displacement between the walls in the same floor level. The foundation rigidity study in section 7.5 shows that a wall-to-wall connection behaves rigidly for the tested wall sections. Assuming a somewhat similar behaviour in the

orthogonal direction would mean that a pressure contact condition would be more accurate. The modelling complications becomes governing in this case and the deformation reduction should be noted.

8.6 Timber frame shear wall rocking behaviour

The actual rocking behaviour of a timber frame shear wall is not a rigid-body motion and the estimation of the behaviour as compression of the sill plate and elongation of the hold-down combined with the axial deformation of the studs as presented in method B might be a better interpretation. The allowed sill plate deformation does however influence the stiffness evaluation harshly. In the report the parameter is set based on the material strength leading to a very stiff wall in comparison to the rigid-body behaviour assumed in method A. The calibration of the allowed deformation to show equal displacement under unit load is made to showcase the load case specific deformation distribution. At the same time this load case dependency makes the alteration arbitrary. Rigorous tests are needed on the actual behaviour and the dependencies on material strength and cross-section level to further interpret the timber frame rocking behaviour.

8.7 Friction and weak axis capacities

As shown in section 7.4 considering friction and weak axis strength capacities of connectors brings significant reductions to deformations. The consideration of weak axis capacities is optional and can be added to increase the stiffness of the system. Based on the connector types and wall properties used in the conducted tests it is deemed viable to consider weak axis capacities since the deformation reduction reaches above 20% in both horizontal and vertical direction. The horizontal stiffness of the hold-downs does not demand an inclusion of more elements to the model since the stiffness of the already present linear spring along the wall base is simply increased. To account for the vertical stiffness a tension-only spring is however needed per angle bracket as the proposed modelling strategy models the vertical stiffness with discrete connector positions. To reduce the modelling effort an option could be to include the horizontal capacity and leave the vertical capacity out. Friction will naturally only affect the horizontal deformation and in the conducted tests the deformation reduction is just over 10%. Adding friction to the model does, just like the horizontal capacity of the hold-downs, not increase the number of elements in the model as stiffness is only added to already present springs. The friction force is however load case dependent which in a large scale model would increase work load for setting up the load cases.

8.8 Model linearization

The linearization performed in section 7.9 proves that a conversion from a non-linear model to a linear equivalent model with equal global deformation magnitudes is

possible. The conversion however implies an altered position of the center-of-rotation leading to a downward shift of the vertical displacement. The stacking of walls will then induce an accumulation of under-estimated global rocking deformation. With this deviance in mind this method can still be a good alternative for the purpose of linear dynamic analysis (modal analysis) as the automatic linearization applied by the studied softwares when calculating a non-linear model linearly is shown unreliable in section 7.8. The linearized model is only briefly discussed in this thesis and investigation on the behaviour with regards to the eigenfrequency of the structure is needed to claim viability of the conversion from non-linearity. As there is a risk that the bedding of equivalent stiffness springs will dampen the model differently under cyclic loads then in the proposed modelling strategy.

9
Further studies

1. Point loads and asymmetric load distributions
Within this thesis the behaviour of shear walls are studied under evenly distributed vertical and horizontal loads. Further investigations on the behaviour under point loads and asymmetric load distributions would be an interesting and natural next step.
2. Energy dissipation
Longer wall lengths might be positive to balance the ratio between rocking and shear deformation. However from a seismic analysis point of view the vertical joints between the wall panels plays an important role for the ductility of the structure dissipating the seismic energy. If the structure is too stiff the risk for brittle failures at connection points increases.

Bibliography

[1] Casagrande, D., Rossi, S., Sartori, T. & Tomasi, R. (2015), Proposal of an analytical procedure and a simplified numerical method for elastic response of single-storey timber shear walls. *Construction and Building Materials*, http://dx.doi.org/10.1016/j.conbuildmat.2014.12.114

[2] Aondio, P., Glaser, P. & Kreuzinger, H. (2020). FE-Berechnung von geklebtem Brettsperrholz - Teil 1:Theorie. *Bauingeniuer*, vol. 95(1), p. 22-25.

[3] Gavric, I. (2012), Seismic Behaviour of Cross-Laminated Timber Buildings. University of Trieste, http://dx.doi.org/10.13140/RG.2.2.29320.67845

[4] Gavric, I., Fragiacomo, M. & Cecotti, A. (2014), Cyclic behaviour of typical metal connectors for cross-laminated (CLT) structures, *Materials and Structures* vol. 48, p. 1841–1857. http://dx.doi.org/10.1617/s11527-014-0278-7

[5] Gavric, I., Fragiacomo, M. & Cecotti, A. (2015), Cyclic behaviour of CLT wall systems: Experimental tests and analytical prediction models. *Journal of Structural Engineering*, vol. 141(11), https://ascelibrary.org/doi/10.1061/%28ASCE%29ST.1943-541X.0001246

[6] Fragiacomo, M. (2013), Seismic Behaviour of Cross-Laminated Timber Buildings: Numerical Modelling and Design Provisions. Focus Solid Timber Solutions - Proceedings of the European Conference on Cross-Laminated Timber, TU Graz, COST Action FP1004, p. 166-182

[7] Tomasi, R. (2013), Seismic behavior of Connections for Buildings in CLT. Focus Solid Timber Solutions - Proceedings of the European Conference on Cross-Laminated Timber, TU Graz, COST Action FP1004, p. 138-151

[8] Wallner-Novak, M., Koppelhuber, J. & Pock, K. (2013), Information Cross-Laminated Timber Structural Design Basic Design and Engineering Principles According to Eurocode. *proHolz Austria*, p. 134-137

[9] Lukacs, I., Björnfot, A. & Tomasi, R. (2018), Strength and Stiffness of cross-laminated timber (CLT) shear walls: State-of-the-art of analytical approaches. *Engineering Structures*, vol. 178, p. 136-147,

https://doi.org/10.1016/j.engstruct.2018.05.126

[10] Hummel, J., Seim, W. & Otto, S. (2016). Steifigkeit und Eigenfrequenzen im mehrgeschossigen Holzbau. *Bautechnik*, vol. 93, p. 781-794.

[11] Hummel, J. & Seim, W. (2016). Assessment of dynamic characteristics of multi-storey timber buildings. World Conference on Timber Engineering 2016, https://www.researchgate.net/publication/330354311

[12] Popovski, M., Gagnon, S., Mohammad, M. & Chen, Z. (2019). *Canadian CLT handbook 2019 Edition*. vol. 1.

[13] D'Arenzo, G., Casagrande, D., Reynolds, T. & Fossetti, M. (2019). In-plane elastic flexibility of cross laminated timber floor diaphragms. *Construction and Building Materials*. vol. 209, p. 709-724, https://doi.org/10.1016/j.conbuildmat.2019.03.060

[14] Dlubal Software GmbH. (2016). RF-LAMINATE: Design of Laminate Surfaces. https://www.dlubal.com/-/media/Files/website/documents/manuals/rfem-and-rstab-add-on-modules/others/rf-laminate/rf-laminate-manual-en.pdf?mlid=A1793038DDBA4F60A129F84FD9B33209

[15] Gustafsson, A., Crocetti, R., Just, A., Landel, P., Olsson, J., Pousette, A., Silfverhielm, M. & Östman, B. (2019). *The CLT Handbook*. Swedish Wood.

[16] Kuhn, B. (2018). Considering end releases between surfaces. Dlubal Software GmbH. https://www.dlubal.com/en/support-and-learning/support/knowledge-base/001549

[17] Flatscher, G. (2017), Evaluation and approximation of timber connection properties for displacement-based analysis of CLT wall systems. *Monographic Series TU Graz/Timber Engineering & Technology*, vol. 6, DOI 10.3217/978-3-85125-557-7

[18] Schickhofer, G., Bogensperger, T., Moosbrugger, T., Augustin, M., Blaß, H., Ebner, H., Ferk, H., Fontana, M., Frangi, A., Hamm, P., Jöbstl, R. A., Richter, A., Thiel, A., Traetta, G. & Uibel, T. (2010), *BSPhandbuch Holz-Massivbauweise in Brettsperrholz Nachweise auf Basis des neuen europäischen Normenkonzepts*, ed. 2, Verlag der Technischen Universität Graz.

[19] SOFiSTiK. (2020). SOFiSTiK (Version 2020-8) [Computer software]. https://www.sofistik.de/

[20] TimberTech. (2013). TimberTech (Version 92) [Computer software]. https://en.timbertech.eu/

[21] Acord. (2022). Acord (Version 6.1) [Computer software]. https://acord.io/

[22] Acord. (2020). Acord-BAT 3D Manuel d'utilisation (Version 6.1). p. 120-125. https://acord.io/telechargements/manuels/

[23] DIN. (2016). DIN EN 338:2016, Structural timber - Strength classes. Deutsches Institut für Normung DIN.

[24] Jung, P. (2009), Bemessung von Scheiben. Holzbautag Biel 2009. p. 5. https://www.forum-holzbau.com/pdf/hbt09_jung_pirmin.pdf

[25] Aira, J.R., Arriaga, F., Íñiguez-González, G., Crespo, J. (2014). Static and kinetic friction coefficients of Scots pine (Pinus sylvestris L.), parallel and perpendicular to grain direction. Mater. Construcc. 64 [315], http://dx.doi.org/10.3989/mc.2014.03913

A

Appendix 1

A.1 Calculation of transformed section method for wall section 2

Stiffness matrix elements are calculated for a 1,25m long wall with properties of wall section 2 using the transformed section method as laid out in section 2.5.1.

Table A.1: Input data for the transformed section method of wall section 2. Young's modulus and shear modulus given in MPa.

Layer	**Mat.**	**Thickness [mm]**	**Dir. [°]**	$\mathbf{E}_0$	$\mathbf{E}_{90}$	$\mathbf{G}_{xz}$	$\mathbf{G}_{yz}$	$\mathbf{G}_{xy}$
1	C24	20	0	11000	370	690	69	690
2	C24	20	90	11000	370	690	69	690
3	C24	20	0	11000	370	690	69	690
4	C24	20	90	11000	370	690	69	690
5	C24	20	0	11000	370	690	69	690

Table A.2: Reduction factors for wall section 2.

Reduction factor	**Value**	**Reference**
κ_{33}	1	With glued short edges, Aondio et al. (2020)
κ_{44}	0.194	Gustafsson et al. (2019), Table 3.10
κ_{55}	0.152	Gustafsson et al. (2019), Table 3.10
κ_{88}	1	With glued short edges, Aondio et al. (2020)

Bending stiffness averaged over area:

$$E_{xx} = \frac{\sum_{i=1,3,5}^{n} E_0 A_i + \sum_{j=2,4}^{n-1} E_{90} A_j}{A_{tot}} = 6748\text{MPa} \tag{A.1}$$

$$E_{yy} = \frac{\sum_{i=1,3,5}^{n} E_{90} A_i + \sum_{j=2,4}^{n-1} E_0 A_j}{A_{tot}} = 4622\text{MPa} \tag{A.2}$$

Shear stiffness averaged over area and reduced with reduction factors in table A.2:

$$G_{xy} = \frac{\sum_{i=1}^{n} G_{xy,i} A_i}{A_{tot}} = 690\text{MPa} \tag{A.3}$$

$$G_{xz} = \kappa_{44} * \frac{\sum_{i=1,3,\ldots}^{n} G_{90} t_i + \sum_{j=2,4,\ldots}^{n-1} G_0 t_j}{t_{tot}} = 86\text{MPa} \tag{A.4}$$

$$G_{yz} = \kappa_{55} * \frac{\sum_{i=1,3,\ldots}^{n} G_0 t_i + \sum_{j=2,4,\ldots}^{n-1} G_{90} t_j}{t_{tot}} = 48\text{MPa} \tag{A.5}$$

Stiffness matrix elements:

$$D_{11} = E_{xx} \frac{t^3}{12} = 562.3\text{kNm} \tag{A.6}$$

$$D_{22} = E_{yy} \frac{t^3}{12} = 385.2\text{kNm} \tag{A.7}$$

$$D_{33} = G_{xy} \frac{t^3}{12} = 57.5\text{kNm} \tag{A.8}$$

$$D_{44} = G_{xz} \frac{5t}{6} = 7139.2\text{kN/m} \tag{A.9}$$

$$D_{55} = G_{yz} \frac{5t}{6} = 4020.4\text{kN/m} \tag{A.10}$$

$$D_{66} = E_{xx} t = 674800.0\text{kN/m} \tag{A.11}$$

$$D_{77} = E_{yy} t = 462200.0\text{kN/m} \tag{A.12}$$

$$D_{88} = G_{xy} t = 69000.0\text{kN/m} \tag{A.13}$$

A.2 Calculation of transformed section method for wall section 3

Stiffness matrix elements are calculated for a 1,25m long wall with properties of wall section 3 using the transformed section method as laid out in section 2.5.1.

Table A.3: Input data for the transformed section method of wall section 3. Young's modulus and shear modulus given in MPa.

Layer	**Mat.**	**Thickness [mm]**	**Dir. [°]**	$\mathbf{E}_0$	$\mathbf{E}_{90}$	$\mathbf{G}_{xz}$	$\mathbf{G}_{yz}$	$\mathbf{G}_{xy}$
1	C24	40	0	11000	370	690	69	690
2	C24	20	90	11000	370	690	69	690
3	C24	40	0	11000	370	690	69	690
4	C24	20	90	11000	370	690	69	690
5	C24	40	0	11000	370	690	69	690

Table A.4: Reduction factors for wall section 2.

Reduction factor	**Value**	**Reference**
κ_{33}	1	With glued short edges, Aondio et al. (2020)
κ_{44}	0.219	Gustafsson et al. (2019), Table 3.10
κ_{55}	0.147	Gustafsson et al. (2019), Table 3.10
κ_{88}	1	With glued short edges, Aondio et al. (2020)

Bending stiffness averaged over area:

$$E_{xx} = \frac{\sum_{i=1,3,5}^{n} E_0 A_i + \sum_{j=2,4}^{n-1} E_{90} A_j}{A_{tot}} = 8343\text{MPa} \tag{A.14}$$

$$E_{yy} = \frac{\sum_{i=1,3,5}^{n} E_{90} A_i + \sum_{j=2,4}^{n-1} E_0 A_j}{A_{tot}} = 3028\text{MPa} \tag{A.15}$$

Shear stiffness averaged over area and reduced with reduction factors in table A.2:

$$G_{xy} = \frac{\sum_{i=1}^{n} G_{xy,i} A_i}{A_{tot}} = 690\text{MPa} \tag{A.16}$$

$$G_{xz} = \kappa_{44} * \frac{\sum_{i=1,3,\ldots}^{n} G_{90} t_i + \sum_{j=2,4,\ldots}^{n-1} G_0 t_j}{t_{tot}} = 117\text{MPa} \tag{A.17}$$

$$G_{yz} = \kappa_{55} * \frac{\sum_{i=1,3,\ldots}^{n} G_0 t_i + \sum_{j=2,4,\ldots}^{n-1} G_{90} t_j}{t_{tot}} = 33\text{MPa} \tag{A.18}$$

Stiffness matrix elements:

$$D_{11} = E_{xx}\frac{t^3}{12} = 2847.6\text{kNm} \tag{A.19}$$

$$D_{22} = E_{yy}\frac{t^3}{12} = 1033.4\text{kNm} \tag{A.20}$$

$$D_{33} = G_{xy}\frac{t^3}{12} = 235.5\text{kNm} \tag{A.21}$$

$$D_{44} = G_{xz}\frac{5t}{6} = 15614.7\text{kN/m} \tag{A.22}$$

$$D_{55} = G_{yz}\frac{5t}{6} = 4395.3\text{kN/m} \tag{A.23}$$

$$D_{66} = E_{xx}t = 1334800\text{kN/m} \tag{A.24}$$

$$D_{77} = E_{yy}t = 484400\text{kN/m} \tag{A.25}$$

$$D_{88} = G_{xy}t = 110400\text{kN/m} \tag{A.26}$$